Drinking Water Risk Assessment: Public Health Impacts of Alternative Disinfection Byproduct Control Strategies

by

John Alexander Meyer

B.S., University of Colorado at Boulder, 2014

A thesis submitted to the Faculty of the College of Engineering and Applied Science of the University of Colorado in partial fulfillment of the requirement for the degree of

Master of Science

Department of Civil, Environmental and Architectural Engineering

2016

The thesis entitled:

Drinking Water Risk Assessment: Public Health Impacts of
Alternative Disinfection Byproduct Control Strategies

written by John Alexander Meyer

has been approved for the
Department of Civil, Environmental, and Architectural Engineering

_____

Dr. R. Scott Summers

_____

Dr. Chad Seidel

_____

Dr. Rajagopalan Balaji

DATE: _____.

The final copy of this thesis has been examined by the signatories, and we find that both the content and the form meet acceptable presentation standards of scholarly work in the above mentioned discipline.

Abstract

Meyer, John A. (M.S., Environmental Engineering)

Drinking Water Risk Assessment: Public Health Impacts of Alternative Disinfection Byproduct Control Strategies

Thesis Directed by Professor R. Scott Summers

Chemical agents in drinking water can pose significant human health risks. Evaluating the combined effects from multiple contaminants can provide new insights into how best to manage that risk and protect public health. The Relative Health Indicator (RHI) is a semi-quantitative metric developed to harmonize the cancer and non-cancer impacts from a wide range of drinking water contaminants, thereby allowing for comparison of the relative health risks posed by multiple waterborne constituents. The goals of this study were to use the RHI to assess the impact water age dynamics through distribution systems can have on population-based disinfection by-product (DBP) risk exposures and to evaluate the public health benefits afforded by several DBP control strategies.

Analysis of different network models revealed that system water age dynamics have a significant impact on population-weighted DBP exposures. As DBP regulatory compliance strategies, optimized coagulation processes and granular activated carbon (GAC) adsorption at the treatment plant were found to provide superior public health protection than GAC and aeration technologies applied within the distribution system when population-weighted RHI values were considered. The relative efficiencies of distribution system technologies tended to be equivalent to those applied at the treatment plant as evidenced by normalizing population-weighted RHI reductions to treatment process flow rates. Booster chlorination cannot be used to achieve DBP compliance but did demonstrate moderate population-weighted RHI reductions.

Acknowledgements

First and foremost I would like to thank my family for supporting me in my academic endeavors for the past two decades. I would never have reached this point without their steadfast love and support.

I would also like to acknowledge the countless friends who had my back through all of my six years at CU. While there are far too many to name everyone individually, each person played a unique role in my support system and helped to create a community for me to share with in the trials, tribulations, joys, and triumphs of being a young adult.

Very special thanks are in order for Dr. Chad Seidel and Dr. Scott Summers who have mentored me through my graduate studies and helped set me up for success as I begin a career in the water industry. I also give very high praise to Dr. Fernando Rosario and Dr. Chris Corwin for strongly encouraging me to continue my education beyond a bachelor's degree. I have been very fortunate to study under some other fantastic minds at CU including Dr. Diane McKnight, Dr. Dick Kuchenrither, Dr. Balaji Rajagopalan, Dr. Joseph Kasprzyk, Dr. Rita Klees and Dr. Karl Linden.

Finally, I would like to acknowledge all past and present members of the Engineers Without Borders Peru Program. My experience working and playing with EWB-CU the past several years has opened my eyes up to the bigger picture of how the world works and what it means to be a global citizen.

Funding for this research was provided by the United States Environmental Protection Agency Science to Achieve Results (STAR) Program Grant #83560301.

Table of Contents

List of Tables

List of Figures

CHAPTER 1: INTRODUCTION

1.1 Background

Humans are constantly exposed to a multitude of chemical and microbial constituents in air, food, water, soil, and other media. While many of these are benign, some can pose significant human health risks and induce both cancer and non-cancer health outcomes. Drinking water is a primary source of exposure to various risk agents including pathogens, heavy metals, nitrate and nitrite, natural and anthropogenic organic contaminants, disinfection byproducts, and radionuclides.

Risk reduction is mandated by the 1996 Amendments of the Safe Drinking Water Act (SDWA) as stated in Section 1412(b)(1)(A) General Authority, "…in the sole judgement of the Administrator, regulation of such contaminant presents a meaningful opportunity for health risk reduction for persons served by public water systems." To date, over 90 contaminants have been regulated under the SDWA. However, with recent advances in analytical techniques, the number of constituents detected in water has dramatically increased. This has spurred an elevated concern surrounding the health hazards that these constituents might pose. The challenge arises in actually quantifying the risks associated with mixtures of contaminants and the level of risk reduction which can be achieved through various treatment processes.

Researchers (Seidel et al., 2014) developed the Relative Health Indicator (RHI) metric as a semi-quantitative means of evaluating the cumulative risk posed by multiple waterborne contaminants by harmonizing the cancer and non-cancer health outcomes presented by exposure to chemical and microbial constituents. Using this methodology, RHI project researchers deduced that microbes constitute the number one risk agent in the United States. However, they conceded that the microbial RHI methodology offers significant room for improvement due to

the extensive overarching assumptions that had to be made to mitigate the lack of available utility operational data. RHI developers also determined that several disinfection byproduct (DBP) species are among the top ten risk agents nationally (Seidel et al., 2014). These findings highlight the need for future policy decisions and treatment strategies to focus on balancing adequate disinfection with DBP control.

The Stage 2 Disinfectants and Disinfection Byproducts Rule, promulgated in January of 2006, requires all drinking water systems to conduct an Initial Distribution System Evaluation to identify locations with high DBP concentrations to be used as monitoring sites for total trihalomethanes (TTHM) and the five regulated haloacetic acid species (HAA5). Monitoring for these contaminant groups is based on a locational running annual average (LRAA) with TTHM and HAA5 maximum contaminant levels (MCLs) of 80 µg/L and 60 µg/L, respectively (USEPA, 2005b).

Due to increasingly stringent regulatory requirements, it is important for drinking water providers to consider DBP formation through the treatment plant and distribution system when deciding which treatment approaches to pursue. One model that is commonly applied to predict DBP formations is the United State Environmental Protection Agency (USEPA) Water Treatment Plant Model (WTP Model) (Harrington et al., 1992; Solarik et al., 2000). The WTP Model predicts the behavior of water quality with an empirically-based, central tendency modeling approach that accounts for NOM removal, disinfectant decay, and DBP formation through the treatment plant and distribution system. Combining risk assessment metrics, such as the RHI, with modeled water quality predictions could be a useful way to assess which treatment strategies provide the best public health protection.

While tools such as the WTP Model can be effective at relating water age to DBP yields, actual population exposures to these constituents could be significantly impacted by system layout, usage patterns and community spatial distribution in relation to the treatment plant. For example, Uber et al. (2004) demonstrated that storage tanks can significantly increase both the median water age and water age variability in subsequent distribution system sections. Considering factors that affect water age in conjunction with DBP formation kinetics could have significant implications for public health protection in the drinking water community.

1.2 Objectives of Study

The overall goal of this work was to evaluate population-based DBP risk exposure. Specific objectives included:

1. Analyzing the effects of distribution system water age dynamics on population-weighted DBP risk exposures.

2. Evaluating the relative health protectiveness of optimized coagulation, granular activated carbon applied at the treatment plant or in the distribution system, distribution system aeration, and booster chlorination as DBP control strategies.

1.3 Literature Review

1.3.1 Environmental Exposures and Health Risk

Exposure to potentially hazardous constituents can occur though any one of a number of routes including inhalation, ingestions, dermal absorption, or injection (Doull, Curtis, & Klaassen, 1986; Loomis, 1970). To effectively protect public health, it is important to understand the hazards that these substances pose, the specific health outcomes they induce, and the mechanisms by which they are transported through the environment.

Typical health risk assessment for a chemical of interest follows a four step process of: 1) hazard identification, 2) exposure assessment, 3) dose response assessment for cancer and non-cancer effects, and 4) risk characterization of cancer and non-cancer health outcomes (OEHHA, 2001). While risk assessment has historically considered contaminants on individual bases, there recently has been a shift towards cumulative risk assessment approaches which consider multiple contaminants, exposure pathways, external stressors, and health outcomes (NRC, 1993; 2009; Sexton, 2012; Williams et al., 2012).

This paradigm shift towards cumulative risk assessment over the past several decades has been accompanied by a fair amount of criticism. Covello (1990) and Slovik (1991) point out that risk comparisons across numerous constituents will inevitably rest on several assumptions, simplifications, and limitations due to lack of knowledge about the synergistic and antagonistic effects of interacting substances, variable subpopulation sensitivities, and complex environmental transport mechanisms. Reflecting these sentiments, the USEPA Science Advisory Board has asserted that a cumulative risk assessment “promises a level of sophistication in risk analysis that currently does not exist”, and “much work remains to be done and much experience

is yet to be gained before we will be able to assess cumulative risks posed by multiple stressors and/ or multiple exposures over time" (USEPA, 2000b).

The health risk posed by a given chemical is traditionally quantified as the product of the probability and severity of the adverse health effects that it induces. The probability of negative health impacts is further defined as the product of constituent exposure and toxicity. When assessing carcinogenic effects, the cancer slope factor is used as a measure of toxicity (USEPA, 2005a). For non-cancer health impacts, toxicity is defined by the reference dose of a given risk agent adjusted by a statistically derived uncertainty factor (USEPA, 1987). Studies have shown that exposure to chemical constituents can be accurately quantified by modeling the fate and transport of various contaminants through different environmental media. This type of exposure assessment seeks to link chemical concentrations in environmental media and human contact based on average daily intake or as a time-averaged contact concentration (McKone & MacLeod, 2003).

There are several metrics for assessing the severity of health outcomes. For example, when analyzing carcinogenic effects, the age dependent adjustment factor is often used to define the severity of impacts on subpopulations at various stages of life (USEPA, 2011). When developing methods to evaluate health impacts posed by drinking water contaminants, Seidel et al., (2014) adopted quantitative severity factors by mapping critical effects of various health outcomes to specific diseases identified by the World Health Organization's (WHO) Disability Adjusted Life Years (DALYs) weightings. Other studies have characterized severity from dose response thresholds such as the no observed adverse effect level, the lowest observed adverse effect level, the frank effect, and lethality (Hertzberg, 1989; Hertzberg & Miller, 1985).

1.3.2 Drinking Water Risk Assessment

Drinking water treatment plays an important role in public health protection. While advances in treatment technology and more stringent regulations help to reduce drinking water health risks, the relative benefits achieved can vary significantly. In the early 20th century, utilities started incorporating filtration and disinfection processes into their facilities. As a result, the U.S. experienced a significant reduction in microbial diseases at a cost of $500 (in 2003 dollars) per death averted which constitutes a benefit: cost ratio of 23: 1 (Cutler & Miller, 2005). Conversely, lowering the regulatory standard for arsenic in drinking water from 50 parts per billion (ppb) to 10 ppb cost an estimated $4 million per death averted at a benefit: cost ratio of less than 1: 1 (USEPA, 2000).

As aforementioned, risk reduction is mandated by the SDWA. It is implicit in this that that drinking water risk be qualified either quantitatively or qualitatively. Smith et al. (1992) expressed the cancer risk from arsenic in drinking water as the number of individuals expected to experience negative health outcomes in a sample population of 1000. Regli et al. (1991) used a similar metric when determining levels of disinfection required for *Giardia* and enteric virus disinfection. Cantor et al. (1998) used odds ratios to describe the risks associated with chlorination byproducts. Similarly, Ward et al. (1996) also used odds ratios to express the risk of non-Hodgkin's lymphoma from nitrate in rural drinking water supplies.

The major limitation of approaches similar to those described above is that they only consider individual contaminants and specific health outcomes. Recently, there has been a push from regulators to approach risk susceptibility in a more holistic manner. The USEPA has directed program offices to "consider a broader scope that integrates multiple sources, effects, pathways, stressors, and populations for cumulative risk analyses in all cases for which relevant

data are available" (USEPA, 1997). In 2010, the USEPA Office of Water revealed a new strategy for the protection of drinking water and public health. This approach built upon four main principles:

1. Address contaminants as groups rather than one at a time so that enhancement of water protection can be achieved cost effectively

2. Foster development of new drinking water technologies to address health risks posed by a broad array of contaminants

3. Use the authority of multiple statutes to help protect drinking water

4. Partner with states to share more complete data from monitoring at public water systems (USEPA, 2010).

Thus far, the incorporation of cumulative risk assessment principles in the drinking water industry has been limited to disinfection byproducts (Teuschler et al., 2004). One of the primary barriers to developing cumulative risk assessment approaches for waterborne contaminants is an incomplete understanding of the underlying science governing how risk agents interact (Covello, 1990; Seidel et al., 2014; Slovic, 1991; USEPA, 200b). Furthermore, there is an innate conflict between regulatory standards implemented on a national level and the geographic heterogeneity of drinking water contaminant occurrence (Seidel et al., 2014).

1.3.3 The Relative Health Indicator Metric

In Water Research Foundation Project #4310, "Identifying Meaningful Opportunities for Drinking Water Health Risk Reduction in the United States", Seidel et al. (2014) developed the Relative Health Indicator (RHI) as a semi-quantitative cumulative risk assessment framework to harmonize the cancer and non-cancer health impacts associated with microbial and chemical contaminants in drinking water. The overall goal of the RHI project was to help utilities prioritize risk reduction strategies and to better communicate the health impacts of drinking water risk agents to consumers and policy makers.

RHI developers considered 91 drinking water contaminants including: 68 of the 69 USEPA Six Year Review 2 (6YR2) chemicals (fluoride was omitted); 8 DBPs including 4 trihalomethanes (chloroform, bromodichloromethane, dibromochloromethane, bromoform), 2 haloacetic acids (dichloroacetic acid and trichloroacetic acid), chlorate, and bromate; lead and copper; 12 chemical contaminants from the USEPA Unregulated Contaminants Monitoring Rule 2 (UCMR2) dataset which includes 6 nitrosamines (NDEA, NDMA, NDBA, NDPA, NMEA, NPYR), 3 parent acetanilides (acetochlor, alachlor, metolachlor) and 3 explosives (1,3-dinitrobenzene, TNT, RDX); and microbial contaminants including total coliform, fecal coliform and *E. coli*.

The RHI metric is partitioned into cancer and non-cancer components with the overall RHI of a given constituent representing the sum of its cancer and non-cancer RHI values. RHI values for individual contaminants can then be summed to produce a cumulative RHI value for a given drinking water. For a given chemical, RHI quantification methodology is outlined as follows:

$$Constituent\ RHI = Cancer\ RHI + NonCancer\ RHI \quad (1.1)$$

$$Cancer\ RHI = Cancer\ Toxicity * Cancer\ Severity * Exposure \quad (1.2)$$

$$Cancer\ Toxicity = \frac{CSF * 2(\frac{L}{d})}{70\ (kg)} \quad (1.3)$$

- CSF = Cancer Slope Factor
- 2(L/d) represents human daily consumption of water
- 70(kg) is the standard default body weight used for risk calculations

$$NonCancer\ RHI = NonCancer\ Toxcity * NonCancer\ Severity * Exposure \quad (1.4)$$

$$NonCancer\ Toxicity = \frac{0.01 * 2(\frac{L}{d})}{70(kg) * RfD * UFc} \quad (1.5)$$

- 0.01 represents a 1% population incidence rate derived from Dourson et al. (1996)
- 2(L/d) represents human daily consumption of water
- 70(kg) is the standard default body weight used for risk calculations
- RfD = Reference Dose (oral)
- UFc = Uncertainty Factor used for RfD derivation

In equations 1.2 and 1.4 above, cancer and non-cancer severity scores were derived from DALYs developed by the WHO in the Global Burden of Disease Report (WHO, 2008) by "mapping" critical effects from the USEPA Integrated Risk Information System database to

specific diseases identified in the WHO weightings with the underlying assumption that a critical effect is prognostic of a certain disease. This methodology makes risk estimates slightly subjective, however, it avoids the needs for complex bio-mathematical models which currently do not exist. RHI cancer health outcomes were assigned a uniform severity score of 0.29 as derived by professional judgement.

Although it is not a major component of this work, RHI researchers also developed a methodology for quantifying microbial risk which could then be added to the cumulative "risk cup" for a given drinking water. For this, only non-carcinogenic microbial health effects were considered. Ultimately, the authors concluded that there is significant room for improvement in the microbial RHI quantification due to the overarching assumptions that had to be made in light of a lack of available utility operational data.

1.3.4 Drinking Water Distribution System Modeling

Modeling distribution system hydraulics and contaminant transport has a number of useful applications including homeland security, emergency response planning, process optimization, and sensor placement selection. Uber et al. (2004) explain the inherent conflict between protecting distribution system information in the interest of preventing terrorism and the need for researchers to access network data in order to improve modeling capabilities. The authors identified two viable solutions: 1) fabricate "prototype" network models that reflect both the hydraulics and water quality behavior of real systems, 2) develop methods to visually transform real systems so they cannot be readily identified.

There are numerous examples of the former strategy found in literature. Alperovits & Shamir (1977) developed a hypothetical two loop system which has since been used to assess

various optimization algorithms (Kessler & Shamir, 1989; Geem, 2006). Walski et al. (1987) created Anytown, USA as the basis for "Battle of the Network [Optimization] Models". Similarly, "Battle of the Water Sensor Networks" used hypothetical systems Network 1 and Network 2 (Ostfeld et al., 2008), and "Battle of the Water Calibration Networks" used C-Town (Ostfeld, 2012). The EPANET example networks Net2 and Net3 have been used for numerous research purposes (Rossman, 2000; Berry et al. 2006; Watson et al. 2010; Pasha and Laney 2009; Hart et al. 2011). Other examples of hypothetical systems developed specifically for research purposes include Micropolis and Mesopolis (Brumbelow et al., 2004), and Exnet (Farmani et al., 2004).

Converse to these prototype network approaches, Jolly et al. (2014) created a research database of 12 small and medium sized models based on real drinking water distribution systems in Kentucky. All of the models were slightly modified to mask the identity of each specific community. The authors selected the systems based on a range of attributes including system size, the number of pumps, the number of tanks, the number of reservoirs and system topology (branched, gridded or looped), to create robust set of networks. Each model incorporates a previously developed diurnal demand curve (AWWA, 2012) and constraints to simulate utility pump schedules.

Whether a hypothetical or real system model is used, simulated distribution system analysis does have some notable limitations. Maier (2003) and Khu & Keedwell (2005) assert that algorithm testing on a singular system model could lead to erroneous results due to lack of robustness and interchangeability among different networks. Furthermore, Walski (2001) points out that solutions derived from network models may not necessarily be practical or feasible when applied to a given real world scenario.

1.4 Report Organization

Chapter 2 of this report details a study evaluating the health protectiveness of several DBP mitigation strategies using the RHI metric in conjunction with alternative treatment models. This study also assessed the extent to which distribution system water age dynamics can impact population-weighted DBP health risks and how that could influence a utility's selection of an appropriate DBP control technology. The methods used for this study are described in greater detail in Appendix A and a full set of sensitivity analysis results can be found in Appendix B. This report closes in Chapter 3 with brief summaries of each of these studies and final remarks on how they fit into the larger context of drinking water treatment and public health protection.

CHAPTER 2: PUBLIC HEALTH IMPACTS OF DBP MITIGATION

2.1 Introduction

Promulgated in January of 2006, the Stage 2 Disinfectants and Disinfection Byproducts Rule (D/DBP Rule) tightened total trihalomethane (TTHM) and haloacetic acid (HAA5) regulations by requiring disinfection byproduct (DBP) monitoring to occur at distribution system locations with high DBP concentrations as determined by an Initial Distribution System Evaluation (USEPA, 2005b). It further mandated DBP maximum contaminant levels (MCLs) to be quantified on locational running annual averages (LRAAs), which consider average concentrations at each individual monitoring location, rather than running annual averages (RAAs), which consider cumulative average concentrations across multiple monitoring sites.

Balancing conflicting treatment goals can often present challenges for drinking water providers. A common regulatory hurdle is achieving compliance with increasingly stringent DBP regulations while simultaneously maintaining an adequate disinfectant residual throughout the distribution system. Alternative treatment strategies may achieve the same LRAA monitoring goals, thereby ensuring that all consumers are exposed to DBP concentrations below the regulatory limit. However, there could be significant differences in the level of risk reduction that each approach offers when the overall population-weighted exposure is considered. The goals of this study were to assess how distribution system water age dynamics might affect DBP public health risks, and to evaluate the overall public health protectiveness of several treatment strategies that drinking water providers might pursue to achieve both DBP and secondary disinfection compliance.

2.2 DBP Mitigation Strategies

Disinfection byproducts have been linked to negative health outcomes including cancer (Bull & Kopfler, 1991) as well as adverse reproductive and developmental effects (Bielmeir et al., 2001; Waller et al., 1998). There are three primary approaches utilities can pursue for DBP mitigation: 1) use alternative disinfectants which produce lower DBP yields; 2) remove precursor natural organic matter (NOM) in raw water sources; 3) remove DBPs after formation. This study primarily focuses on the latter two of these strategies.

A long-established treatment approach is coagulation with hydrolyzing metal salts such as aluminum sulfate (alum), ferric sulfate, and ferric chloride. While coagulation processes are typically used to remove particles and reduce turbidity, they can also have the added benefit of reducing organic carbon concentrations. The D/DBP Rule stipulates a total organic carbon (TOC) removal criteria which, for most utilities, can be met by a process referred to as enhanced coagulation (USEPA, 1999). DBP precursor removal beyond that required can be achieved by optimizing the coagulation process for NOM removal at pH values below 6 (Crozes et al., 1995; Edwards, 1997; Tseng et al., 1996; Qin et al., 2006).

High pressure membranes (Ates et al., 2009; Siddiqui et al., 2000) and ion exchange processes (Boyer & Singer, 2005; Tan et al., 2005) can reduce dissolved organic carbon (DOC) concentrations resulting in significantly lower trihalomethane and haloacetic acid formation potentials. Precursory compounds can also be removed through oxidation by OH-radicals (Ferguson et al., 1990; Wallace et al., 1988), ozone (Myers, 1990; Tan et al., 1990), and advanced oxidation processes with ultraviolet radiation (Chin & Bérubé, 2005; Lamsal et al., 2011; Wallace et al., 1988; Zhou & Smith, 2002).

Granular activated carbon (GAC) can also be used to remove precursor NOM, resulting in lower post-treatment DBP yields (Chiu et al. 2012, Jacangelo et al., 1995; Owen et al., 1998). As an added advantage, GAC can be used after chlorination to also remove both preformed THMs and HAAs (Babi et al., 2003; 2007; Clark & Lykins, 1991; Speth & Miltner, 1990; 1998). This approach, however, is less common because NOM has been shown to be more adsorbable than DBPs (Snoeyink et al. 1999) and chlorine is readily adsorbed thereby prompting the need for post-GAC rechlorination.

There are several other treatment options for removing preformed DBPs from drinking water. Trihalomethanes are amenable to aeration due to their relatively high volatilities. A number of THM aeration technologies exist including surface aeration, packed tower aeration, tray aeration, spray aeration, and bubble aeration. This study specifically focuses on the latter two of these technologies as localized treatments within the distribution system. Spray aeration, which uses a nozzle in the head space of a tank to create small water droplets, has been reported to achieve up to 99.5% TTHM removal (Brooke & Collins, 2011). Parameters which can impact the THM removal efficiency of spray aeration units include nozzle type, spray angle, droplet size, nozzle pressure, and air-water contact time (Ghosh et al. 2015; Schneider et al., 2015). Bubble aeration introduces air to a system using mechanical diffusers which produce small bubbles that travel up through a water column. The mass transfer of stripping compounds from solution in this manner is controlled by Henry's Law equilibrium dynamics (Mackay et al., 1979) resulting in varying removal efficiencies for different THM species. The use of aeration to reduce TTHM concentrations in finished drinking waters has the added benefit of not significantly impacting chlorine residual (Brook & Collins, 2011; Sherant, 2008; Johnson et al., 2009; Tarquin et al., 2005), thus eliminating the need for post-treatment rechlorination. While

effective at removing THMs, aeration does not reduce HAA concentrations as these compounds have relatively low volatilities nor does it remove DBP precursory compounds.

A common water treatment practice is to apply a single high chlorine dose in order to maintain a disinfectant residual through the far reaches of the distribution network. This can, however, produce high levels of DBP formation, as well as cause taste and odor problems due to extremely high chlorine concentrations at consumer's taps (Amy et al, 1987; Boccelli et al., 2003; Clark, 1998). Reducing the amount of chlorine applied at the treatment plant and incorporating additional small doses throughout the distribution system, in a process known as "booster chlorination", can dampen initial DBP formations and help to reduce aesthetic issues. Boccelli (1999) demonstrated that booster chlorination reduces the total mass of chlorine required to maintain an adequate disinfection residual when compared to the conventional practice of applying a single dose at the plant. However, the author also determined that booster chlorination provides no reduction in the DBP formation at the maximum residence time. While not viable as a strategy for achieving compliance with TTHM or HAA5 regulations under the LRAA monitoring framework, booster chlorination is another approach utilities might pursue to abate population-weighted health risk by reducing the DBP concentrations in certain areas of the distribution system.

2.3 Objectives of Study

The study objective was to assess how water age dynamics impact population-weighted DBP health risks under the same baseline treatment scenario in several different distribution systems. Building upon this, booster chlorination, optimized coagulation, GAC adsorption, and aeration were modeled across a range of source water quality parameters to compare how each

strategy might be used to reduce population-weighted DBP risk exposure. This work also sought to look beyond risk reduction and demonstrate how each approach would impact chemical use and process flow rates to illustrate the challenge utilities face in balancing risk reduction with technical feasibility when deciding which alternative technologies to pursue.

2.4 Methods

2.4.1 Source Water Quality Parameters

For all analyses, source water pH and alkalinity were held constant at their respective 50^{th} percentile values of large U.S. water treatment plants from the Information Collection Rule database (McGuire et al., 2002). Source water temperature, TOC, and bromide (Br^-) were varied across a range of values that was deemed to be representative of scenarios in which drinking water systems may encounter DBP regulatory compliance issues. Source water ultraviolet absorbance at 254 nanometers (UVA) was assumed to be empirically related to source water TOC via a constant TOC-based specific ultraviolet absorbance ((T)SUVA) value of 2.5 L/mg-m. Summaries of the constant and variable source water parameter values are shown in Table 2.1 and Table 2.2.

Table 2.1: Source water parameters held constant across all analyses.

Parameter	Units	Value
pH	-	7.6
Alkalinity	mg/L as $CaCO_3$	93
(T)SUVA	L/(mg-m)	2.5
Flow Rate	GPM	1000

Table 2.2: Combinations of source water temperature, TOC and Br^- values analyzed.

Temperature ($°C$)	TOC (mg/L)	Br^- (mg/L)
10	3.5	0.01
		0.05
		0.1
	4.0	0.01
		0.05
		0.1
	4.5	0.01
		0.05
		0.1
18	3.0	0.01
		0.05
		0.1
	3.5	0.01
		0.05
		0.1
	4.0	0.01
		0.05
		0.1
24	2.5	0.01
		0.05
		0.1
	3.0	0.01
		0.05
		0.1
	3.5	0.01
		0.05
		0.1

2.4.2 Treatment Modeling

Each of the modeled treatment approaches are described briefly below. In all cases chlorine decay and DBP formation were modeled at the effluent of the filter and contact tank, as well as at 12 hour time-steps through the distribution system. The treatment model equations and algorithms used in this study were based on the U.S. Environmental Protection Agency Water Treatment Plant (WTP) Model (Center for Drinking Water Optimization, 2001) and the detailed descriptions can be found in Appendix A.

Baseline Treatment

NOM removal, disinfectant decay and DBP formation were modeled for a baseline conventional conventional filtration treatment train of: 1) coagulant (alum) addition, 2) rapid mix, 3) flocculation, 4) sedimentation, 5) free chlorine addition, 6) anthracite over sand filtration, 7) contact tank disinfection, 8) pH adjustment and 9) distribution. The assumed baseline model parameters are shown in Table 2.3

Table 2.3. The applied alum dose was optimized to meet the enhanced coagulation regulatory requirements as set forth by the USEPA (1999) and the applied chlorine dose was optimized to maintain a residual concentration greater than 0.2 mg/L through the distribution system. Prior to distribution, caustic soda was used to raise the pH above 8.

Table 2.3: Baseline treatment model specifications.

Parameter	Value
Coagulation	
Alum Dose	Optimized to meet enhanced coagulation regulations
Disinfection	
Chlorine Dose	Optimized to maintain a residual concentration >0.2 mg/L
Filter Volume	15,0000 gallons
Filter T10/Residence Time Ratio	0.5
Filter T50/Residence Time Ratio	1
Contact Tank Volume	45,000 gallons
Contact Tank/T10 Residence Time Ratio	0.5
Contact Tank T50 Residence Time Ratio	1
Distribution	
Pre-Distribution Caustic Soda Dose	Optimized to bring pH above 8 (±5 mg/L)
Max Distribution System Residence Time	10 days (240 hours)

Booster Chlorination

Although not an effective strategy for bringing the baseline treatment system into compliance for TTHM or HAA5, booster chlorination was also modeled to evaluate how it might impact population-weighted DBP health risks for cases in which the baseline treatment system did not produce DBP concentrations exceeding their regulatory MCLs. The baseline alum dose was applied in order to remain in compliance with enhanced coagulation regulations (USEPA, 1999). The chlorine dose applied prior to filtration was optimized to maintain a chlorine residual greater than 0.2 mg/L through half of the distribution system and the pre-distribution caustic soda addition was adjusted to bring the pH above 8 under this new chlorination scenario. A second optimized chlorine dose was applied at half of the total distribution residence time to maintain a residual greater than 0.2 mg/L through the remainder of the system. In order to produce results consistent with the findings of Boccelli (1999) under the WTP Model framework, the rechlorination UVA was adjusted so the DBP concentrations at the end of the system were approximately equal to those of the baseline case.

Optimized Coagulation

Optimized coagulation, was modeled as an alternative treatment strategy which modified the baseline treatment processes to ensure both TTHM and HAA5 stayed below their respective regulatory MCLs of 80 µg/L and 60 µg/L throughout the distribution system. pH was initially reduced to 6 with a sulfuric acid addition to enhance TOC removal during coagulation (Crozes et al., 1995; Qin et al., 2006). The applied optimal alum and chlorine doses required to achieve the compliance for both classes of DBPs while maintaining a disinfectant residual greater than 0.2

mg/L were determined iteratively. Consistent with the baseline approach, a caustic soda addition was used to raise the pH above 8 prior to distribution.

GAC Adsorption

GAC adsorption was modeled both at the effluent of the treatment plant as well as within the distribution system as alternative treatment strategies to achieve TTHM and HAA5 compliance. For both scenarios, the baseline treatment specifications remained unaltered. It was assumed that two GAC units could be implemented in series as a lead-lag system to mitigate the temporal effects of constituent breakthrough, thereby producing steady-state THM, HAA, and TOC removals of 99%. A post-treatment rechlorination dose was applied to maintain a residual greater than 0.2 mg/L throughout the remainder of the distribution system. Under both GAC application scenarios, the fraction of flow treated was optimized to meet the specified treatment goals upon rechlorination. For the distribution system GAC application scenario, the adsorption unit was modeled at the highest residence time possible while still ensuring that DBP concentrations were kept below their respective MCLs prior to treatment.

Distribution System Aeration

Spray and bubble aeration were modeled as alternative treatments applied within the distribution system to keep TTHM below its regulatory MCL. The baseline treatment specifications remained unaltered for this approach. Spray aeration was modeled using species specific THM removal equations proposed by Cecchetti et al. (2014) with an assumed air-to-water ratio of 25,000. Bubble aeration was modeled using a THM removal equation proposed by Matter-Müller et al. (1981) with an assumed air-to-water ratio of 60 and system pressure of 25

psig. The Henry's Law coefficient for each THM species was adjusted for temperature (Staudinger & Roberts, 2001) and pressure (Zwerneman, 2012) accordingly. The placement of aeration units with the distribution system and the fraction of flow treated were optimized to meet the specified treatment goals at all points the distribution system. In some cases, this required multiple units to be implemented at different residence times.

2.4.3 DBP Relative Health Risk Estimation

The Relative Health Indicator (RHI) developed by Seidel et al. (2014) was used to evaluate DBP health risks for each of the modeled treatment strategies described above. Individual species RHI values were calculated for four trihalomethanes (chloroform, bromodichloromethane, dibromochloromethane, bromoform) and two haloacetic acids (dichloroaceticacid, trichloroaceticacid) at 12 hour distribution system time-steps based on the THM and HAA formation curves produced each modeled treatment approach. Cancer slope factors and reference doses have not been defined for the other three regulated haloacetic acid species (monochloroacetic acid, bromoacetic acid, dibromoacetic acid), thus, no cancer or non-cancer RHI contributions can be quantified for those constituents. The six individual DBP species RHI values were added to get a cumulative RHI value at each time-step. Details about the RHI quantification methodology can be found in Appendix A.

2.4.4 RHI Population Weighting

Distribution system models KY2, KY7, and KY12, developed by Jolly et al. (2014), were assessed using EPANET extended period simulations (Rossman, 2000) with a total duration of two weeks.

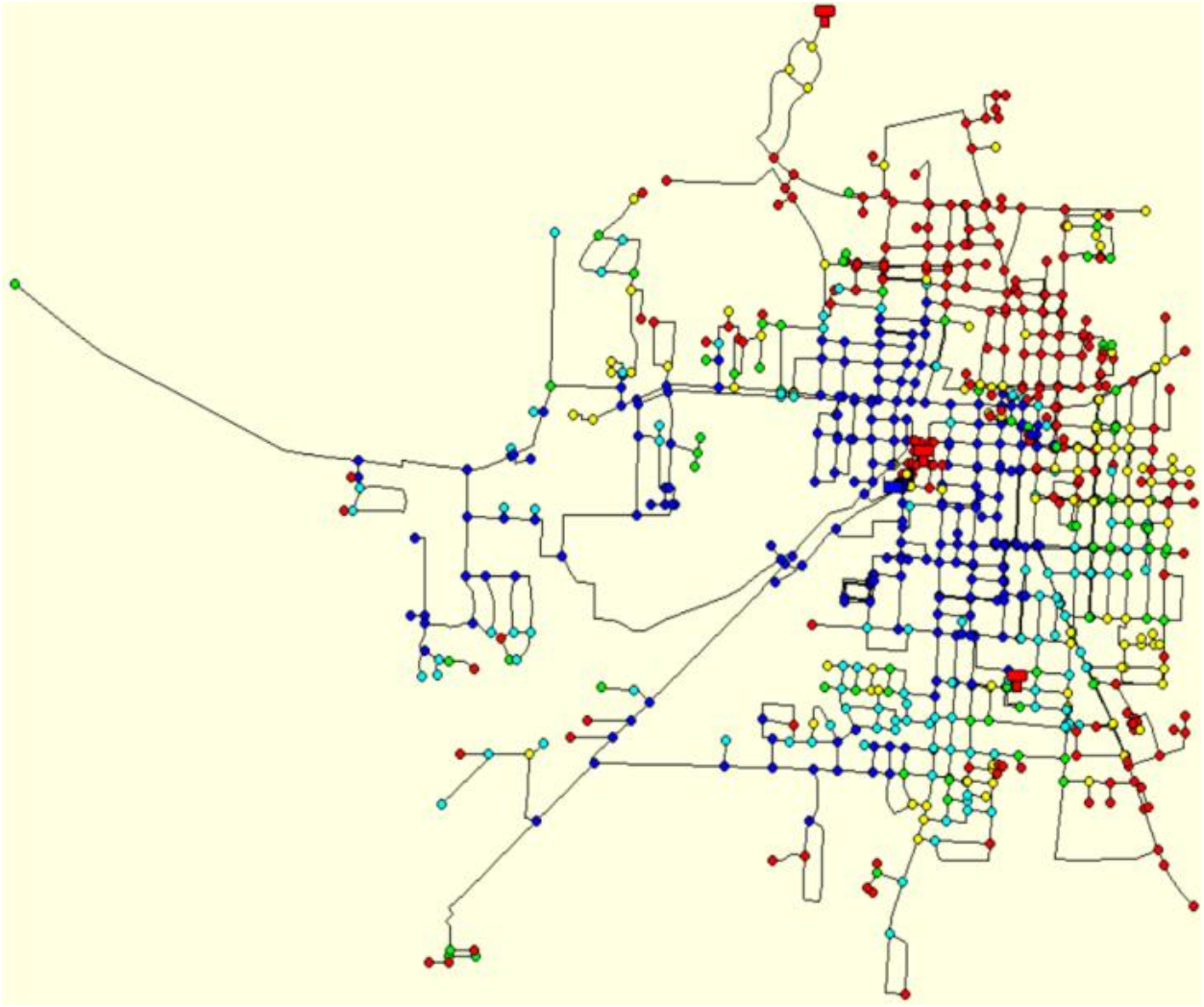

Figure 2.1: Distribution system EPANET model KY2 developed by Jolly et al. (2014).

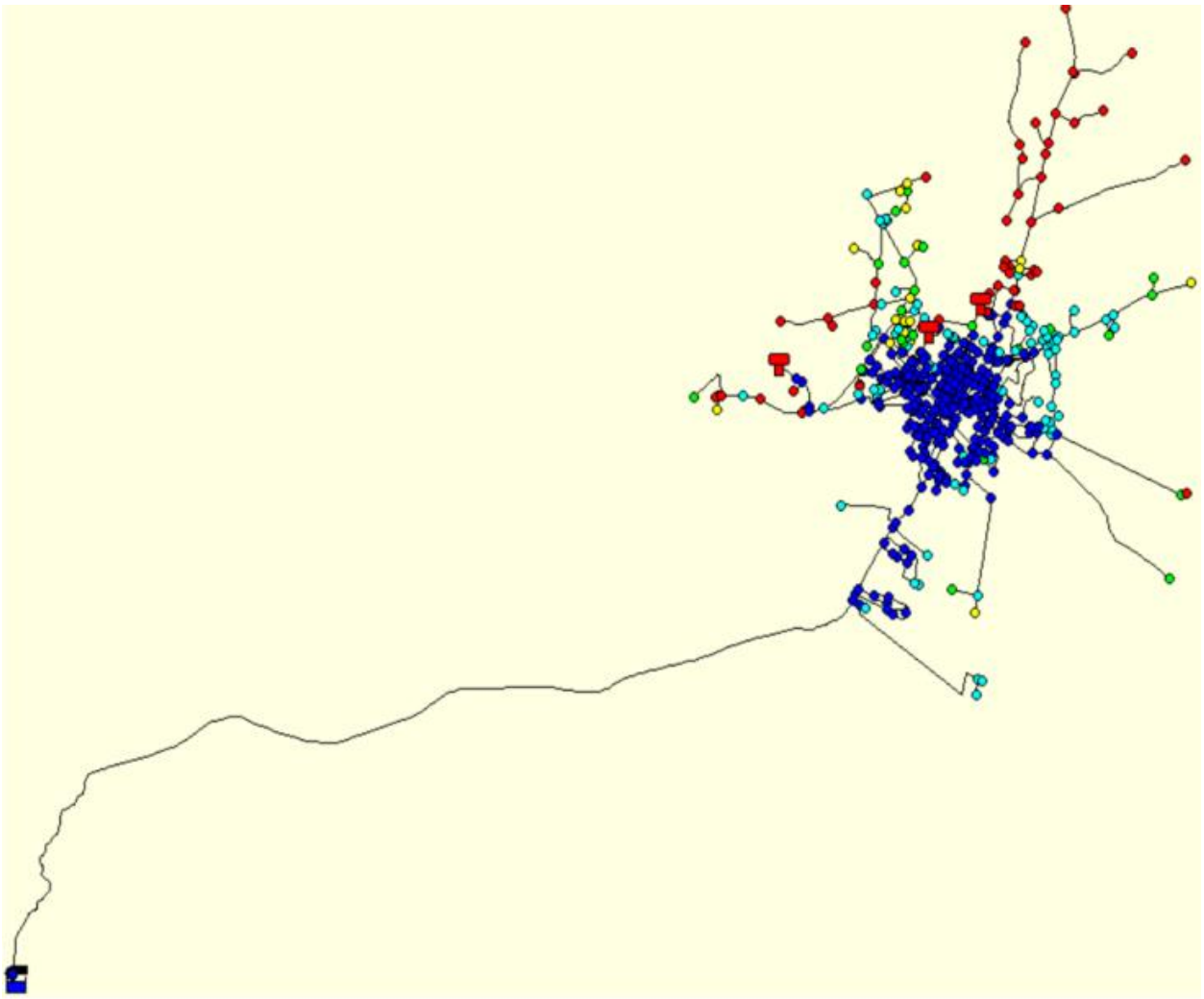

Figure 2.2: Distribution system EPANET model KY7 developed by Jolly et al. (2014).

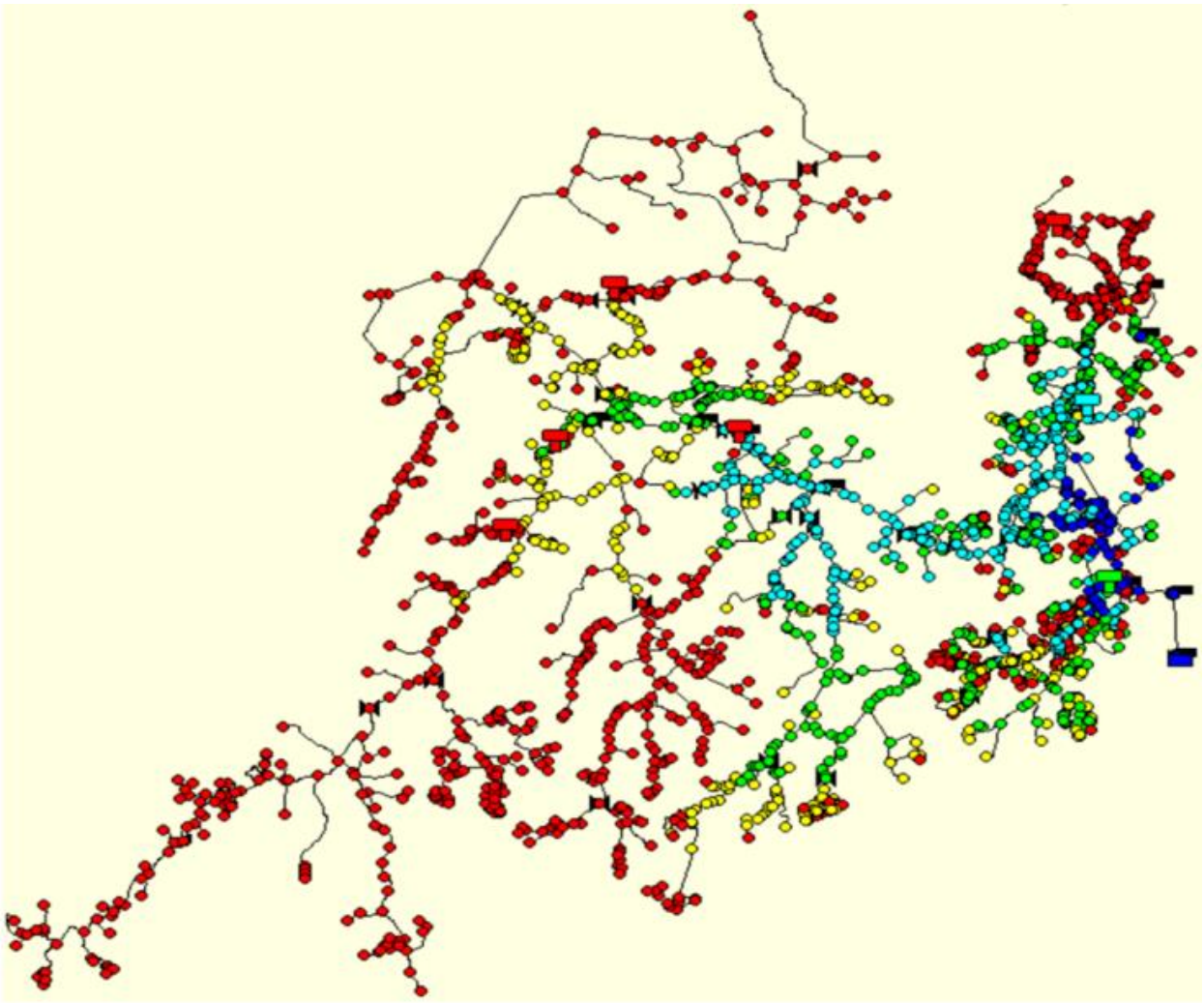

Figure 2.3: Distribution system EPANET model KY12 developed by Jolly et al. (2014).

Cumulative distribution functions (CDFs) of water age at the point of consumption were derived for each system using nodal base demand as a proxy for population and the median water age at each node during the last 24 hours of simulation. High median nodal water ages were truncated to 240 hours to match maximum distribution system residence time used for treatment modeling. As illustrated in Table 2.4, less than 5% of each CDF had to be truncated to the maximum water age of 240 hours. Thus, each system was deemed acceptable to be considered in conjunction with the modeled treatment strategies.

Table 2.4: Fraction of each distribution system model truncated at 240 hours.

Model	Fraction of CDF Truncated at 240 hours
KY2	0.000
KY7	0.041
KY12	0.014

Each simulation incorporated the original demand flow rates as reported by Jolly et al. (2014). It was assumed that the resulting CDF curves were applicable to the treatment models which all used an assumed treatment plant flow rate of 1000 GPM.

Population-weighted RHI values for all three of the modeled systems were calculated by integrating under a curve relating their respective water age CDFs to the RHI values at each time-step produced under the different treatment scenarios. The relative risk reductions achieved by alternative treatment strategies for a given source water quality scenario were calculated as the percent reduction in population-weighted RHI each one provided relative to the baseline. The RHI population-weighting methodology is described in greater detail in Appendix A.

2.4.5 Demonstrating Alternative Treatment Operational Requirements

To demonstrate how operational requirements could affect the technical feasibility of each of the treatment approaches described above, a set water quality treatment scenario (source water temperature = 10 °C; TOC = 4.0 mg/L; Br^- = 0.10 mg/L) applied to distribution system model KY7 was explored in-depth. Daily chemical use rates were calculated by multiplying individual doses by the flow rates at which they were applied. All in-plant chemical additions were assumed to be applied to the initial flow rate of 1000 GPM. The rechlorination flow rate for GAC adsorption at the effluent of the treatment plant was determined by multiplying the initial flow rate by the fraction of flow treated. Distribution system flow rates were calculated as the

product of the initial flow rate and the remaining fraction of a given system's CDF at the time of interest. The booster chlorination dose was assumed to be applied to the flow rate at the half way point (120 hours) in the distribution system. The treated stream flow rate for distribution system GAC was determined by multiplying the total flow rate at the point of interest by the fraction of flow treated. Flow rates for the spray and bubble aeration systems were calculated in a similar manner.

2.5 Results and Discussion

2.5.1 Baseline Population Weighted DBP Risk for Different Distribution System Models

The water age CDFs derived for the three distribution system models considered in this study are shown in Figure 2.4.

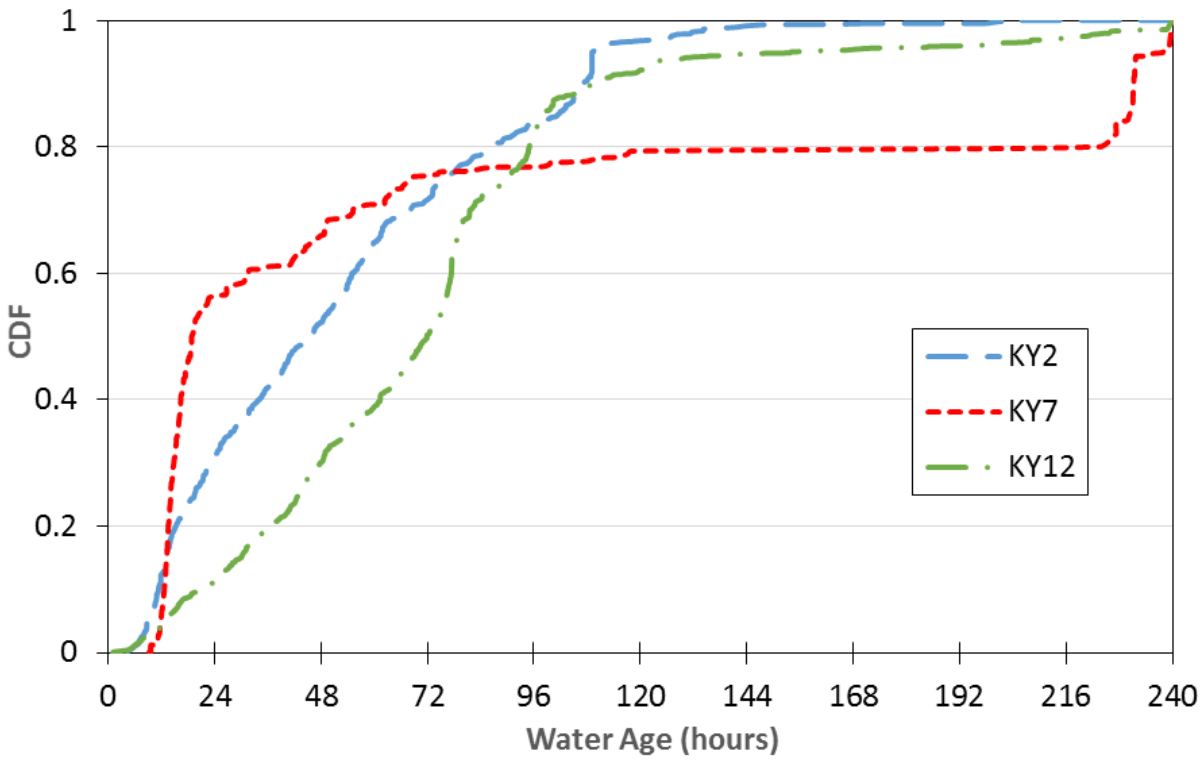

Figure 2.4: CDFs of the water age served for distribution system models KY2, KY7, and KY12 truncated to a maximum water age of 240 hours.

KY7 had high consumption at low distribution system residence times resulting in a 50th percentile median water age of roughly 19 hours. Consumption leveled off around 72 hours resulting in the final 20 percent occurring at water ages greater than 224 hours. KY2 demonstrated a more steady consumption pattern with a 50th percentile median water age of roughly 46 hours. For this system, more than 90% of consumption occurred at a median water age of less than 108 hours. Similarly, KY12 demonstrated a steady consumption pattern that was lagged through the early distribution system residence times, resulting in 50th and 90th percentile median water ages of roughly 72 and 110 hours, respectively.

The baseline treatment conditions and finished water quality conditions for each of the 27 scenarios evaluated are given in Appendix Table B-1. The resulting TTHM and HAA5

concentrations as a function of time for these scenarios are given in Appendix Table B-2and summarized in Table 2.5.

Table 2.5: Summary of baseline source water quality modeling scenarios.

Scenario #	*Source Water Parameters*			*Baseline DBPs*			
	Temperature (°C)	*TOC (mg/L)*	*Br^- (mg/L)*	*TTHM MCL Exceedance (day)*	*Max TTHM (µg/L)*	*HAA5 MCL Exceedance (day)*	*Max HAA5 (µg/L)*
1	10	3.5	0.01	-	68.3	-	55.3
2			0.05	8.5	84.4	-	50.9
3			0.1	6.0	93.0	-	46.8
4		4.0	0.01	-	76.7	7.5	62.9
5			0.05	5.5	94.7	-	58.2
6			0.1	4.0	104.3	-	54.0
7		4.5	0.01	-	73.6	7	63.7
8			0.05	6.5	90.9	-	59.1
9			0.1	4.5	100.1	-	54.9
10	18	3.0	0.01	-	71.4	-	56.6
11			0.05	7.0	88.1	-	51.1
12			0.1	5.0	97.1	-	46.2
13		3.5	0.01	9.5	82.1	5.5	66.7
14			0.05	4.5	101.1	9.5	60.8
15			0.1	3.0	111.4	-	55.5
16		4.0	0.01	6.0	92.7	2.0	77.0
17			0.05	3.0	114.1	4.0	70.8
18			0.1	2.0	125.6	6.5	65.1
19	24	2.5	0.01	-	69.1	-	54.1
20			0.05	8.0	85.2	-	47.8
21			0.1	5.5	94.0	-	42.4
22		3.0	0.01	9.0	83.0	6.5	64.2
23			0.05	4.0	102.2	-	57.4
24			0.1	3.0	112.6	-	51.5
25		3.5	0.01	5.5	95.4	2.5	75.6
26			0.05	2.5	117.3	4.5	68.5
27			0.1	2.0	129.1	8.5	62.0

TTHM and HAA5 formation kinetics for Scenario #1 for the baseline treatment are shown in Figure 2.5A, as an example. The DBP formation kinetics for all 27 scenarios under baseline conditions are given in Appendix B. In this case the maximum DBP values occur at 10

days and both TTHM and HAA5 are below their respective MCLs. A summary of the MCL exceedances is shown in Table 2.6. In three scenarios neither the TTHM nor HAA5 MCLs were violated. In 22 scenarios the TTHM MCL was violated and in only 11 scenarios the HAA5 MCL was violated. There were 13 scenarios in which only the TTHM MCL was violated, while only two scenarios in which only the HAA5 MCL was violated and in 9 scenarios both the TTHM and the HAA5 MCLs were violated. The higher levels of TTHM formation is reflective of that reported in the ICR (McGuire et al., 2002).

Table 2.6: Summary of MCL exceedances under baseline treatment.

Number of MCL exceedances	Type of MCL exceedance
3	none
5	TTHM Violation < 10 µg/L
17	TTHM Violation ≥ 10 µg/L
8	HAA5 Violation < 10 µg/L
3	HAA5 Violation ≥ 10 µg/L

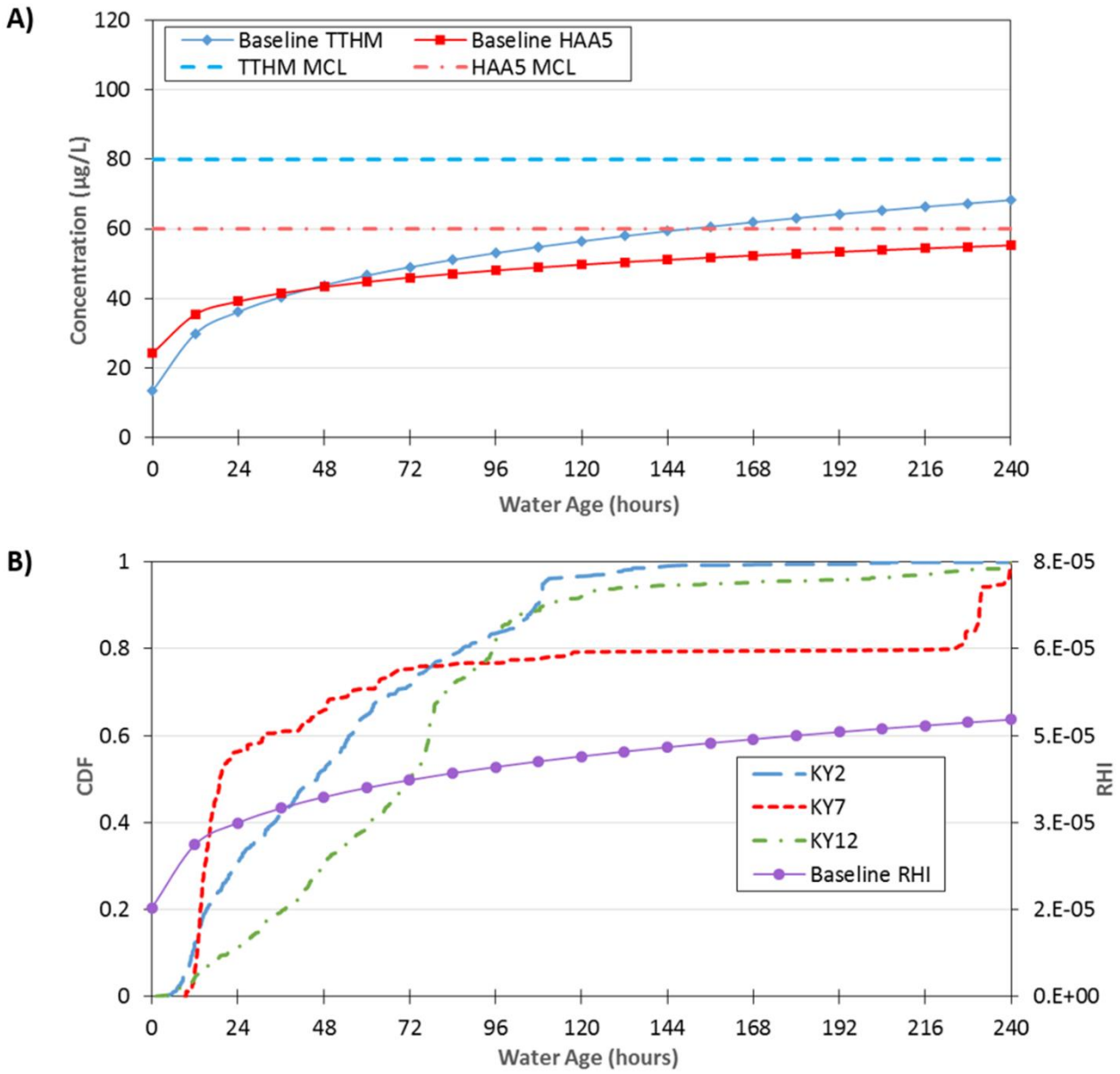

Figure 2.5: Example baseline treatment model results for Scenario #1 (source water temperature = 10 °C; TOC = 3.5 mg/L; Br^- = 0.01 mg/L). A) TTHM and HAA5 formations. B) RHI curve with distribution system model water age CDFs.

The RHI associated with the DBPs formed in Scenario #1 as a function of water age is shown in Figure 2.5B. Weighting this baseline RHI curve by each of the three distribution system water age CDFs resulted in the population-weighted RHI values shown in Table 2.7. A

summary of the population-weighted RHI results for each of the 27 water quality scenario is shown in Appendix B for each of the three distribution systems.

Table 2.7: Sample population-weighted RHI results for three different distribution systems under the baseline treatment for Scenario #1 (source water temperature = 10 °C; TOC = 3.5 mg/L; Br^- = 0.01 mg/L.

Distribution System Model	Population-Weighted RHI
KY2	3.29×10^{-5}
KY7	3.32×10^{-5}
KY12	3.60×10^{-5}

KY2 and KY7 had similar population-weighted RHIs with that of KY2 being marginally smaller. This shows that the benefits of a large amount of early consumption in KY7 were tempered by the 20% of the population served at high water ages. Conversely, KY12 had a 10% higher population-weighted RHI than KY2 as a result of having a lagged consumption pattern. This trend held true across all source water qualities analyzed under the baseline treatment scenario (Appendix B).

These findings illustrate that, when considering the population of a community as a whole, distribution system water age dynamics can have a moderate impact on public health. Nonetheless, it is important to point out that the DBP risks for individuals at the point of maximum exposure (i.e. the last house in the distribution line) remains the same if the total residence time is equivalent across all systems.

2.5.2 Public Health Impact of Booster Chlorination

As shown in Table 2.5 for three of the source water quality scenarios (numbers 1, 10 and 19) evaluated in this study, the baseline treatment model produced TTHM and HAA5

concentrations that remained below their respective regulatory MCLs through the entire distribution system. Booster chlorination in the distribution system, which does not alter the maximum DBPs formed, was evaluated for the potential to decrease the population-weighted RHIs. In each of these cases, booster chlorination altered the DBP formation kinetics and the resulting RHI values in a manner similar to that illustrated in Figure 2.6 for Scenario #1, which resulted in moderate reductions in population-weighted RHI values as shown in Table 2.8.

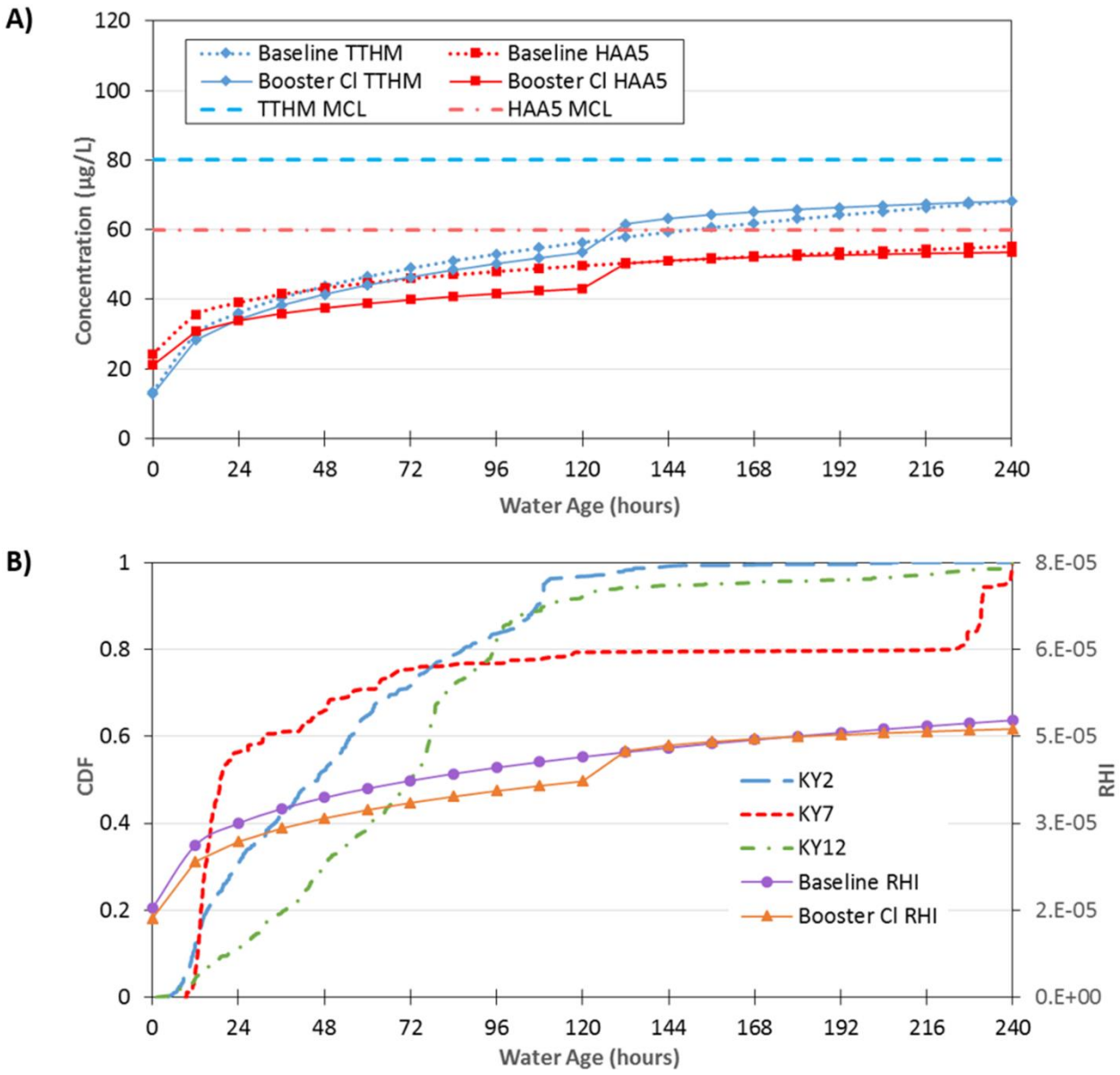

Figure 2.6: Example baseline and booster chlorination treatment model results for Scenario #1 (source water temperature = 10 °C; TOC = 3.5 mg/L; Br^- = 0.01 mg/L). A) TTHM and HAA5 formations. B) RHI curve with distribution system model water age CDFs.

Table 2.8: Population-weighted RHI percent reduction achieved by booster chlorination for source water scenarios where the baseline was in compliance for DBP regulations.

Source Water Parameters	System Model		
	KY2	*KY7*	*KY12*
Scenario #1 *Temperature = 10 °C* *TOC = 3.5 mg/L* *Br^- = 0.01 mg/L*	10.0	8.2	9.5
Scenario #10 *Temperature = 18 °C* *TOC = 3.0 mg/L* *Br^- = 0.01 mg/L*	9.9	8.1	9.4
Scenario #19 *Temperature = 24 °C* *TOC = 2.5 mg/L* *Br^- = 0.01 mg/L*	9.0	7.1	8.5

The average decrease in population-weighted RHI value was about 9% for these systems and water quality conditions. There were only marginal differences in the levels of DBP risk reduction achieved by booster chlorination among the various distribution system models. KY2 exhibited slightly higher reductions because over 96% of its consumption occurred at residence times less than 120 hours where the second chlorine dose was applied.

These findings demonstrate that utilities which do not face DBP compliance issues can attain meaningful public health benefits by implementing booster chlorination as a secondary disinfection strategy. In this study, only a single booster chlorine dose was considered; in practice, this approach might be further optimized by using several smaller doses applied at different distribution system locations. There may, however, be practical limitations which could constrain the utilization of this technique in a given water system such as the location of existing infrastructure to support chemical additions (storage tanks, pump stations, etc.), temporal variability in demand patterns, and primary disinfection requirements.

2.5.3 Relative Risk Reduction Achieved by Treatment Approaches for TTHM Compliance

The baseline treatment model yielded 13 scenarios in which MCL compliance for HAA5 was achieved, but the TTHM MCL was exceeded. A summary of the baseline DBP formations produced for each source water quality scenario, as well as the population-weighted RHI values for each system under alternative treatment models can be found in Appendix B. Comparisons of the population-weighted RHI reductions achieved by each viable treatment technology in this subset of trials are shown in Figure 2.7.

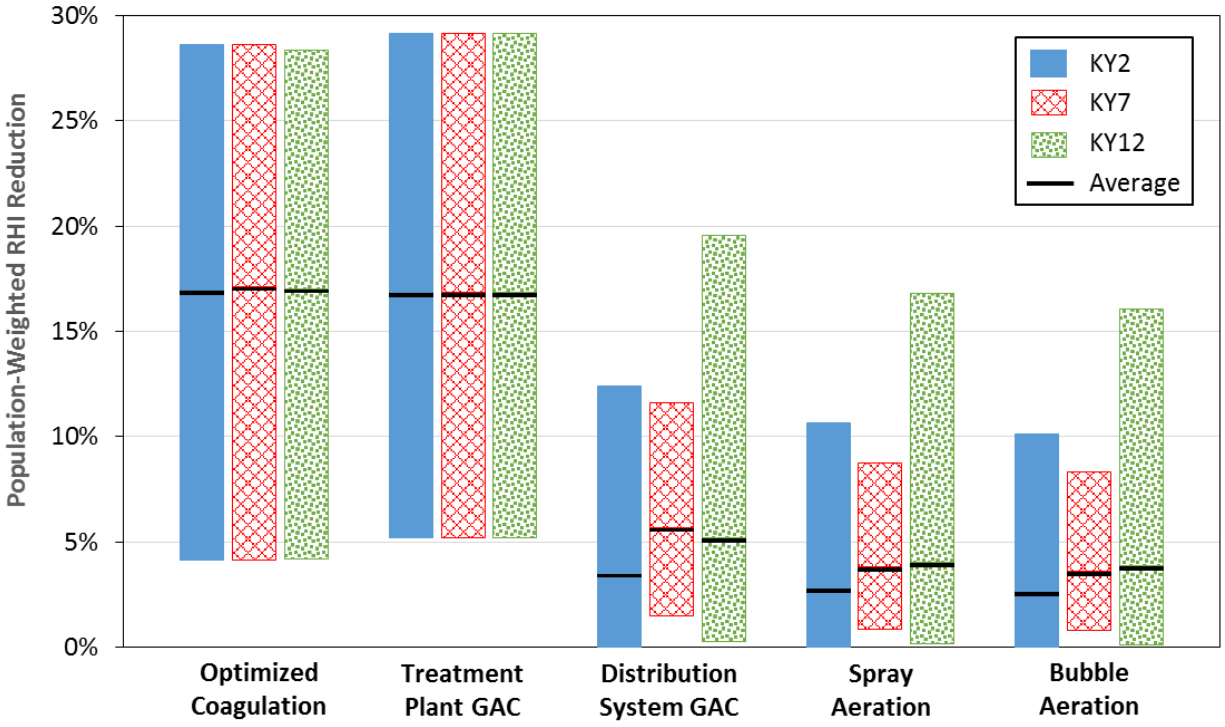

Figure 2.7: Minimum to maximum range of population-weighted RHI reductions achieved for scenarios in which the baseline treatment only violated the TTHM regulatory MCL (n=13).

In each case, optimized coagulation and GAC adsorption at the treatment plant provided the highest reduction of population-weighted RHI with neither approach demonstrating significantly better performance than the other. Distribution system water age (demand) patterns

had little influence on the level of relative risk reduction achieved by these two strategies as the entire population benefited from lower DBP exposures.

Treatments applied within the distribution system were less effective in reducing the population-weighted RHI. Of the three distribution system technologies evaluated for THM removal, GAC provided the highest RHI reductions as it had the added benefit of also removing HAAs. Spray aeration demonstrated slightly better RHI reduction than bubble aeration, particularly for the higher water temperature scenarios, because it removed a larger fraction of the more toxic brominated THM species.

The residence time at which distribution system treatments were applied for a given scenario directly affected the fraction of the total population that benefited from lower DBP exposures. Hence, the relative risk reductions afforded by these technologies were highly variable. Overall, KY12 experienced the greatest population-weighted RHI reductions from distribution system treatment because its consumption was lagged and greater portions of the total population benefited. On average, KY7 achieved similar risk reductions to KY12 and demonstrated less variability because 20% of the population at the far reaches of the system benefited even in cases where treatment was applied within the last 36 hours of residence time compared to less than 4% in each of the other two systems.

As a rough measure of the relative efficiency of each treatment strategy, population-weighted RHI reductions were normalized to flow as shown in Figure 2.8. Note that this analysis just considered the total flow rate at the point of treatment and did not factor in the fractions of flow treated by individual adsorption or aeration units.

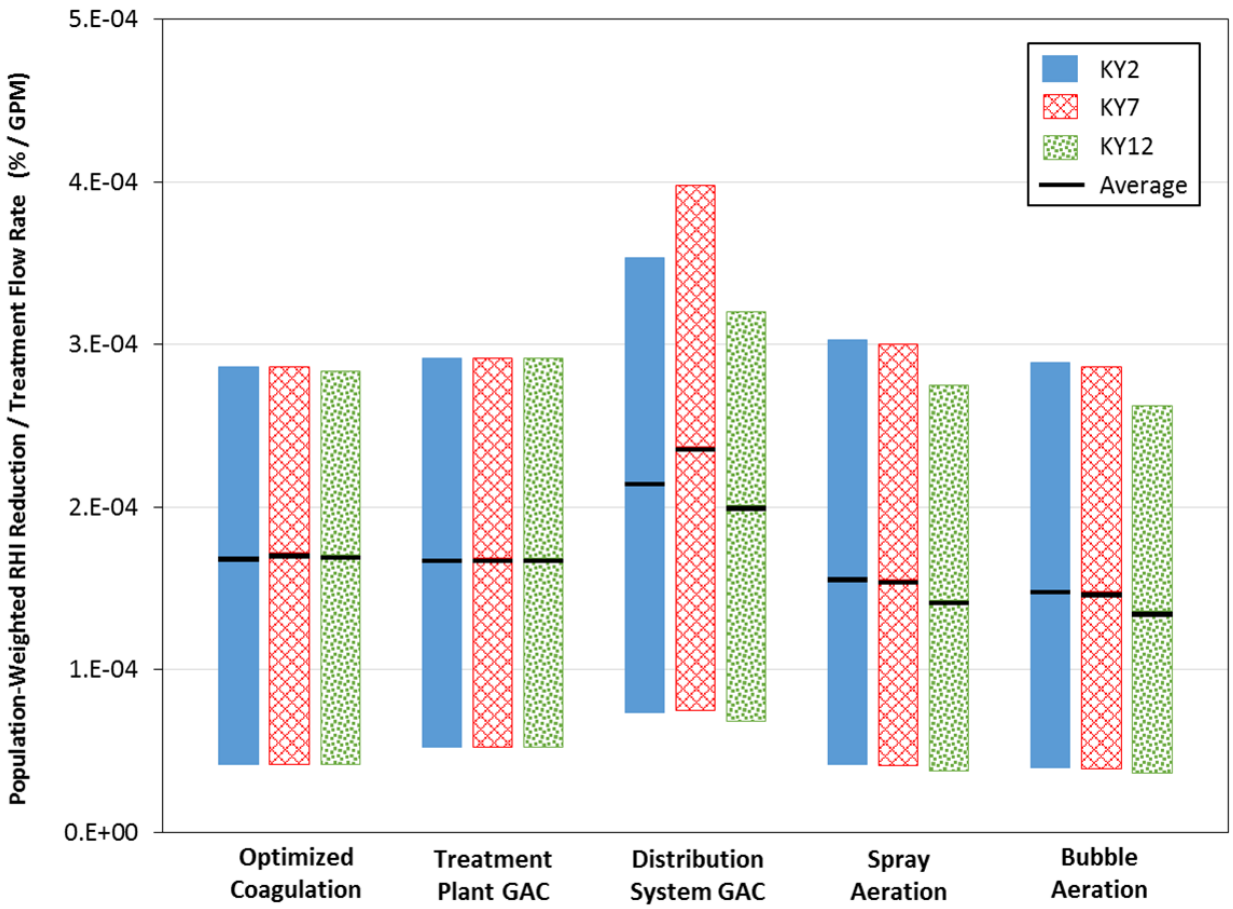

Figure 2.8: Minimum to maximum population-weighted RHI reductions achieved normalized to the flow rate at the point of treatment for cases in which the baseline treatment only violated the TTHM regulatory MCL (n=13).

While optimized coagulation and GAC adsorption at the plant effluent provided the highest levels of population-weighted RHI reduction, because they were applied at the maximum system flow rate, these proved to have no significant advantage compared to distribution system aeration technologies when the relative efficiencies were considered. Both aeration technologies were applied at lower flow rates, but only removed THM, thereby limiting their capacity for reducing RHI values. Distribution system GAC exhibited the most efficient RHI reductions as the result of being applied at low flow rates and removing both THM and HAA species.

Distribution system technologies were most efficient when applied to KY7 because of the 20% of consumption occurred at high water ages allow for greater population-weighted RHI reductions. The efficiency of distribution system technologies applied to KY2 were similar to those of KY7 because its flow rate at the point of treatment after 96 hours (when most TTHM violations occurred) was incredibly low. KY12 experienced slightly less efficient risk DBP risk reductions than the other two systems under distribution system treatment because it did not strike as favorable of a balance between low flow rates and high population-weighted RHI reductions.

2.5.4 Relative Risk Reduction Achieved by Treatment Approaches for HAA5 Compliance

The baseline treatment model yielded DBP formations that exceeded the HAA5 regulatory MCL for nine of the source water quality scenarios evaluated in this study. In seven of these cases, the baseline TTHM formation curve also violated its MCL. Comparisons of the population-weighted RHI reductions achieved by each viable treatment technology in this subset of nine HAA5 regulatory violation scenarios are shown in Figure 2.9.

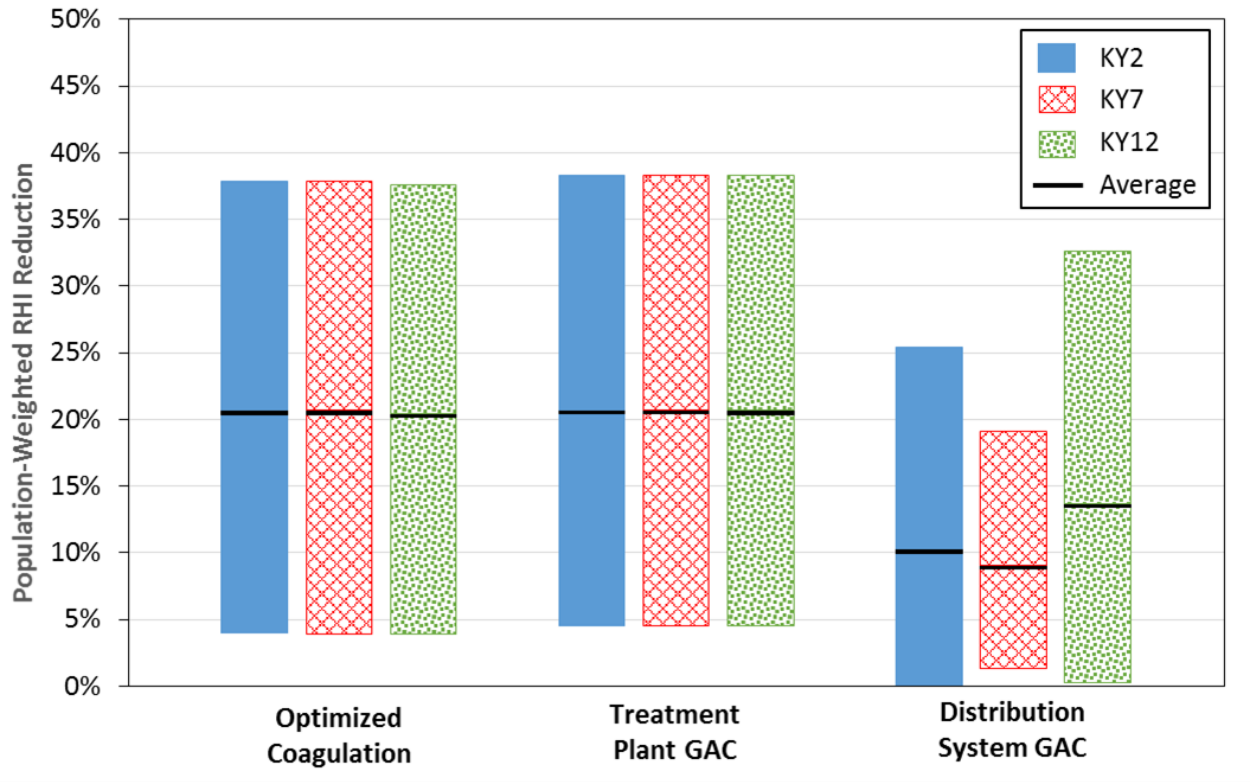

Figure 2.9: Minimum to maximum population-weighted RHI reductions achieved for cases in which the baseline treatment violated the HAA5 regulatory MCL (n=9).

Similar to the findings for TTHM compliance strategies, treatment approaches applied at the plant provided the highest levels of population-weighted RHI reduction with very little difference in performance exhibited by optimized coagulation and GAC adsorption. Again, distribution system consumption patterns did not impact the relative risk reductions afforded by these two in-plant treatment options.

Because HAAs had to be removed to achieve full regulatory compliance, GAC was the only viable distribution system treatment option in these scenarios. Distribution system GAC displayed the greatest population-weighted RHI reductions for system KY12 because the lagged consumption pattern permitted a large portion of total population to benefit from lower DBP exposures. KY7 experienced the lowest levels of DBP risk reduction under distribution system

treatment because the high early consumption limited the relative fraction of the population who benefited compared to the other two systems. This result is different than the cases in which only TTHM violations occurred where distribution system treatments were typically applied in the latter half of the distribution system. The population-weighted RHI reductions for each technology were normalized to flow as shown in Figure 2.10.

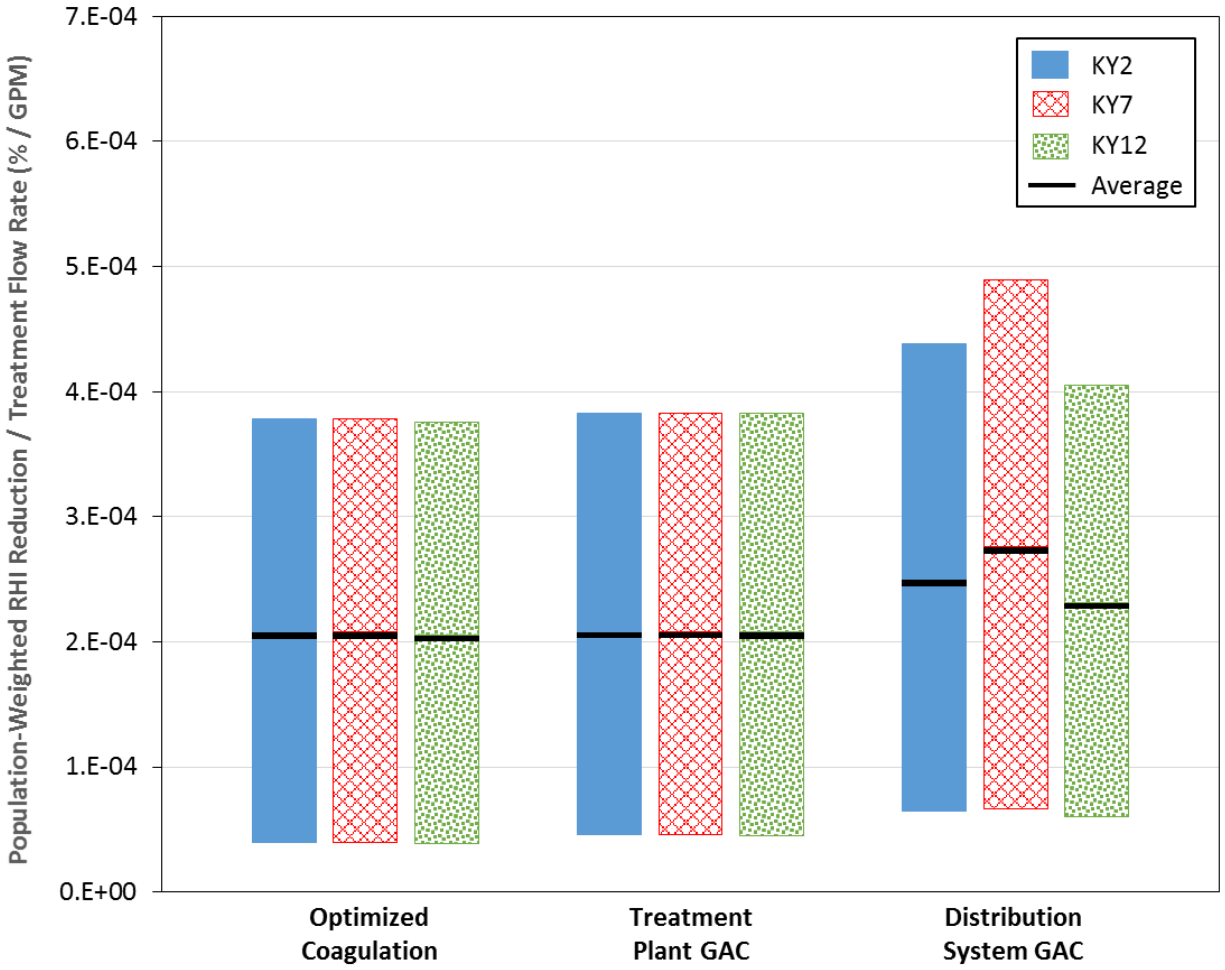

Figure 2.10: Minimum to maximum population-weighted RHI reductions achieved normalized to the flow rate at the point of treatment for cases in which the baseline treatment violated the HAA5 MCL (n=9).

Again, distribution system GAC provided more efficient means of reducing population-weighted RHI values than in-plant treatments because of lower flow rates. This technology proved to be most efficient when applied to KY7, because of the favorable combination of lower flow rates and a high potential for meaningful DBP risk reduction resulting from the late spike in consumption.

The findings of this study demonstrate that TTHM and HAA5 control strategies applied at the treatment plant provide higher levels of relative risk reduction than localized distribution system technologies. Nevertheless, due to the smaller volumes of water that have to be addressed, the relative efficiency of distribution system treatment as a means of reducing population-weighted DBP risk exposure is approximately equivalent to strategies applied at the plant. Because the public health benefits of all treatment approaches are highly variable, utilities should evaluate all potential options and determine which approaches strike an acceptable balance between public health protection, financial sustainability, and technical feasibility.

2.5.5 Demonstration of Alternative Treatment Requirements

Under Scenario # 6, source water quality conditions where temperature was 10 °C, TOC was 4.0 mg/L, and Br^- was 0.1 mg/L, the baseline treatment model produced the DBP formation shown in Figure 2.11.

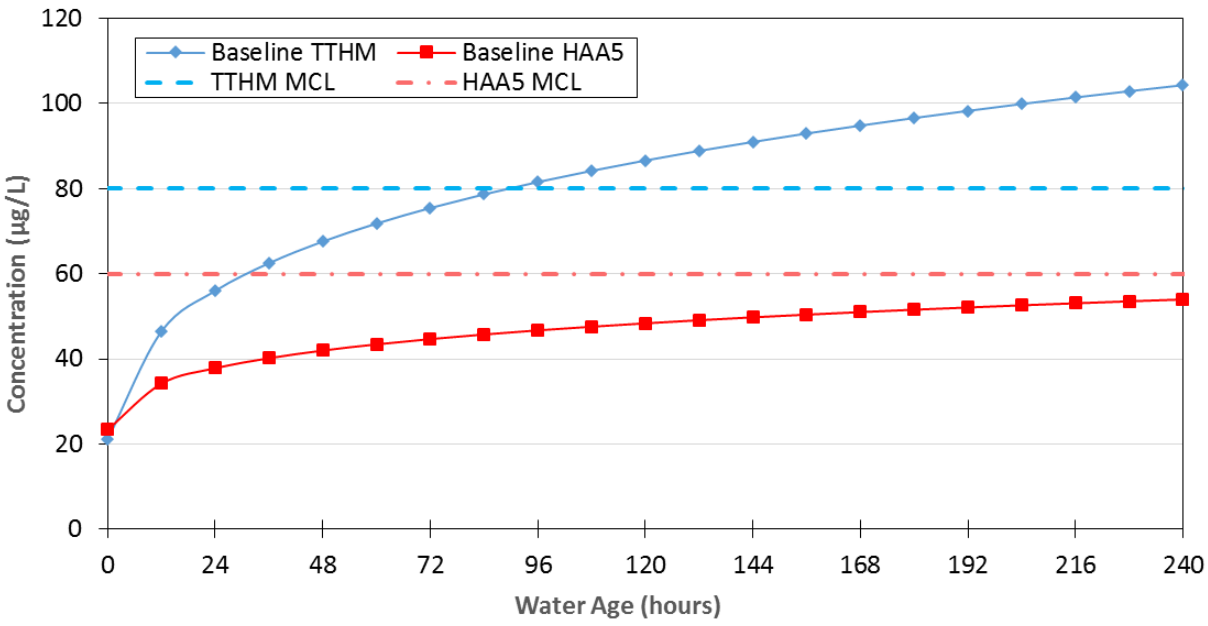

Figure 2.11: TTHM and HAA5 formations produced by the baseline treatment model for Scenario #6 (source water temperature = 10 °C; TOC = 4.0 mg/L; Br-= 0.1 mg/L).

In this case, TTHM violated its regulatory MCL at 96 hours while HAA5 remained in compliance. Thus, all alternative treatment approaches (except booster chlorination) were viable options for achieving DBP compliance.

As shown in Figure 2.12, system model KY7 has an isolated branch where a water age is elevated in relation to the rest of the system. At the particular time shown, this branch is the primary location where TTHM violations would occur under the specified treatment scenario with water ages exceeding 96 hours. Although water ages fluctuated throughout the two week simulation, for demonstrative purposes it was assumed that the conditions shown at this particular time were relatively static and the system could be brought into compliance by implementing distribution system technologies at the primary tank which supplies the non-compliant branch.

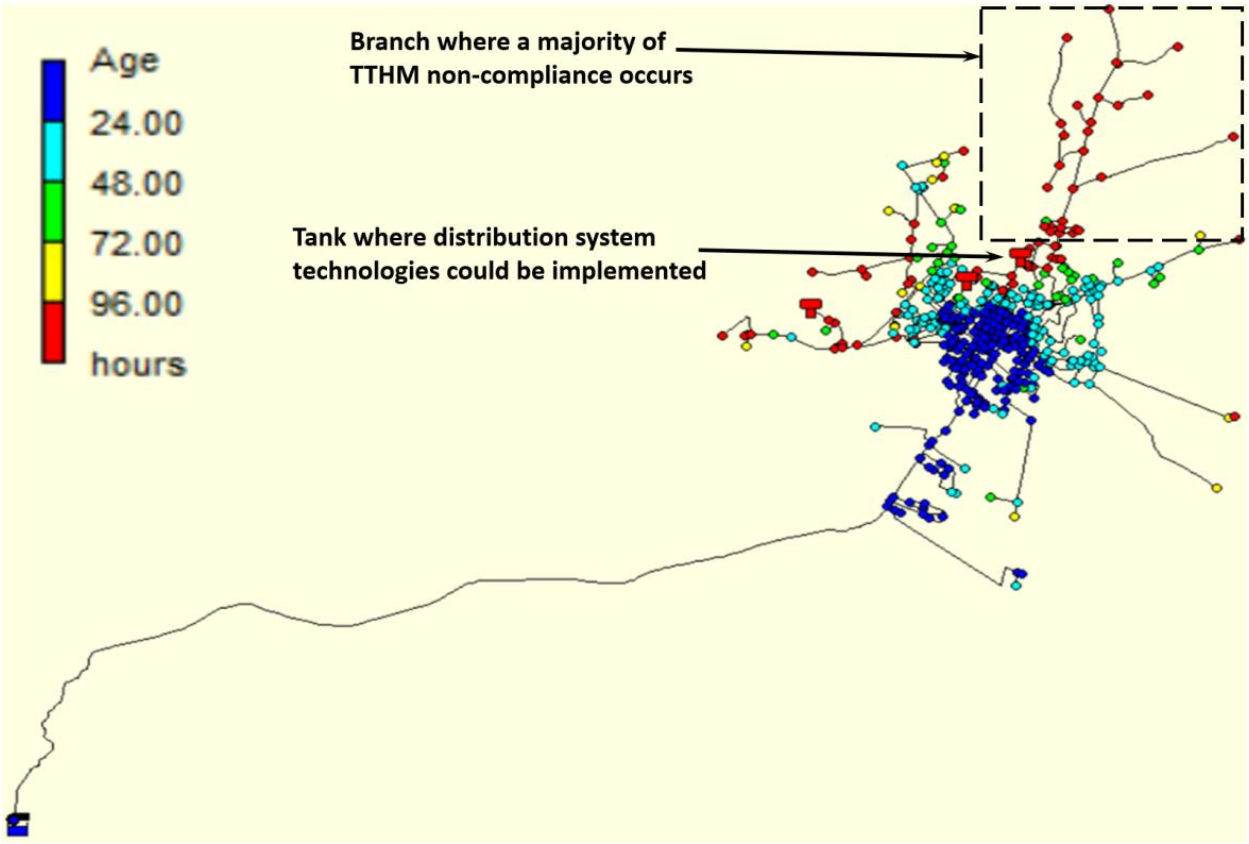

Figure 2.12: EPANET distribution system model KY7 developed by Jolly et al. (2014).

The DBP formations produced by the alternative treatment models applied to this scenario are shown in Figure 2.13.With the exception of booster chlorination, all treatment approaches brought the baseline system into compliance.

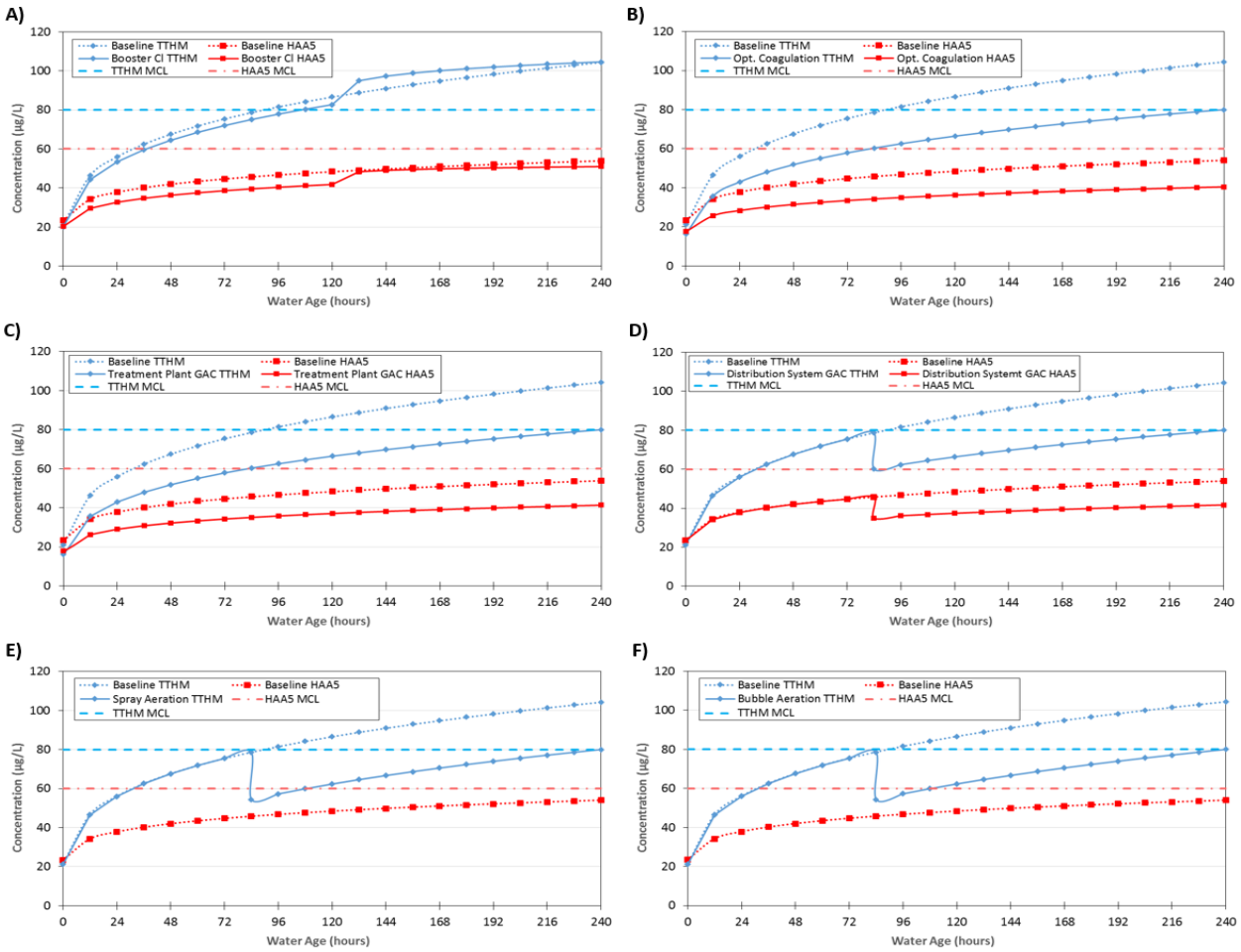

Figure 2.13: DBP formations produced by alternative treatment models for source water temperature = 10 °C; TOC = 3.0 mg/L; Br^- = 0.10 mg/L. A) Booster chlorination; B) Optimized coagulation; C) Treatment plant GAC; D) Distribution system GAC; E) Spray aeration; F) Bubble aeration.

The population-weighted RHI values quantified for each treatment approaches using the KY7 water age CDF are shown in Figure 2.14.

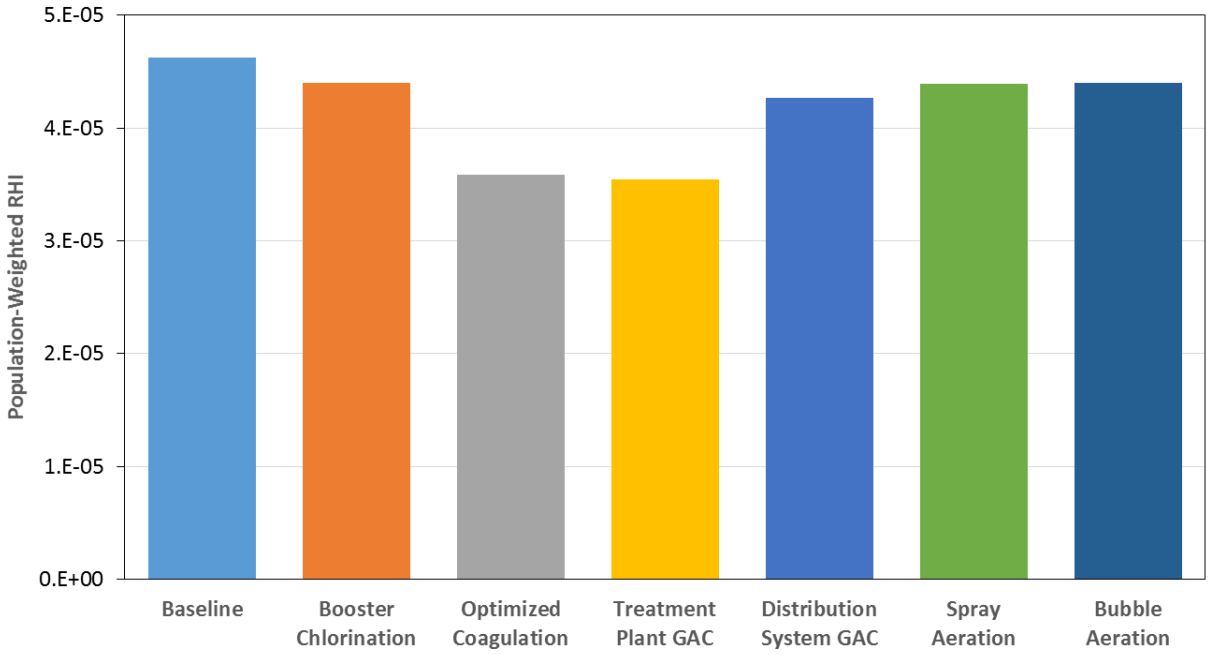

Figure 2.14: Population-weighted RHI values for each alternative treatment technology for system KY7 with Scenario #6 (source water temperature = 10 °C; TOC = 4.0 mg/L; Br^- = 0.10 mg/L).

The operational requirements quantified for each of the modeled treatment approaches under this scenario are shown in Table 2.9.

Table 2.9: Operational requirements for alternative treatment approaches for source water temperature = 10 °C; TOC = 4.0 mg/L; Br^- = 0.10 mg/L.

	Baseline	Booster Chlorination	Optimized Coagulation	TP GAC	DS GAC	Spray Aeration	Bubble Aeration
Sulfuric Acid Use Rate (10^3 kg/day)	-	-	327	-	-	-	-
Alum Use Rate (10^3 kg/day)	218	218	234	218	218	218	218
Chlorine Use Rate (10^3 kg/day)	21	18	17	24	21	21	21
Caustic Soda Use Rate (10^3 kg/day)	131	120	398	131	131	131	131
GAC Treatment Flow Rate (GPM)	-	-	-	238	56	-	-
Aeration Treatment Flow Rate (GPM)	-	-	-	-	-	81	115

Although booster chlorination did not bring the system into compliance, it did curtail chlorine and caustic soda usage while simultaneously reducing population-weighted RHI. Utilities which do not face DBP compliance issues could consider this strategy as a means to lower operational costs and better protect public health.

Optimized coagulation provided a high level of population-weighted RHI reduction but was very chemically intensive compared to the other treatment options. GAC applied at the treatment plant effluent also provided a high level of DBP risk reduction and only demonstrated a marginal increase in chlorine use. By comparison, GAC applied in the distribution system reduced the population-weighted RHI to a lesser extent but required a 76% lower treatment flow rate. From an operations standpoint, this would necessitate less frequent replacement of the adsorptive media resulting in lower operational costs.

Aeration had no impact on chemical use. While both aeration technologies provided similar levels of relative risk reduction, the spray system had a 27% lower treatment flow rate. However, because the mechanisms by which each of these technologies operate are markedly

different, it is difficult to infer which would ultimately require lower operating costs without performing further design analytics.

The purpose of this exercise was to demonstrate how utilities would need to consider operational requirements in conjunction with population-weighted cumulative risk assessment when choosing among different treatment technologies. It is important to recognize that this scenario was a highly idealized case in which implementing distribution system technologies at a single location was feasible for achieving regulatory compliance. Most distribution systems are far more complex and would likely require treatment at multiple points servicing different areas thereby increasing the level of required operations and maintenance inputs.

2.6 Summary and Conclusions

This study analyzed how distribution system water age dynamics impact community disinfection byproduct risk exposures. In general, systems which serve large portions of the population at low water ages present lower overall relative health risks than those with lagged consumption patterns. To better protect public health, utilities should aim to incorporate efficient distribution system management practices that prioritize lowering water age, such as effective storage tank management, reducing the number of dead-end locations.

This study also evaluated the relative risk reduction implications of several treatment strategies utilities can pursue to achieve compliance with DBP regulations. These ranged from in-plant process modifications to localized treatment technologies applied within the distribution system. In-plant treatment approaches benefit entire populations served and yield lower overall DBP health risks regardless of distribution system consumption patterns. Nevertheless, with larger flow rates at the treatment plant, these strategies could require a substantially higher

degree of operational input and have lower efficiencies. By comparison, distribution system technologies only benefit certain segments of a community, however, these localized treatments have to address a just fraction of the total flow thereby reducing the required operational input. Due to the complexities of water system hydraulics, incorporation of these technologies to achieve regulatory compliance may not be feasible, or could otherwise require multiple treatment units to be implemented at several different locations.

Disinfection byproducts are just one class of drinking water contaminants which can pose significant human health risks. Future research should seek to address the cumulative risks posed by a wider range of drinking water constituents and the public health benefits afforded by technologies which can synergistically treat for multiple classes of contaminants.

CHAPTER 3: SUMMARY AND CONCLUSIONS

The goal of the research was to improve our understanding of how health risk assessment across multiple DBP species can be incorporated into a number of practical applications. The effects of distribution system water age dynamics on population-weighted disinfection byproduct risks were evaluated using three distribution network models in conjunction with cumulative RHI estimates for modeled DBP species formation curves. Building upon this, several DBP control strategies were modeled to compare how alternative approaches impact community relative health risks and the feasibility of implementing such measures under different distribution scenarios. Overall, it was demonstrated that approaches incorporated at the treatment plant provide superior public health protection than those applied in the distribution system because they benefit entire community populations. However, in-plant approaches also must address greater flow rates, and associated treatment costs, thereby increasing the required operational inputs on a unit volume basis. Still, these may be more practical in many cases as they centralize operations whereas distribution system treatments may require many localized treatment units to be dispersed throughout transmission networks to achieve regulatory compliance.

This work demonstrated how relative risk assessment across multiple contaminants can provide useful insights into the public health benefits afforded by different drinking water treatment strategies. Specifically, it established a framework in which the risk reductions achieved different DBP control strategies can be compared relative to one another. The principles established here could be extended to a wider range of pollutants and treatment technologies. By using this type of approach, utilities can make more informed decisions about which treatment options provide the most efficient means of reducing drinking water health risk.

The RHI was used as a means of conveying information about the combined health impacts of multiple DBP species. While this metric provides a useful framework for performing these types of analyses, there is still much work to be done in developing more robust cumulative risk assessment methods that pertain to drinking water.

There are a number of research needs to be addressed so cumulative risk assessment practices can be further progressed in the drinking water industry. Analytical techniques for detecting trace concentrations of emerging contaminants need to be leveraged so the full range of constituents encountered in drinking water can be accurately described. Along with this, epidemiological science should aim to improve our understanding of how multiple risk agents interact to induce various health outcomes. Given the current lack of information about the synergistic and antagonistic effects of various pollutants, the RHI simply assumes that these agents interact additively, thereby limiting the capacity for it to accurately quantify the impact of exposure to combinations of waterborne constituents. Finally, efficient treatment practices which address several classes of contaminants simultaneously need to be identified so as to increase the sustainability of providing safe drinking water as natural resources continue to become scarcer.

Concurrently evaluating the impacts of multiple drinking water contaminants can provide new insights into how the water industry can better manage and mitigate public health risks. Nevertheless, drinking water is just one source of exposure to potentially hazardous agents. Drinking water risk assessment must be incorporated into the larger context of environmental risk exposure in order to more fully understand how to better provide more effective and equitable public health protection.

References

Alperovits, E., & Shamir, U. (1977). Design of optimal water distribution systems. *Water Resources Research*, *13*(6), 885–900.

American Water Works Association. (2012). *AWWA manual M32- Computer modeling of water distribution systems*. Denver, CO.

Amy, G., Chadik, P., & Chowdhury, Z. (1991). Developing models for predicting trihalomethane formation potential and kinetics. *Journal of the American Water Works Association*, *79*(7), 89–97.

Amy, G., Siddiqui, M., Ozekin, H., Zhu, H., & Wang, C. (1998). *Empirically Based Models for Predicting Chlorination and Ozonation Byproducts: Haloacetic Acids, Chloral Hydrate, and Bromate* (No. CX 819579). Cincinnati, OH: USEPA Office of Ground Water and Drinking Water.

Ates, N., Yilmaz, L., Kitis, M., & Yetis, U. (2009). Removal of disinfection byproduct precursors by UF and NF membranes in low-SUVA waters. *Journal of Membrane Science*, *328*(1-2), 104–112.

Babi, K., Koumenides, K., Nikolaou, A., Makri, C., Tzoumerkas, F., Lekkas, T., & Mihopoulos, N. (2003). Pilot-plant experiments for the removal of THMs, HAAs, and DOC from drinking water by GAC adsorption- Galatsi Water Treatment Plant, Athens. *Global NEST International Journal*, *5*(3), 177–184.

Babi, K., Koumenides, K., Nikolaou, A., Makri, C., Tzoumerkas, F., & Lekkas, T. (2007). Pilot study of the removal of THMs, HAAs and DOC by GAC adsorption. *Desalination*, *210*, 215–225.

Berry, J., Hart, W., Phillips, C., Uber, J., & Watson, J.-P. (2006). Sensor placement in municipal water networks with temporal integer programming models. *Journal of Water Resources Planning and Management*, *132*(4), 218–224.

Bielmeier, S., Best, D., Guidici, D., & Narotsky, M. (2001). Pregnancy loss in the rat caused by bromodichloromethane. *Toxicological Sciences*, *59*(2), 309–315.

Boccelli, D. (1999). *Booster Disinfection: Bulk Decay Kinetics, Byproduct Formations, and Model Development.* Master's Thesis. University of Cincinnati, Cincinnati, OH.

Boccelli, D., Tryby, M., Uber, J., & Summers, R. (2003). Optimal scheduling of booster disinfection in water distribution systems. *Water Research*, *37*(11), 2654–2666.

Boyer, T., & Singer, P. (2005). Bench-scale testing of a magnetic ion exchange resin for removal of disinfection byproduct precursors. *Water Research*, *39*(7), 1265–1276.

Brooke, E., & Collins, M. (2011). Posttreatment Aeration to Reduce THMs. *Journal of the American Water Works Association*, *103*(10), 84–96.

Brumbelow, K., Torres, J., Guikema, S., Bristow, E., & Kanta, L. (2007). Virtual cities for water distribution and infrastructure system research. *Proc. World Environmental and Water Resources Congress*. ASCE. Reston, VA.

Bull, R., & Kopfler, R. (1991). *Health effects of disinfectants and disinfection byproducts*. Denver, CO: American Water Works Association Research Foundation.

Cantor, K., Lynch, C., Alavanja, M., Hildesheim, M., Dosemeci, M., Lubin, J., & Craun, G. (1998). Drinking Water Source and Chlorination Byproducts I. Risk of Bladder Cancer. *Epidemiology*, *9*(1), 21–28.

Cecchetti, A., Roakes, H., & Collins, M. (2014). Influence of selected variables on trihalomethane removals by spray aeration. *Journal of the American Water Works Association*, *106*(5), E242–E252.

Center for Drinking Water Optimization. (2001). *Water Treatment Plant Model Version 2.0 User's Manual*. Boulder, CO: University of Colorado.

Chin, A., & Bérubé, P. (2005). Removal of disinfection byproduct precursors with ozone-UV advanced oxidation process. *Water Research*, *39*(10), 2136–2144.

Chiu, C., Westerhoff, P., & Ghosh, A. (2012). GAC removal of organic nitrogen and other DBP precursors. *Journal of the American Water Works Association*, *104*(7), E406–E415.

Clark, R. (1998). Chlorine demand and TTHM formation kinetics: a second order model. *Journal of Environmental Engineering*, *124*(1), 16–24.

Clark, R., & Lykins, B. J. (1991). *Granular Activated Carbon, Deign, Operation, and Cost* (2nd ed.). Michigan, U.S.A.: Lewis Publishers.

Covello, V. (1990). Risk comparisons and risk communication: issues and problems in comparing health and environmental risks. In R. Kaperson & P. Stallen, *Communicating Risks to the Public: International Perspectives* (pp. 29–124). Dordrecht: Kluwer Academic Publishers.

Crozes, G., White, P., & Marshall, M. (1995). Enhanced coagulation. *Journal of the American Water Works Association*, *87*, 78–89.

Cutler, D., & Miller, G. (2005). The role of public health improvements in health advances: The twentieth-century United States. *Demography*, *42*(1), 1–22.

Denbigh, K., & Turner, J. (1971). *Chemical Reactor Theory: An Introduction* (2nd ed.). Cambridge, UK: Cambridge University Press.

Doull, J., Curtis, D., & Klaassen, M. (1986). *Casarett and Doull's Toxicology: The Basic Science of Poisons*. New York, NY: Macmillan Publishing Co., Inc.

Dourson, M., Felter, S., & Robinson, D. (1996). Evolution of science-based uncertainty factors in non cancer risk assessment. Regulatory Toxicology and Pharmacology, 24, 108–120.

Dugan, N., Summers, R., Miltner, R., & Shukairy, H. (1995). An Alternative Approach to Predicting Chlorine and Chloramine Residual Decay. Presented at the AWWA Water Quality Technology Conference.

Edwards, M. (1997). Predicting DOC removal during enhanced coagulation. *Journal of the American Water Works Association*, *89*(5), 78–89.

Farmani, R., Savic, D., & Walters, G. (2004). "EXNET" benchmark problem for multi-objective optimization of large water systems. *Modell. Control for Particip. Plann. Manage. Water Syst.* IFAC Workshop. Venice, Italy.

Ferguson, D., McGuire, M., Koch, B., Wolfe, R., & Aieta, E. (1990). Comparing PEROXONE and ozone for controlling taste and odor compounds, disinfection byproducts, and microorganisms. *Journal of the American Water Works Association*, *82*(4), 181–191.

Geem, Z. (2006). Optimal cost design of water distribution networks using harmony search. *Engineering Optimization*, *38*(3), 259–277.

Ghosh, A., Seidel, C., Townsend, E., Pacheco, R., & Corwin, C. (2015). *Reducing Volatile Disinfection Byproducts in Treated Drinking Water Using Aeration Technologies*. Denver, CO: Water Research Foundation Web Report #4441.

Harrington, G., Chowdhury, Z., & Owen, D. (1992). Developing a Computer Model to Simulate DBP Formation During Water Treatment. *Journal of the American Water Works Association*, *84*(11), 78–87.

Hart, W., Murray, R., & Phillips, C. (2011). Minimize impact or maximize benefit: the role of objective function in approximately optimizing sensor placement for municipal water distribution networks. *Proc. World Environmental and Water Resources Congress*. ASCE. Reston, VA.

Hertzberg, R. (1989). Fitting a model to categorical response data with application to species extrapolation to toxicity. *Health Physics, 57*, 405–409.

Hertzberg, R., & Miller, M. (1985). A statistical model for species extrapolation using categorical response data. *Industrial Health, 1*(4), 43–57.

Isabel, R., Solarik, G., Koechling, M., Anzek, M., & Summers, R. (2000). Modeling Chlorine Decay in Treated Waters. Presented at the AWWA Annual Conference.

Jacangelo, J., DeMarco, J., Owen, D., & Randtke, S. (1995). Selected processes for removing NOM: an overview. *Journal of the American Water Works Association*, *87*(1), 64–77.

Johnson, B., Lin, J., Rexing, M., Fang, J., Chan, L., Jacobson, L., & Sampson, P. (2009). *Localized Treatment for Disinfection By Products*. Denver, CO: Water Research Foundation Project #3103.

Jolly, M., Lothes, A., Bryson, S., & Ormsbee, L. (2014). Research Database of Water Distribution System Models. *Journal of Water Resources Planning and Management*, *140*(4), 410–416.

Kessler, A., & Shamir, U. (1989). Analysis of linear programming gradient method for optimal supply of water networks. *Water Resources Research*, *25*(7), 1469–1480.

Khu, S.-T., & Keedwell, E. (2005). Introducing more choices (flexibility) in the upgrading of water distribution networks: the New York City tunnel example. *Engineering Optimization*, *37*(3), 291–305.

Koechling, M. (1998). *Assessment and modeling of chlorine reactions with natural organic matter: impact of source water quality and reaction conditions* (Doctoral Dissertation). University of Cincinnati, Cincinnati, OH.

Koechling, M., Rajbhandari, A., & Summers, R. (1998). Use of Humic/Nonhumic Distribution of Natural Organic Matter for Predicting Bulk Chlorine Decay. Presented at the AWWA Annual Conference.

Lamsal, R., Walsh, M., & Gagnon, G. (2011). Comparison of advanced oxidation processes for the removal of natural organic matter. *Water Research*, *45*(10), 3263–3269.

Levenspiel, O. (1972) *Chemical Reaction Engineering* (2nd ed.). New York, NY: John Wiley & Sons.

Loomis, T. (1970). *Essentials of Toxicology*. Philadelphia, PA: Lea and Febiger.

Mackay, D., Shui, W., & Sutherland, R. (1979). Determination of air-water Henry's law constants for hydrophobic pollutants. *Environmental Science and Technology*, *13*(3), 333–337.

Maier, H. (2003). Ant colony optimization for design of water distribution systems. *Journal of Water Resources Planning and Management*, *129*(3), 200–209.

Matter-Müller, C., Gujer, W., & Giger, W. (1981). Transfer of Volatile Substances from Water to the Atmosphere. *Water Research*, *15*(11), 1271–1279.

McGuire, M., McLain, J., & Obolensky, A. (2002). *Information Collection Rule Data Analysis*. AWWA Research Foundation.

McKone, T., & MacLeod, M. (2003). Tracking multiple pathways of human exposure to persistent multimedia pollutants: regional, continental, and global scale models. *Annual Review of Environmental Resources*, *28*, 463–492.

Myers, A. (1990). Evaluating alternative disinfectants for THM control in small systems. *Journal of the American Water Works Association*, *82*(6), 77–84.

National Research Council. (1993). *Pesticides in the Diets of Infants & Children*. Washington, D.C.: National Academy Press.

OEHHA. (2001). *A Guide to Health Risk Assessment*. California Environmental Protection Agency Office of Environmental Health Hazard Assessment.

Otsfeld, A. et al. (2008). The battle of the water sensor networks (BWSN): A design challenge for engineers and algorithms. *Journal of Water Resources Planning and Management*, *134*(6), 556–568.

Otsfeld, A. et al. (2012). The battle of the water calibration networks. *Journal of Water Resources Planning and Management*, *138*(5), 523–568.

Owen, D., Chowdhury, Z., Summers, R., Hooper, S., & Solarik, G. (1998). *Removal of DBP Precursors by GAC Adsorption*. Denver, CO: AWWA Research Foundation.

Prasha, M., & Lansey, K. (2009). WDS water quality parameter estimation and uncertainty. *Proc. World Environmental and Water Resources Congress*. ASCE. Reston, VA.

Qin, J., Oo, M., Kekre, K., Knops, F., & Miller, P. (2006). Impact of coagulation on enhanced removal of natural organic matter in treatment of reservoir water. *Separation and Purification Technology*, *49*(3), 295–298.

Regli, S., Rose, J., Haas, C., & Gerba, C. (1991). Modeling the Risk From Giardia and Viruses in Drinking Water. *Journal of the American Water Works Association*, *83*(11), 76–84.

Rossman, L. (2000). *EPANET 2 user's manual*. Cincinnati, OH: United States Environmental Protection Agency.

Schneider, O., LeChevallier, M., Yang, J., Hughes, D., & Reed, H. (2015). *Localized Control of Disinfection Byproducts by Spray Stripping in Storage Tanks*. Denver, CO: Water Research Foundation Web Report #4413.

Seidel, C., Ghosh, A., Tang, G., Hubbs, S., Raucher, R., & Crawford-Borwn, D. (2014). *Identifying Meaningful Opportunities for Drinking Water Health Risk Reduction in the United States*. Denver, CO: Water Research Foundation Web Report #4310.

Sexton, K. (2012). Cumulative Risk Assessment: An Overview of Methodological Approaches for Evaluating Combined Health Effects from Exposure to Multiple Environmental Stressors. *Journal of Environmental Research and Public Health*, *9*(2), 370–390.

Sherant, S. (2009). *Trihalomethane Control by Aeration*. Master's Thesis. Pennsylvania State University.

Siddiqui, M., Amy, G., Ryan, J., & Odem, W. (2000). Membranes for the control of natural organic matter from surface waters. *Water Research*, *34*(13), 3355–3370.

Slovic, P. (1991). Beyond numbers: A broader perspective on risk perception and risk communication. In D. Mayoand & R. Hollander, *Acceptable evidence: Science and values in risk management* (pp. 48–65). New York, NY: Oxford University Press.

Smith, A., Hopenhayn-Rich, C., Bates, M., Goeden, H., Hertz-Picciotto, I., Duggan, H., & Smith, M. (1992). Cancer risks from arsenic in drinking water. *Environmental Health Perspectives*, *97*, 259–267.

Snoeyink, V., Kirisits, M., & Pelekani, C. (1999). Adsorption of disinfection byproduct precursors. In *Formation and Control of Disinfection Byproducts in Drinking Water* (pp. 259–284). Denver, CO: American Water Works Association.

Solarik, G., Summers, R., Sohn, J., Swanson, W., Chowdhury, Z., & Amy, G. (2000) Extensions and Verifications of the Water Treatment Plant Model for DBP Formation. *Journal of the American Chemical Society, Natural Organic Matter and Disinfection Byproducts Symposium (March 21 - 25, 1999)*.

Speth, T., & Miltner, R. (1990). Technical note: Adsorption capacity of GAC for synthetic organics. *Journal of the American Water Works Association*, *82*(2), 72–75.

Speth, T., & Miltner, R. (1998). Technical note: Adsorption capacity of GAC for synthetic organics. *Journal of the American Water Works Association*, *90*(4), 171–174.

Staudinger, J., & Roberts, P. (2001). A critical compilation of Henry's law constant temperature dependence relations for organic compounds in dilute aqueous solutions. *Chemosphere*, *44*, 561–576.

Stumm, W., & Morgan, J. (1981). *Aquatic Chemistry: An Introduction Emphasizing Chemical Equilibria in Natural Waters*. New York, NY: John Wiley & Sons.

Tan, L., Amy, G., Rigby, M., Renna, J., & Kemp, K. (1990). Ozonation of colored groundwater pilot-scale and full-scale experiences. *Ozone: Science and Engineering*, *13*(1), 109–125.

Tan, Y., Kilduff, J., Kitis, M., & Karanfil, T. (2005). Dissolved organic matter removal and disinfection byproduct formation control using ion exchange. *Desalination*, *176*(1-3), 189–200.

Tarquin, A., Rico, F., Zammarron, A., & Rittmann, D. (2005). Removal of THMs is Drinking Water Using an Induced Draft Stripping Tower. Proceedings of the AWWA Water Quality Technology Conference.

Teefy, S., & Singer, P. (1990). Performance and Analysis of Tracer Tests to Determine Compliance with the SWTR. *Journal of the American Water Works Association*, *82*(12), 88–98.

Teuschler, L., Rice, G., Wilkes, C., Lipscomb, J., & Power, F. (2004). A feasibility study of cumulative risk assessment methods for drinking water disinfection byproduct mixtures. *Journal of Toxicology and Environmental Health Part A*, *67*, 755–777.

Tseng, T., Edwards, M., & Chowdhury, Z. (1996). American Water Works Association National Enhanced Coagulation and Softening Database.

Uber, J., Murray, R., & Janke, R. (2004). Use of Systems Analysis to Assess and Minimize Water Security Risks. *Journal of Contemporary Water Research and Education*, (129), 34–40.

U.S. Environmental Protection Agency. (1987). *Reference Dose (RfD): Description and Use in Health Risk Assessments. Integrated Risk Information System (IRIS): Appendix A* (No. EPA/600/8-66/032a). Washington, D.C.: USEPA Office of Health and Environmental Assessment.

U.S. Environmental Protection Agency. (1997). *Memorandum - Cumulative Risk Assessment Guidance - Phase I Planning and Scoping*. Washington, D.C.: USEPA.

U.S. Environmental Protection Agency. (1999). *Enhanced Coagulation and Enhanced Precipitative Softening Guidance Manual* (No. EPA 815-R-99-012). Cincinnati, OH: USEPA Office of Water.

U.S. Environmental Protection Agency. (2000). *Arsenic in Drinking Water Rule Economic Analysis* (No. EPA 815-R-00-026). Washington, D.C.: USEPA Office of Ground Water and Drinking Water.

U.S. Environmental Protection Agency. (2000b). *Supplementary Guidance for Conducting Health Risk Assessment of Chemical Mixtures* (No. EPA/630/R-00/002). USEPA Risk Assessment Forum Technical Panel.

U.S. Environmental Protection Agency. (2005a). *Guidelines for Carcinogen Risk Assessment* (No. EPA/630/P-03/001F). Washington, D.C.: USEPA Risk Assessment Forum.

U.S. Environmental Protection Agency. (2005b). National Primary Drinking Water Regulations: Stage 2 Disinfectants and Disinfection Byproducts Rule. *Fed Reg.*, 68:159:49.

U.S. Environmental Protection Agency. (2010). *A New Approach to Protecting Drinking Water and Public Health* (No. EPA 815F10001). Washington, D.C.: USEPA Office of Water.

U.S. Environmental Protection Agency. (2011). *Age Dependent Adjustment Factor (ADAF) Application*. Washington, D.C.: USEPA Office of Water Policy.

Wallace, J., Vahadi, B., Fernandes, J., & Boyden, B. (1988). The combination of ozone/hydrogen peroxide and ozone/UV radiation for reduction of trihalomethane formation potential in surface water. *Ozone: Science & Engineering*, *10*(1), 103–112.

Waller, K., Swan, S., DeLorenze, G., & Hopkins, B. (1998). Trihalomethanes in drinking water and spontaneous abortion. *Epidemiology*, *9*(2), 134–140.

Walski, T. (2001). The wrong paradigm- Why water distribution optimization doesn't work. *Journal of Water Resources Planning and Management*, *127*(4), 203–225.

Walski, T., Brill, E., Gessler, J., Goulter, I., Jeppson, R., Lansey, K., Ormsbee, L. (1987). Battle of the network models: Epilogue. *Journal of Water Resources Planning and Management, 113(2),*191–203.

Ward, M., Mark, S., Cantor, K., Weisenburger, D., Correa-Villaseñor, A., & Zahm, S. (1996). Drinking Water Nitrate and the Risk of Non-Hodgkin's Lymphoma. *Epidemiology*, *7*(5), 465–471.

Watson, J.-P., Hart, W., Woodruff, D., & Murray, R. (2010). Formulating and analyzing multi-stage sensor placement problems. *Proc. Water Distribution System Analysis*. ASCE. Reston, VA.

Williams, P., Dotson, G., & Maier, A. (2012). Cumulative Risk Assessment (CRA): Transforming the Way We Assess Health Risks. *Environmental Science and Technology*, *46*, 10868–10874.

World Health Organization. (2008). *The global burden of disease: 2004 update*. Geneva.

Zhou, H., & Smith, D. (2002). Advanced Technologies in Water and Wastewater Treatment. *Journal of Environmental Engineering and Science*, *1*(4), 247–264.

Zwerneman, J. (2012). *Investigating the Effect of System Pressure on Trihalomethane Post Treatment Diffused Aeration*. Master's Thesis. University of New Hampshire.

Appendices

Appendix A: Treatment Technology Modeling Methods

Appendix A.1: Chemical Addition pH Adjustment Methods

Several treatment processes modeled as part of this study used aluminum sulfate (alum), free chlorine, sulfuric acid, or caustic soda additions. Changes in pH induced by chemical additions were modeled with methods similar to those used in the USEPA Water Treatment Plant (WTP) Model as outlined in the WTP Model Version 2.0 User's Manual by the Center for Drinking Water Optimization (CDWO) at the University of Colorado at Boulder (CDWO, 2001). pH was based on equilibrium conditions and was assumed to change immediately after chemical addition. Kinetics of dissolution processes were not taken into account when making pH adjustments. Water hardness considerations and the associated precipitation of calcium carbonate and magnesium carbonate were not included as part of the pH adjustment methodology.

The concentration of hydrogen ions in solution prior to chemical addition was determined from the initial pH:

$$[H^+]_o = 10^{(-pH_o)} \quad \text{(A.1.1)}$$

The concentration of hydroxide ions in solution prior to chemical addition was calculated as follows:

$$[OH^-]_o = \frac{K_w}{[H^+]_o} \quad \text{(A.1.2)}$$

In equation A.1.2 K_w is the water ionization constant which was assumed to be dependent on temperature and was calculated as follows (Stumm and Morgan, 1981):

$$K_w = 10^{(-\frac{4470.99}{T}+6.0875-0.01706T)} \quad \text{(A.1.3)}$$

Where T is the temperature in Kelvin. The total concentration of carbonate in solution was defined as:

$$C_{T,CO_3} = [H_2CO_3] + [HCO_3^-] + [CO_2^{2-}] \quad \text{(A.1.4)}$$

In the equation above, $[H_2CO_3]$ is the concentration of dissolved carbon dioxide (carbonic acid) in solution (moles/L), $[HCO_3^-]$ is the concentration of the bicarbonate ion (moles/L), and $[CO_3^{2-}]$ is the concentration of the carbonate ion (moles/L). Carbonic acid speciation was determined using the following expressions:

$$[HCO_3^-] = \alpha_1 C_{T,CO_3} \quad \text{(A.1.5)}$$

$$[CO_2^{2-}] = \alpha_2 C_{T,CO_3} \quad \text{(A.1.6)}$$

Where α_1 and α_2 are the dissociation percentages of bicarbonate and carbonate respectively. These parameters were calculated as:

$$\alpha_1 = \frac{K_1[H^+]}{[H^+]^2+K_1[H^+]+K_1K_2} \quad \text{(A.1.7)}$$

$$\alpha_2 = \frac{K_1 K_2}{[H^+]^2 + K_1[H^+] + K_1 K_2} \quad \text{(A.1.8)}$$

Where K_1 and K_2 are the acid dissociation constants of carbonic acid and the bicarbonate ion respectively. It was assumed that K_1 and K_2 are temperature dependent (Stumm and Morgan, 1981) and were adjusted using relative to their respective standard values at 25 °C and an ionic strength of zero:

$$K_1 = \exp\left\{\left[\left(\frac{7700\frac{J}{mole}}{8.314\frac{J}{^\circ K * mole}}\right)\left(\frac{1}{298.15\ ^\circ K} - \frac{1}{T}\right)\right] - 14.5\right\} \quad \text{(A.1.9)}$$

$$K_2 = \exp\left\{\left[\left(\frac{14900\frac{J}{mole}}{8.314\frac{J}{^\circ K * mole}}\right)\left(\frac{1}{298.15\ ^\circ K} - \frac{1}{T}\right)\right] - 23.7\right\} \quad \text{(A.1.10)}$$

In the equations above, 7700 (J/mole) and 14900 (J/mole) represent the standard enthalpy changes for carbonic acid and the bicarbonate ions respectively, 8.314 (J/Kelvin-mole) is the ideal gas constant, 298.15 (°K) is the standard temperature, T is the system temperature (°K), and 14.5 and 23.7 are the natural logs of K_1° and K_2° at the standard temperature of 298.15 °K.

Alkalinity was defined by the following expression (Stumm and Morgan, 1981):

$$Alkalinity = [HCO_3^-] + 2[CO_2^{2-}] + [OH^-] - [H^+] \quad \text{(A.1.11)}$$

Substituting the expressions for bicarbonate and carbonate and hydroxide into equation A.1.11 yields the following:

$$Alkalinity = (\alpha_1 + 2 * \alpha_2) * \ C_{T,CO_3} + [OH^-] - [H^+] \quad \text{(A.1.12)}$$

All pH calculations were based on a closed system assumption. The concentration of carbonate in solution was calculated by rearranging equation A.1.12:

$$C_{T,CO_3} = (Alk_0 + [H^+]_o - [OH^-]_o)/(\alpha_{1,o} + 2 * \alpha_{2,0}) \quad \text{(A.1.13)}$$

Where Alk_0 is the initial alkalinity and $[H^+]_o$, $[OH^-]_o$, $\alpha_{1,o}$ and $\alpha_{2,o}$ were based on conditions prior to any chemical additions. Alkalinity was also defined to maintain electroneutrality as:

$$Alkalinity = C_B - C_A \quad \text{(A.1.14)}$$

Where C_B is the concentration of all positively charge ions excluding hydrogen (eq/L), and C_A is the concentration of all negatively charged ions excluding hydroxide, bicarbonate, and carbonate (eq/L). Equations A.1.13 can also be written as:

$$Alkalinity = C_{B'} + 2[Ca^{2+}] + [CaOH^+] + 2[Mg^{2+}] + [MgOH^+] + [NH_4^+] - C_{A'} - [OCl^-] \quad \text{(A.1.15)}$$

Where parameters $C_{B'}$, and $C_{A'}$ are defined as:

$$C_{B'} = [HCO_3^-] + 2[CO_3^{2-}] + [OH^-] \quad \text{(A.1.16)}$$

$$C_{A'} = [H^+] \quad \text{(A.1.17)}$$

Because water hardness was not taken into account for this study and none of the chemicals used were associated with calcium, magnesium or ammonia addition, equation A.1.14 was simplified to:

$$Alkalinity = C_{B\prime} - C_{A\prime} - [OCl^-] \quad \text{(A.1.18)}$$

In the equation above, *[OCl^-]* is the concentration of hypochlorite in solution. This parameter was calculated as:

$$[OCl^-] = \frac{C_{T,OCl}}{1+\frac{[H^+]}{K_{HOCl\_OCl^-}}} \quad \text{(A.1.19)}$$

Where $C_{T,OCl}$ is the total concentration of hypochlorite in solution (moles/L), and $K_{HOCl\_OCl^-}$ is the dissociation constant of hypochlorus acid. $K_{HOCl\_OCl^-}$ was assumed to be dependent on temperature and was calculated as follows:

$$K_{HOCl\_OCl^-} = exp\left\{\left[\left(\frac{13800\frac{J}{mol}}{8.314\frac{J}{°K*mol}}\right)\left(\frac{1}{298.15\ °K} - \frac{1}{T}\right)\right] - 17.5\right\} \quad \text{(A.1.20)}$$

Substituting the equilibrium expression for the hypochlorite ion into equation A.1.17 gives the following:

$$Alkalinity = C_{B\prime} - C_{A\prime} - \frac{C_{T,OCl}}{1+\frac{[H^+]}{K_{HOCl\_OCl^-}}} \quad \text{(A.1.21)}$$

Chemical additions were assumed to impact alkalinity on a stoichiometric basis with each mole of alum added reducing alkalinity by 6 (eq/L), each mole of free chlorine added reducing alkalinity by 1 (eq/L), each mole of sulfuric acid added reducing alkalinity by 2 (eq/L), and each mole of caustic soda added increasing alkalinity by 1 (eq/L). Using the alkalinity adjustments for chemical additions, equation A.1.21 becomes:

$$Alkalinity = C_{B'} - C_{A'} - \frac{C_{T,OCl}}{1+\frac{[H^+]}{K_{HOCl_{OCl^-}}}} - 6 * [alum] - [free\ chloine] - 2 * [sulfuric\ acid] + [caustic\ soda]$$

(A.1.22)

Where *[alum]*, *[free chlorine]*, *[sulfuric acid]*, and *[caustic soda]* are the cumulative concentrations of each chemical added at a given point (moles/L). This includes all additions made during previous treatment processes. The final pH after chemical addition was determined by setting the alkalinity expressions in equation A.1.12 and equation A.1.22 equal to each other and iteratively solving for $[H^+]$. A schematic for the overall process is shown in Figure A-1.

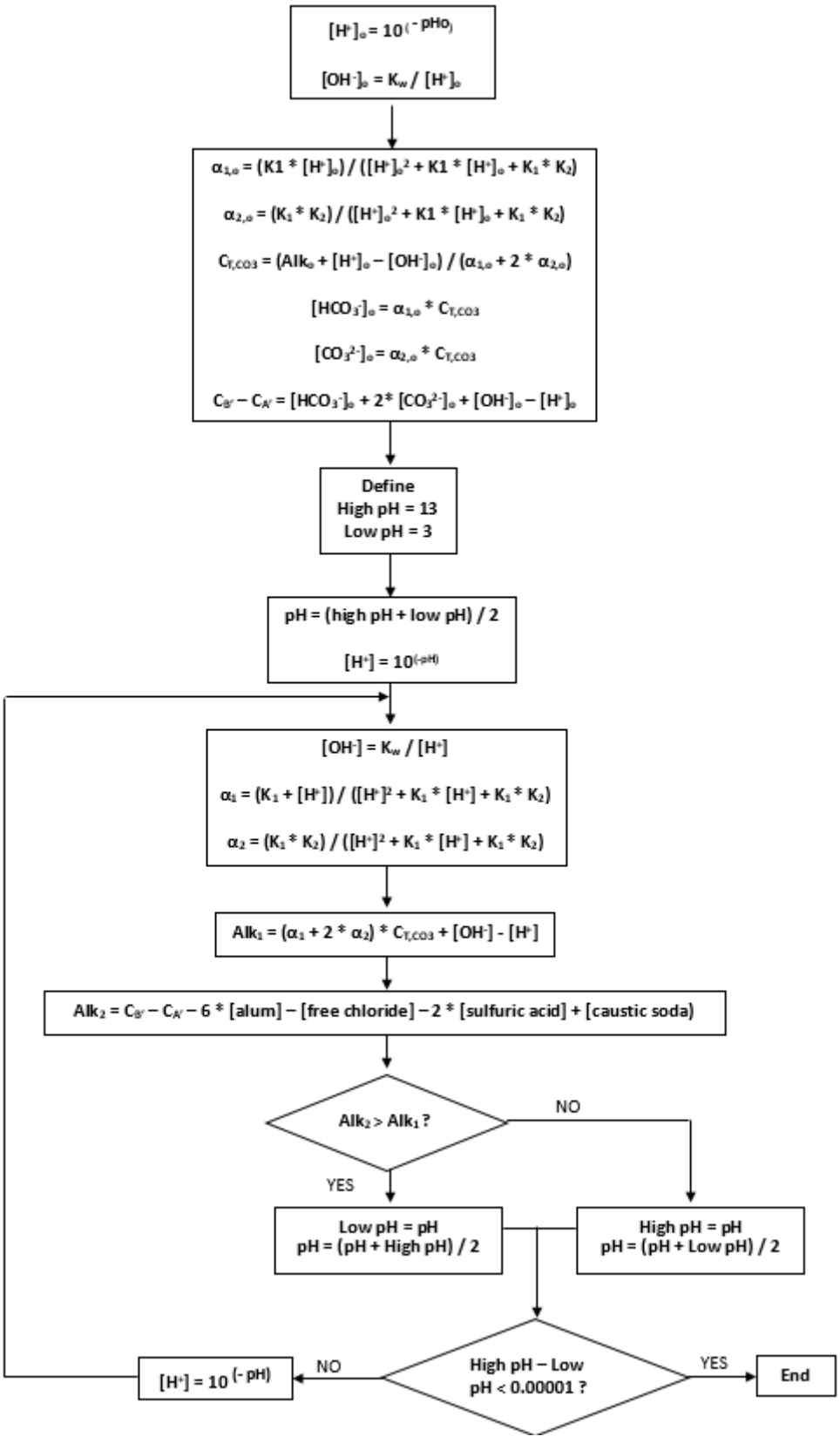

Figure A-1: Iterative process used for calculating pH changes from chemical addition.

Appendix A.2: Baseline Treatment Approach Modeling Methods

The baseline treatment approach for this study was modeled as a conventional filtration plant with a treatment train of: 1) coagulant (alum) addition, 2) rapid mix, 3) flocculation, 4) sedimentation, 5) free chlorine addition, 6) anthracite over sand filtration, 7) contact tank disinfection, 8) pH adjustment, and 9) distribution. All model equations came from the WTP Model Version 2.0 User's Manual (CDWO, 2001; Solarik et al., 2000). The assumed filter and contact tank hydraulic parameters used for this study are shown in Table A-1. Because chlorine addition was modeled before filtration, the hydraulic parameters for the rapid mix, flocculation, and sedimentation basins were not relevant.

Table A-1: Filter and contact tank hydraulic parameters.

Unit Process	Basin Volume (gallons)	Basin T_{10}/Detention Time Ratio	Basin T_{50}/Detention Time Ratio
Filter	15000	0.5	1
Contact Tank	45000	0.5	1

The alum dose applied to the raw source water was optimized to achieve the required TOC removals for enhanced coagulation (USEPA, 1999). This was determined by initially assuming an applied alum dose of 2 mg/L for which pH was adjusted using the methodology described in Appendix A.1. Consistent with the WTP Model approach TOC removal by coagulation was calculated based on methods proposed by Edwards (1997). Although these model equations were originally developed for dissolved organic carbon (DOC) and the DOC-based specific ultraviolet absorbance (SUVA), TOC and (T)SUVA were assumed to be acceptable substitutes. The fraction of non-sorbable TOC which cannot be removed by coagulation was calculated as:

$$Fraction\ nonsorbable\ TOC = K_1 * ((T)SUVA)_{raw} + K_2 \quad \text{(A.2.1)}$$

Where, $((T)SUVA)_{raw}$ is the (T)SUVA value prior to coagulant addition (L/mg-m), and K_1 and K_2 are empirical fitting constants. Using the "General Al Specific" best-fit predictive model from Edwards (1997), coefficients K_1, and K_2 were given values of -0.075 and 0.56, respectively. The sorbable TOC concentration was calculated as:

$$Sorbable\ TOC\ \left({}^{mg}/_{L}\right) = (1 - fraction\ of\ nonsorbable\ TOC) * TOC_{raw}\ \left({}^{mg}/_{L}\right) \quad \text{(A.2.2)}$$

A Langmuir isotherm was used to model the sorptive equilibrium between aluminum hydroxide surface and sorbable TOC:

$$\frac{x}{M} = \frac{ab[C]_{eq}}{1+b[C]_{eq}} \quad \text{(A.2.3)}$$

Where x is the concentration of TOC removed (mg/L), M is the concentration of Al^{3+} and metal hydroxide formed (mmoles/L), a is the maximum TOC sorption per mM of alum (mg TOC/mM Al^{3+}), b is the sorption constant for sorbable TOC to hydroxide surface (L/mg TOC), and $[C]_{eq}$ is the sorbable concentration of TOC in solution at equilibrium (mg/L). a was approximated as a function of pH:

$$a = x_3 pH^3 + x_2 pH^2 + x_1 pH \quad \text{(A.2.4)}$$

Where x_1, x_2, and x_3 are fitting constants. Using the "General Al Specific" best-fit predictive model from Edwards (1997), coefficients, b, x_1, x_2, and x_3 from equations A.2.3 and A.2.4 above

were given values of 0.147, 284, -74.2, and 4.91, respectively. For simplicity, a constant *z* was established:

$$z = ((1 - (T)SUVA_{raw} * K_1 - K_2) * TOC\ (^{mg}/_{L})) \quad \text{(A.2.5)}$$

Substituting *a*, *b*, and *z* into the Langmuir equation, C_{eq} was determined as:

$$C_{eq}\ (^{mg}/_{L}) = \frac{\sqrt{b^2*[z-a*M]^2+2*b*[z+a*M]+1}+b*[z-a*M]-1}{2*b} \quad \text{(A.2.6)}$$

The concentration of TOC remaining after coagulation was calculated as follows:

$$TOC\ (^{mg}/_{L}) = C_{eq}\ (^{mg}/_{L}) + nonsorbable\ TOC\ (^{mg}/_{L}) \quad \text{(A.2.7)}$$

If the TOC removal achieved was not sufficient comply with enhanced coagulation requirements based on the source water TOC and alkalinity (USEPA, 1999), the alum dose was increased by 2 mg/L and this process was repeated until this condition was met.

UVA removal by coagulation was predicted by the WTP Model equation derived from the American Water Works Association (AWWA) Water Industry Technical Action Fund (WITAF) database (Tseng et al., 1996):

$$UVA_{removed} = 5.716(UVA_{raw})^{1.0894}(Dose_{coagulant})^{0.306}(pH)^{-0.9513} \quad \text{(A.2.8)}$$

Where UVA_{raw} is the UVA prior to coagulant addition (cm^{-1}), $Dose_{coagulant}$ is the concentration of Al^{3+} added (meq/L), and *pH* is the pH adjusted for alum addition.

The applied chlorine dose was optimized to maintain a residual free chlorine concentration greater than 0.2 mg/L throughout the entire distribution system. This approach was based on the assumption that primary disinfection requirements were being met and secondary disinfection was the primary driver for chlorine dose determination. For chlorine decay calculations, the filter and contact tank were both modeled as a certain number of equally sized continuous flow stirred tank reactors (CFSTRs) in series based on the ratio of basin T_{10}/T_{50} as determined by dividing each basin's T_{10}/Detention Time ratio by its T_{50}/Detention Time ratio. Details about this modeling approach can be found elsewhere (Denbigh & Turner, 1971; Harrington, et al., 1992; Levenspiel, 1972; Teefy and Singer, 1990). Both basins had T_{10}/T_{50} ratios of 0.5 resulting in each being modeled as 5 CFSTRs in series. The distribution system was assumed to follow plug flow reactor (PFR) behavior which was approximated as 25 CFSTRs in series.

The filter effluent chlorine concentration was calculated using a Monod-type kinetic reaction (Dugan et al., 1995; Isabel et al., 2000; Koechling et al., 1998) for coagulated waters:

$$C_t = \{-0.8404(C_o)\} * \ln\left(\frac{C_o}{C_t}\right) + \left\{-0.404\ \left(\frac{C_o}{UVA}\right)^{-0.9108}\right\} * TOC * time + C_o \qquad \text{(A.2.9)}$$

Where C_o is chlorine dose at the influent of a given modeled CFSTR (mg/L), *UVA* is the UV absorbance prior to chlorine addition (cm^{-1}), *TOC* is the total organic carbon concentration at the point of chlorination (mg/L), *time* is the CFSTR detention time (hours), and C_t is the

concentration of chlorine at the effluent of the CFSTR (mg/L). C_t was iteratively calculated for each filter CFSTR. The C_t calculated for a given CFSTR was used as C_o for the next modeled CFSTR in series.

Chlorine decay in the contact tank was modeled using the same process described above with the effluent chlorine concentration for the last filter CFSTR serving as the influent concentration for the first contact tank CFSTR. Similarly, chlorine decay was modeled at 12 hour residence time intervals throughout the distribution system using the same process. At each time step, the distribution system from the treatment plant effluent to the point of interest was modeled as 25 CFSTRs in series to approximate PFR behavior. The residence time of each of the modeled CFSTRs increased for each time step based 12 hour increase in total residence time. The effluent chlorine concentration for the last contact tank CFSTR (C_t) was assumed to be the influent concentration to first the distribution system CFSTR (C_o). For this study, the distribution system was assumed to have a maximum residence time of 10 days (240 hours).

To determine the optimal chlorine dose, an initial dose of 0.3 mg/L was applied. Consistent with WTP Model algorithms, the adjusted dose used in the chlorine decay and DBP formation equations was calculated to account for instantaneous chlorine demand:

$$[Cl]_{adjusted} = [Cl]_{applied} \left({}^{mg}/_{L}\right) - 0.1 \left({}^{mg}/_{L}\right) \quad \text{(A.2.10)}$$

Using the adjusted chlorine dose, chlorine decay was modeled through the filter, contact tank, and distribution system as described by the process above. If the predicted final chlorine

concentration at the end of the distribution system was not greater than or equal to 0.2 mg/L the applied chlorine dose was increased by 0.1 mg/L and the process was repeated until this condition was met.

The pH was adjusted based on the resulting applied chlorine dose using the methodology described in Appendix A.1 and was assumed to be maintained through the filter and contact tank. Prior to distribution, a caustic soda dose of 2 mg/L was applied and the pH was adjusted accordingly using the methods described in Appendix A.1. If the resulting pH was not greater than or equal to 8, the applied caustic dose was increased by 2 mg/L and the process was repeated until this condition was met.

The filter, contact tank and every 12 hours of distribution system residence time were considered as separate unit processes for DBP formation modeling as shown in Table A-2.

Table A-2: Unit processes used for DBP formation modeling.

Unit Process	Residence Time (hours)
Treatment Plant Filter	0.15
Treatment Plant Contact Tank	0.45
Distribution System Hour $\{X_n\}$ to Hour $\{X_{n+1}\}$ • $X_{n+1} = X_n + 12$ • $n = 0 : 20$ • $X_0 = 0$	12

The concentration of total trihalomethanes (TTHM) formed in each unit process was calculated using the WTP Model equation for coagulated and treated waters which is based on the work of Amy et al. (1998):

$$TTHM\ (^{\mu g}/_{L}) = 23.9(TOC * UVA)^{0.403}(Cl_2)^{0.225}(Br^-)^{0.141}(1.1560)^{(pH-7.5)}(1.0263)^{(Temp-20)}(time)^{0.264} \quad \text{(A.2.11)}$$

In the equation above *TOC* is the total organic carbon concentration at the point of chlorination (mg/L), *UVA* is the UV abosorbance prior to chlorine addition (cm^{-1}), Cl_2 is the applied chlorine dose adjusted for instantaneous demand as determined by equation A.2.10 (mg/L), Br^- is the bromide concentration at the influent of the unit process of interest (µg/L), *pH* is the pH adjusted for all chemical additions prior to the point of interest, *Temp* is the source water temperature (°C), and *time* is the unit process residence time (hours). Individual trihalomethane (THM) species formations in each were calculated using a similar empirical relationship:

$$THM\ (^{\mu g}/_{L}) = A(TOC * UVA)^{a}(Cl_2)^{b}(Br^-)^{c}(D)^{(pH-7.5)}(E)^{(Temp-20)}(time)^{f} \quad \text{(A.2.12)}$$

Where *A, a, b, c, D, E,* and *f* are the species specific coefficients shown in Table A-3.

Table A-3: THM species coefficients used in equation A.2.12 (CDWO, 2001).

THM Species	A	a	b	c	D	E	f
$CHCl_3$	266	0.403	0.424	-0.679	1.1322	1.0179	0.333
$CHCl_2Br$	1.68	0.206	0.114	0.462	1.0977	1.0260	0.196
$CHBr_2Cl$	8.0×10^{-3}	-0.056	-0.157	1.425	1.1271	1.0212	0.148
$CHBr_3$	4.4×10^{-5}	-0.300	-0.221	2.134	1.3907	1.0374	0.143

The bulk formation of six haloacetic acid species of interest (HAA6) in each unit process was calculated with an equation similar to that of TTHM:

$$HAA6\ (^{\mu g}/_{L}) = 30.7(TOC * UVA)^{0.302}(Cl_2)^{0.541}(Br^-)^{-0.012}(0.932)^{(pH-7.5)}(1.022)^{(Temp-20)}(time)^{0.150} \quad \text{(A.2.13)}$$

Individual halo acetic acid (HAA) species formations in each unit process were calculated as:

$$HAA = A(TOC * UVA)^a(Cl_2)^b(Br^-)^c(D)^{(pH-7.5)}(E)^{(Temp-20)}(time)^f \quad \text{(A.2.14)}$$

The HAA species coefficients used in the equation above are shown in Table A-4.

Table A-4: HAA species coefficients used in equations A.2.14 (CDWO, 2001).

HAA Species	A	a	b	c	D	E	f
MCAA	4.58	-0.090	0.662	-0.224	1.042	1.024	0.043
DCAA	60.4	0.397	0.665	-0.558	1.034	1.017	0.222
TCAA	52.6	0.403	0.749	-0.416	0.8739	1.014	0.163
MBAA	2.06×10^{-2}	0.358	-0.101	0.812	0.6526	1.162	0.043
DBAA	9.42×10^{-5}	0.0590	0.182	2.109	1.210	1.007	0.070
BCAA	3.23×10^{-1}	0.153	0.257	0.586	1.181	1.042	0.201

In order to accurately account for bromide incorporation, the concentrations of three additional HAA species formed in each unit process were estimated. Combined with the HAA6 species, these are collectively grouped as HAA9. These concentration were calculated as follows:

$$HAA\ (^{\mu g}/_{L}) = A(TOC * UVA)^a(Cl_2)^b(Br^-)^c(D)^{(pH-8.0)}(E)^{(Temp-20)}(time)^f \quad \text{(A.2.15)}$$

Coefficients used in the equation above for the three additional HAA species as well as bulk HAA9 are shown in Table A-5.

Table A-5: Coefficients used in equation A.2.14 for HAAs and bulk HAA9 (CDWO, 2001).

HAAs	A	a	b	c	D	E	f
CDBAA	3.70×10^{-3}	-0.0162	-0.170	0.972	0.839	1.054	0.685
DCBAA	5.89×10^{-1}	0.230	0.140	0.301	0.700	1.022	0.422
TBAA	5.59×10^{-6}	0.0657	-2.51	2.32	0.555	1.059	1.26
HAA9	10.78	0.25	0.50	0.054	0.894	1.015	0.348

The predicted concentrations of DBPs formed in each unit process were adjusted using WTP Model correction factors:

$$DBP_{corrected}(^{\mu g}/_{L}) = \frac{DBP_{predicted}\,(^{\mu g}/_{L})}{Correction\ Factor} \quad \text{(A.2.16)}$$

The correction factors used for in-plant and distribution system unit processes vary slightly as outlined in Table A-6.

Table A-6: In-plant DBP correction factors used in equation A.2.16.

DBPs	In-Plant Correction Factor	Distribution System Correction Factor
THMs		
$CHCl_3$	1.00	1.10
$CHCl_2Br$	0.92	1.00
$CHBr_2Cl$	0.65	0.46
$CHBr_3$	1.00	1.00
TTHM	1.00	1.00
HAAs		
MCAA	1.00	1.00
DCAA	0.72	1.10
TCAA	1.30	1.30
MBAA	1.00	1.00
DBAA	1.00	1.00
BCAA	0.86	2.00
HAA6	1.10	1.10
HAA9	1.00	1.00

Individual THM species concentrations formed in each unit process were adjusted to remain equivalent to the predicted bulk TTHM concentration formed using proportionality:

$$THM_{n,cadjusted} = \left[\frac{THM_{n,corrected}}{\sum_{i=1}^{4} THM_{i,corrected}}\right] * TTHM_{corrected} \quad \text{(A.2.17)}$$

Where $THM_{n,corrected}$ is the predicted concentration of a single THM specie formed in a given unit process after being corrected with equation A.2.16. The dominator which this is normalized by is the sum of all four corrected THM species formations. *TTHM* is the corrected total trihalomethane concentration formed in the unit process of interest. Individual HAA6 species were adjusted in a similar manner:

$$HAA_{n,adjusted} = \left[\frac{HAA_{n,corrected}}{\sum_{i=1}^{6} HAA_{i},corrected}\right] * HAA6_{corrected} \quad \text{(A.2.18)}$$

The three additional HAA9 species were similarly adjusted to be equivalent to the difference between the corrected bulk HAA9 and HAA6 concentrations:

$$HAA_{n,adjusted} = \left[\frac{HAA_{n,corrected}}{\sum_{i=1}^{3} HAA_{i,corrected}}\right] * (HAA9_{corrected} - HAA6_{corrected}) \quad \text{(A.2.19)}$$

Because only five of the nine HAA species are regulated, a regulatory concentration of haloacetic acid (HAA5) formed in each unit process was calculated by subtracting one unregulated species (BCAA) from the bulk HAA6 concentration:

$$HAA5(^{\mu g}/_{L}) = HAA6_{corrected}(^{\mu g}/_{L}) - BCAA_{adjusted}(^{\mu g}/_{L}) \quad \text{(A.2.20)}$$

The predicted concentrations of individual and bulk DBP species at the effluent of a given unit process were calculated by adding the associated influent concentrations to the predicted concentrations formed within the process as determined by equations A.2.11 – A.2.20. The effluent DBP concentrations for one unit process were used as the influent concentrations for the next unit process in sequence.

The free bromide concentration at the effluent of each unit process was calculated based on stoichiometric DBP incorporation:

$$Br^-_{eff} = Br^-_{inf} - [CHCl_2Br + MBAA + BDCAA + BCAA + 2 * (CHBr_2Cl + DBAA + DBCAA) + 3 * (CHBr_3 + TBAA)] \quad \text{(A.2.21)}$$

Where Br^-_{inf} is the bromide concentration at the influent of a given unit process (moles/L). The total concentration of bromide incorporated into DBPs species on a stoichiometric basis (moles/L) is subtracted from this influent concentration. The bromide concentration at the effluent of a given unit process was assumed to be the influent concentration for the next unit process in sequence and applied accordingly in equations A.2.11 – A.2.15.

The relative cancer and non-cancer health risks of the TTHM and HAA5 species were quantified using the Relative Health Indicator (RHI) as developed by Seidel et al. (2014). A cancer RHI and a non-cancer RHI value were calculated for individual DBP species at the effluent of each unit process. The cancer RHI values were calculated as follows:

$$Cancer\ RHI = Cancer\ Toxicity * Cancer\ Severity * Exposure \quad \text{(A.2.22)}$$

In the equation above, *Cancer Toxicity* is a contaminant-specific toxicity measure of cancer health outcomes (see equation A.2.23 below), *Cancer Severity* is a relative measure of the negative health impacts of cancer health outcomes, and *Exposure* is the concentration of a given contaminant in drinking water (mg/L). Consistent with the methods proposed by Seidel et al., the *Cancer Severity* parameter was assigned a value of 0.29 for all cancer RHI calculations. *Exposure* was assumed to be the predicted concentration of a given DBP species at the unit process of interest. *Cancer Toxicity* values for individual DBP species were calculated as follows:

$$Cancer\ Toxicity = \frac{CSF * 2(\frac{L}{d})}{70\ (kg)} \quad \text{(A.2.23)}$$

Where *CSF* is the cancer slope factor for the contaminant of interest, 2 (L/d) represents human daily consumption of water, and 70 (kg) is the standard default body weight used for risk calculations.

The non-cancer RHI values for each species were calculated in a similar manner to the cancer RHI values:

$$NonCancer\ RHI = NonCancer\ Toxcity * NonCancer\ Severity * Exposure \quad \text{(A.2.24)}$$

Where *NonCancer Toxicity* is a contaminant-specific toxicity measure of non-cancer health outcomes (see equation A.2.25 below), *NonCancer Severity* is a relative measure of the negative health impacts of non-cancer health outcomes, and *Exposure* is the concentration of a given contaminant in drinking water (mg/L). *Non-cancer* Severity values came from those used by Seidel et al. which were derived from disability adjusted life years (DALYs) developed by the World Health Organization (WHO) in the Global Burden of Disease Report (WHO, 2008) by "mapping" critical effects from the USEPA Integrated Risk Information System (IRIS) database to specific diseases identified in the WHO weightings with the underlying assumption that a critical effect is prognostic of a certain disease. *Exposure* was assumed to be the predicted effluent concentration of a given DBP species at the unit process of interest. *NonCancer Toxicity* values for individual DBP species were calculated as follows:

$$NonCancer\ Toxicity = \frac{0.01 * 2(\frac{L}{d})}{70(kg) * RfD * UFc} \quad \text{(A.2.25)}$$

In the equation above, 0.01 represents a 1% population incidence rate derived from Dourson et al. (1996), 2(L/d) represents human daily consumption of water, 70 (kg) is the standard default body weight used for risk calculations, *RfD* is the oral reference dose for a given contaminant, and *UFc* is the uncertainty factor used for reference dose derivation.

RHI values for individual species were calculated as the sum of the associated cancer RHI and non-cancer RHI values:

$$Constituent\ RHI = Cancer\ RHI + NonCancer\ RHI \quad \text{(A.2.26)}$$

RHI values were quantified for 6 DBP species at each the effluent of each unit process including all four trihalomethanes and two haloacetic acids (dichloroaceticacid, trichloroaceticacid). Cancer slope factors and reference doses have not been defined for the other three regulated haloacetic acid species (monochloroacetic acid, bromoacetic acid, dibromoacetic acid), thus, no cancer or non-cancer RHI contributions were quantified for those constituents. A summary of the reference doses, uncertainty factors, non-cancer and cancer severity scores, and cancer slope factors used for each of the DBP species of interest is shown in

Table A-7.

Table A-7: DBP species specific parameters for RHI calculations (Seidel et al., 2014).

Contaminant	RfD (mg/kg/day)	UFc	Non-Cancer Severity	Cancer Slope Factor	Cancer Severity
Trihalomethanes					
Chloroform	1.00E-02	10	0.1		
Bromodichloromethane	0.02	1000	0.01	0.062	0.29
Dibromochlomethane	0.02	1000	0.01	0.084	0.29
Bromoform	2.00E-02	100	0.2	0.0079	0.29
Haloacetic Acids					
Dichloroacetic acid	4.00E-03	300	0.2	0.05	0.29
Trichloroacetic acid	0.02	100	0.2	0.07	0.29

The RHI values for individual DBP species were added to produce a cumulative RHI value at the effluent of each unit process. The resulting total RHI estimates throughout the entire distribution system were for population weighted risk quantification as described in Appendix A.9.

Appendix A.3: Optimized Coagulation Modeling Methods

Optimized coagulation was modeled using the same conventional treatment approach as the baseline scenario described in Appendix A.2 with additional pH adjustments incorporated prior to the coagulation and chlorination steps. A sulfuric acid addition was included at the head of the plant prior to alum addition to lower to the pH to roughly 6. The pH change induced by an initial dose of 5 mg/L was tested using the methodology described in Appendix A.1. If the resulting pH was greater than 6, the dose was increased 5 mg/L until this condition was no longer met. In order to keep the pH above 6, a dose 5 mg/L less than the one which dropped the pH below 6 was applied for modeling purposes. TOC and UVA removal by alum coagulation were modeled using the methods described by equations A.2.1 through A.2.8. A neutralizing caustic soda dose equal to twice the molar concentration of the sulfuric acid addition was applied prior to chlorine addition. The remainder of the treatment plant and distribution system were modeled using the same methods as the baseline treatment scenario with the applied chlorine dose optimized to maintain a chlorine residual greater than 0.2 mg/L at the end of the distribution system, a caustic soda addition to raise the pH above 8 after the contact tank, and DBP formation calculated in the filter, contact tank and every 12 hours of distribution system residence time.

Using the modeling framework described above, the applied alum dose was iteratively optimized to ensure that TTHM and HAA5 concentrations were below their respective regulatory MCLs of 80 µg/L and 60 µg/L at the end of the distribution system.

RHI values for the resulting DBP species concentrations at the effluent of each unit process were calculated using equations A.2.22 through A.2.26. The cumulative RHI values for individual

DBP species were added to produce a total RHI value at the effluent of each unit process. The resulting total RHI estimates throughout the entire distribution system were for population weighted risk quantification as described in Appendix A.9.

Appendix A.4: Distribution System Spray Aeration Modeling Methods

Spray aeration was modeled as a treatment strategy for THM removal within the distribution system. The treatment plant specifications were assumed to be identical those in the baseline approach as described in Appendix A.2. Thus, the baseline the DBP formation curves were applicable for this modeling approach.

Spray aeration units were modeled at specific points within the distribution system so TTHM concentrations stayed below their regulatory concentrations at all residence times. The first aeration unit was applied one time step (12 hours) before the first point at which the baseline TTHM formation curve exceeded its regulatory MCL of 80 µg/L. Removals of individual trihalomethane species by spray aeration were modeled using temperature dependent equations developed by Cecchetti, et al. (2014) as shown Table A-8.

Table A-8: THM species removal equations for spray aeration (Cecchetti, et al., 2014).

THM Specie	Temp (°C)	Removal Equation
$CHCl_3$	2	*% Removal = 12.689 * ln(A/W ratio) - 41.706*
	22	*% Removal = 13.035 * ln(A/W ratio) - 38.929*
	36	*% Removal = 8.459 * ln(A/W ratio) - 8.3222*
$CHCl_2Br$	2	*% Removal = 16.862 * ln(A/W ratio) - 82.652*
	22	*% Removal = 14.487 * ln(A/W ratio) - 53.596*
	36	*% Removal = 9.7368 * ln(A/W ratio) - 41.706*
$CHClBr_2$	2	*% Removal = 17.962 * ln(A/W ratio) - 97.092*
	22	*% Removal = 15.111 * ln(A/W ratio) - 61.488*
	36	*% Removal = 10.761* ln(A/W ratio) - 15.55*
$CHBr_3$	2	*% Removal = 17.148 * ln(A/W ratio) - 88.556*
	22	*% Removal = 14.698 * ln(A/W ratio) - 56.863*
	36	% Removal = 9.9984 * ln(A/W ratio) - 7.6133

In the equations above, *A/W ratio* is the volumetric air-to-water ratio of spray aeration unit. For this study, this was assumed to be 25,000. THM removals at the source water temperature were

determined using linear interpolation between two of the reference temperatures from the table above.

Because aeration does not significantly alter TOC, UVA or residual chlorine concentrations, it was assumed that DBP formation after aeration would follow the baseline curve with the TTHM curve shifted down to a certain extent based on the concentration removed. The required concentration of TTHM to be removed was determined as:

$$C_{required\,removal} = C_{baseline,end\ of\ system} - C_{regulatory\ goal} \quad \text{(A.4.1)}$$

Where $C_{baseline,end\ of\ system}$ is the TTHM concentration at the end of the system for the baseline treatment approach and $C_{regulatory\ goal}$ is the treatment goal of 80 µg/L.

The fraction of the total flow aerated was optimized so TTHM concentration would meet the treatment goal at the end of the system using a mass balance approach as described by Figure A-2.

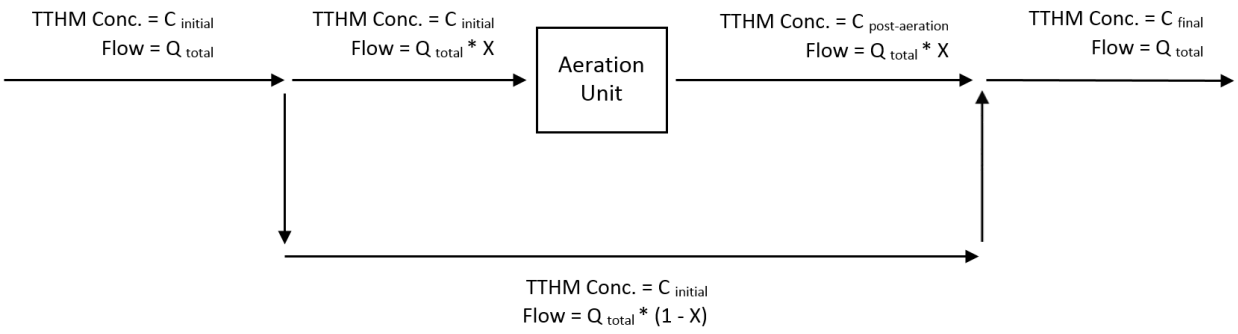

Figure A-2: TTHM mass balance around an aeration unit.

In the figure above, $C_{initial}$ is the TTHM concentration prior to aeration, X is the fraction of the total flow to be aerated, and C_{final} is the final TTHM concentration required to achieve compliance at the end of the distribution system. C_{final} was calculated as follows:

$$C_{final} = C_{initial} - C_{required\ removal} \quad \text{(A.4.2)}$$

Where $C_{required\ removal}$ is the TTHM concentration required to be removed in order to achieve regulatory compliance as calculated by equation A.4.1. The maximum attainable TTHM removal at the point of aeration was determined by summing the individual species removals:

$$C_{\max TTHM\ removal} = (C_{initial,CHCl_3} * \%\ Removal_{CHCl_3}) + (C_{initial,CHCl_2Br} * \%\ Removal_{CHCl_2Br}) + (C_{initial,CHClBr_2} * \%\ Removal_{CHClBr_2}) + (C_{initial,CHBr_3} * \%\ Removal_{CHBr_3}) \quad \text{(A.4.3)}$$

In the equation above, the $C_{initial}$ values represent the concentrations on individual TTHM species prior to aeration. It was assumed that the maximum attainable TTHM removal as calculated above would be achieved if 100% of the flow were aerated. If the maximum attainable TTHM removal was greater than the required TTHM removal as calculated by equation A.6.1, the percent of flow aerated was optimized using a mass balance around the point where the aeration stream and the by-pass stream were re-blended. The optimized fraction of flow to be aerated was calculated as:

$$X = \frac{C_{initial} - C_{final}}{C_{\max TTHM\ removal}} \quad \text{(A.4.4)}$$

If the maximum attainable TTHM removal was less than the required TTHM removal, it was assumed that 100% of the flow was treated and additional aeration units using the same TTHM removal methodology would be implemented before other points in the system exceeding the treatment goal of 80 µg/L. Individual species concentrations after blending were determined using mass balance equations around the re-blending point:

$$C_{final,CHCl_3} = (C_{initial,CHCl_3} * \%\ Removal_{CHCl_3}) * X + C_{initial,CHCl_3}(1 - X) \quad \text{(A.4.5)}$$

$$C_{final,CHCl_2Br} = (C_{initial,CHCl_2Br} * \%\ Removal_{CHCl_2Br}) * X + C_{initial,CHCl_2Br}(1 - X) \quad \text{A.4.6)}$$

$$C_{final,CHClBr_2} = (C_{initial,CHClBr_2} * \%\ Removal_{CHClBr_2}) * X + C_{initial,CHClBr_2}(1 - X) \quad \text{(A.4.7)}$$

$$C_{final,CHBr_3} = (C_{initial,CHBr_3} * \%\ Removal_{CHBr_3}) * X + C_{initial,CHBr_3}(1 - X) \quad \text{(A.4.8)}$$

The final TTHM concentration after re-blending was calculated as the sum of the final concentrations of individual THM species. DBP formation after aeration was modeled to follow the same curve as the baseline approach by setting the change in concentration of each DBP specie over each time step equal to the concentration change for the same time step from baseline treatment approach. If at any point after aeration the resulting TTHM concentration exceeded the treatment goal, an additional aeration unit was modeled one time step (12 hours) before the point of exceedance.

The RHI values associated with individual DBP species at each location before and after spray aeration (where applicable) were calculated using equations A.2.22 through A.2.26. The

cumulative RHI values for individual DBP species were added to produce a total RHI value both before and after spray aeration (where applicable) at each 12 hour time step. The resulting total RHI estimates throughout the entire distribution system were for population weighted risk quantification as described in Appendix A.9.

Appendix A.5: Distribution System Bubble Aeration Modeling Methods

Bubble aeration was modeled using the same overall approach as spray aeration as described in Appendix A.4. The only difference was the percent removals for individual THM species achieved by the aeration unit. For bubble aeration these were calculated as (Matter-Müller et al., 1981):

$$\% \, Removal = \left(1 - \frac{1}{1+\frac{Q_G H_{cc}}{Q_L}}\right) \quad \text{(A.5.1)}$$

Where Q_G is the gas (air) flow rate, Q_L is the liquid (water) flow rate, and H_{cc} is the dimensionless Henry's Law constant for the THM specie of interest at the system temperature and pressure. It was assumed that ratio Q_G/Q_L was constant at a value of 60 which simplified equation A.5.1 to:

$$\% \, Removal = \left(1 - \frac{1}{1+60*H_{cc}}\right) \quad \text{(A.5.2)}$$

H_{cc} for each THM specie was adjusted for temperature using a method proposed by Staudinger & Roberts (2001):

$$H_{cc,T} = \left(H_{cc,20°C}\right) * \left[10^{-B\left(\frac{1}{T}-\frac{1}{293}\right)}\right] \quad \text{(A.5.3)}$$

Where $H_{cc,20°C}$ is the dimensionless Henry's Law constant at 20 °C, B is a temperature dependent relationship constant, and T is the system temperature (°K). The resulting Henry's Law constants

from equation A.5.3 were subsequently adjusted for system pressure using a method proposed by Zwerneman (2012):

$$\frac{1}{H_{cc,P}} = \frac{kP}{1-\frac{1}{H_{cc,T}}} \quad \text{(A.5.4)}$$

Where P is the system pressure (psig), and k is a species specific empirical constant ($psig^{-1}$). $H_{cc,T}$ was assumed to be at atmospheric pressure. For this study, P was assumed to be 25 psig. The parameters used in the equations A.5.3 and A.5.4 above for each THM specie are shown in Table A-9.

Table A-9: THM species parameters used for Henry's Law constant adjustment in equations A.5.3 and A.2.4.

THM Specie	$H_{cc,20°C}$	B	k ($psig^{-1}$)
$CHCl_3$	0.126	1830	0.377
$CHCl_2Br$	0.076	2130	0.674
$CHClBr_2$	0.035	2273	1.21
$CHBr_3$	0.0175	2100	1.81

Using the adjusted Henry's Law constants from the table above, the removals of each THM specie were calculated using equation A.5.2.

The same overall modeling procedure that was used for spray aeration was used for bubble aeration with the first unit implemented one time step (12 hours) before the baseline TTHM concentration exceeded the regulatory MCL of 80 µg/L and the fraction of flow to be aerated was determined using the mass balance approach described by equations A.4.1 through A.4.8. It was also assumed for bubble aeration that the DBP formation curves followed the same shape as

the baseline approach and additional units were modeled one time step (12 hours) before any points where the concentration of TTHM would otherwise exceed the stated treatment goal.

The RHI values associated with individual DBP species at each location before and after bubble aeration (where applicable) were calculated using equations A.2.22 through A.2.26. The cumulative RHI values for individual DBP species were added to produce a total RHI value both before and after bubble aeration (where applicable) at each 12 hour time step. The resulting total RHI estimates throughout the entire distribution system were for population weighted risk quantification as described in Appendix A.9.

Appendix A.6: Distribution System GAC Modeling Methods

Granular activated carbon (GAC) adsorption was modeled as a treatment strategy for THM, HAA, and DBP precursor TOC removal within the distribution system. The treatment plant specifications were assumed to be identical those in the baseline approach as described in Appendix A.2. Thus, baseline the DBP formation curves were applicable for points in the distribution system prior to where GAC was implemented.

GAC adsorption units were modeled at specific locations within the distribution system to keep DBP concentrations below their respective MCLs at all points. The first GAC unit was applied one time step (12 hours) before the first point at which either the baseline TTHM or HAA5 formation curve exceeded 80 µg/L or 60 µg/L, respectively.

Each distribution system GAC adsorption unit was modeled to produce steady state THM, HAA, and TOC removals of 99%. This was based on the assumption that two GAC units could be applied in series as a lead-lag system to eliminate the temporal effects of DBP and TOC breakthrough. Similar to aeration, the fraction of flow treated with GAC adsorption was optimized so both the TTHM and HAA5 concentrations met their MCLs at the end of the distribution system. Although the fraction of flow treated and the by-pass were assumed to be re-blended after GAC adsorption, the two streams were modeled as separate aliquots for chlorine decay and DBP formation through the remainder of the distribution system. Blended DBP concentrations were determined at every 12 hour time-step by weighting the concentrations in each aliquot by their respective fractions of the total flow. This process is described in greater detail by Figure A-3 and equations A.6.1 through A.6.8 below.

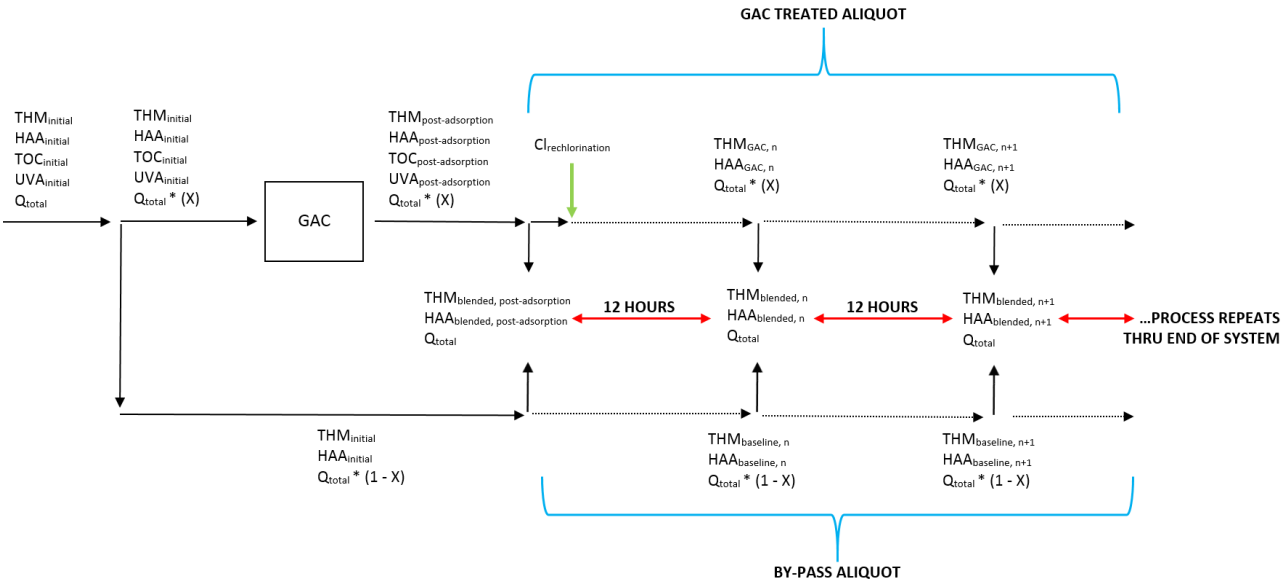

Figure A-3: Distribution system GAC modeling approach.

In the figure above, *X* is the fraction of flow treated by the GAC adsorption unit. The individual and bulk trihalomethane, haloacetic acid species concentrations in the GAC treated aliquot after the adsorption unit were calculated by multiplying their initial concentrations by 0.01 to represent the aforementioned 99% removal rates. The TOC concentration after adsorption was calculated in a similar manner:

$$TOC_{post-adsorption} = 0.01 * TOC_{initial} \quad \text{(A.6.1)}$$

$$THM_{post-adsorption} = 0.01 * THM_{initial} \quad \text{(A.6.2)}$$

$$HAA_{post-adsorption} = 0.01 * HAA_{initial} \quad \text{(A.6.4)}$$

Using and independent data set, it was determined that the (T)SUVA values for chlorinated water treated by GAC could be approximated with constant values of 0.9 L/mg-m. Based on this, the UVA values of the GAC treated aliquot after adsorption were calculated as:

$$UVA_{post-adsorption}(cm^{-1}) = \frac{0.9\left(\frac{L}{mg-m}\right) * TOC_{post-adsorption}\left(\frac{mg}{L}\right)}{100\ (\frac{cm}{m})} \quad \text{(A.6.4)}$$

It was assumed that all chlorine was removed from the GAC treated aliquot and rechlorination was required. Using the resulting $TOC_{post\text{-}adsorption}$ and $UVA_{post\text{-}adsorption}$ values as calculated by equations A.6.1 and A.6.4, the optimal rechlorination dose required maintain a residual concentration greater than 0.2 mg/L in the GAC treated aliquot at was determined iteratively by modeling chlorine decay. For this, the remainder of the distribution system was modeled as 25 CFSTRs in series. An initial chlorine dose of 0.3 mg/L was adjusted using equation A.2.10 and the decay through each modeled CFSTR was calculated using equation A.2.9. If the predicted final chlorine concentration in the GAC treated aliquot at the end of the distribution system was not greater than or equal to 0.2 mg/L, the applied chlorine dose was increased by 0.1 mg/L and the process was repeated until this condition was satisfied. The GAC treated aliquot pH was adjusted based on the applied re-chlorination dose using the methodology described in Appendix A.1.

DBP formation and the associated bromide incorporation in the GAC treated aliquot were modeled every 12 hours through the remainder of the distribution system using equations A.2.11 through A.2.21. It was assumed that DBPs in the by-pass stream aliquot continued to form following the baseline curve. The blended DBP concentrations at every 12 hour time-step through the remainder of the distribution system were calculated by weighting to the GAC treated and by-pass aliquots based on their relative fractions of the total flow:

$$THM_{blended,n} = \left[THM_{GAC,n} * X\right] + \left[THM_{baseline,n} * (1 - X)\right] \quad \text{(A.6.5)}$$

$$HAA_{blended,n} = \left[HAA_{GAC,n} * X\right] + \left[HAA_{baseline,n} * (1 - X)\right] \quad \text{(A.6.6)}$$

The RHI values associated with blended DBP species concentrations at each location were calculated using equations A.2.22 through A.2.26. The cumulative RHI values for individual DBP species were added to produce a total RHI value both before and after GAC adsorption (where applicable) at each 12 hour time step. The resulting total RHI estimates throughout the entire distribution system were for population weighted risk quantification as described in Appendix A.9.

Appendix A.7: WTP Effluent GAC Modeling Methods

As an alternative to treatment within the distribution system, GAC adsorption was also modeled at the effluent of the water treatment plant. This approach used the same methods as described in Appendix A.6 with the GAC unit modeled prior to the distribution system rather than at one time step before either TTHM or HAA5 exceeded their treatment goal concentrations.

Appendix A.8: Booster Chlorination Modeling Methods

Booster chlorination was modeled using the same in-plant treatment train as the baseline approach as described in Appendix A.2 with a second chlorine addition point at half of the distribution system residence time. The alum dose applied to the raw source water was equal to that of the baseline scenario to ensure the system achieved the required TOC removal to comply with enhanced coagulation regulations. The pH changed induced by this change was determined using the methods described in Appendix A.1 and the TOC and UVA were adjusted accordingly using equations A.2.1 through A.2.8. The chlorine dose applied prior to filtration was optimized to maintain a residual free chlorine concentration greater than 0.2 mg/L for half of the distribution system residence time and the caustic soda addition prior to the distribution system was optimized to bring the pH above 8 using the iterative processes described in Appendix A.2. DBP formation and the associated bromide incorporation were modeled through the filter, contact tank and every 12 hours of the first half of the distribution system using equations A.2.11 through A.2.21 based upon these in-plant treatment conditions.

The UVA was adjusted prior to re-chlorination at the half way point in the distribution system to account for the effects of the initial chlorine dose applied in the treatment plant:

$$UVA_{post-Cl2} = 0.06 * UVA_{pre-Cl2} \quad \text{(A.8.1)}$$

In the equation above, $UVA_{pre\text{-}Cl2}$ is the ultraviolet absorbance prior to the initial chlorine addition. Although this adjustment methodology is not consistent with the findings of other studies (Koechling, 1998), it ensures that, under the WTP Model framework, the ultimate DBP

yields at the end of the system are approximately equivalent to those of the baseline case which is constant with the findings of Boccelli (1999).

Using the resulting adjusted UVA as calculated by equation A.8.1, the chlorine concentration required to maintain a residual greater than 0.2 mg/L through the reminder of the distribution system was determined by the same iterative process that was used to calculate the optimized in-plant chlorine dose. The applied booster chlorination dose was determined by subtracting the existing residual concentration at the half way point in the distribution system from this required concentration. The pH was adjusted accordingly using the methods described in Appendix A.1.

THM and HAA formations were modeled for every 12 hours of the remainder of the distribution system. RHI values for the resulting DBP species concentrations at the effluent of each unit process were calculated using equations A.2.22 through A.2.26. The cumulative RHI values for individual DBP species were added to produce a total RHI value at the effluent of each unit process. The resulting total RHI estimates throughout the entire distribution system were for population weighted risk quantification as described in Appendix A.9.

Appendix A.9: Population Weighted Risk Estimation Methods

Cumulative distribution functions (CDFs) for population served in relation to water age at the point of consumption were derived using distribution system models KY2, KY7, and KY12 which were originally created by Jolly et al., (2014). Model developers proportioned base demands at each node from the total system demand based on pipe diameter. Each model incorporated a typical diurnal demand pattern as described by AWWA (2012). Additional details about distribution system model development can be found in the original publication by Jolly et al.

Using EPANET 2.0 software each model was assessed using a 336 hour (2 week) extended period simulation with hydraulic and water quality time steps of 1 hour and 5 min, respectively. The median water age at each node during the last 24 hours of simulation was used to develop CDFs of population served in relation for water age at the point of consumption for each system. This approach was based on the assumption that sufficient time had elapsed for each system in the first 312 hours (13 days) of simulation to reach typical operating conditions. Base demand values were used as a proxy for population at each node for CDF development. Each CDF was truncated to a maximum water age of 240 hours (10 days) to match the DBP risk estimation methodology used for treatment approach modeling as described in Appendix A.2 through A.8.

The distribution system RHI estimates for each alternative technology were weighted using trapezoidal integration under a curve relating RHI to the median water age CDF for each of the three modeled systems. Consistent with the DBP formation modeling methodology, this integration used a 12 hour time step. The population-weighted RHI estimates for each time step

were summed to give an overall population weighted RHI value for each alternative treatment applied to each system. This process is illustrated by Figure A-4 and equations A.9.1 and A.9.2 below.

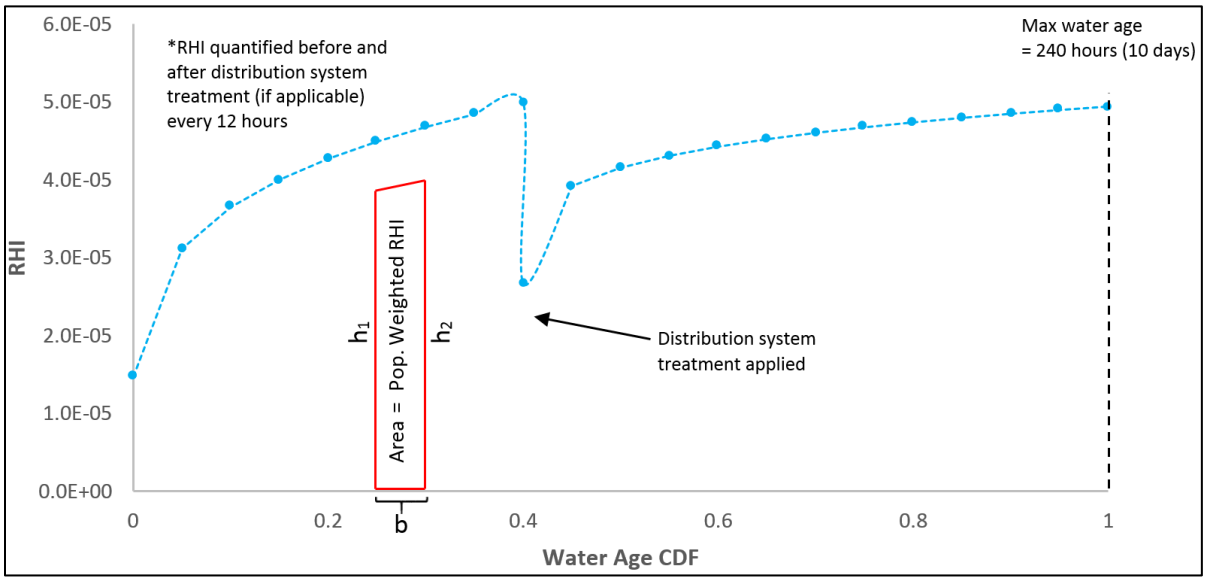

Figure A-4: Trapezoidal integration for population weighted RHI calculation.

$$Population\ Weighted\ RHI_{individual\ timestep} = \frac{(h_1+h_2)}{2} * b \quad \text{(A.9.1)}$$

$$Population\ Weighted\ RHI_{overall} = \sum Population\ Weighted\ RHI_{all\ timesteps} \quad \text{(A.9.2)}$$

In equation A.9.1 above, h_1 is the calculated RHI at a given time, h_2 is the calculated RHI 12 hours later, and b is the difference in median water age CDF values at the two times of interest. When a distribution system treatment technology was applied, as shown in Figure A.1.10 above, the RHI value before treatment was used as h_2 for the 12 hour time step before treatment was implemented and the RHI value after treatment was used as h_1 for the preceding 12 hour time step. The relative risk reductions achieved by each alternative treatment strategy for a given

source water quality scenario were calculated as the percent reduction in population-weighted RHI relative to the baseline.

Appendix B: Treatment Technology Modeling Results

Table B-1: Baseline treatment conditions for 27 Scenarios evaluated (enhanced coagulation regulations satisfied; in-plant chlorine contact time = 1 hour; distribution system pH ~ 8; distribution system residence time = 240 hours, minimum chlorine residual > 0.2 mg/L).

Scenario	Alum Dose (mg/L)	Chlorine Dose (mg/L)	Treated Water Quality at Point of Chlorination			Caustic Soda Dose (mg/L)
			TOC (mg/L)	*UVA (1/cm)*	*pH*	
1	40	3.6	2.58	0.052	6.82	24
2	40	3.6	2.58	0.052	6.82	24
3	40	3.6	2.58	0.052	6.82	24
4	40	3.9	2.97	0.059	6.82	24
5	40	3.9	2.97	0.059	6.82	24
6	40	3.9	2.97	0.059	6.82	24
7	58	3.9	2.92	0.059	6.63	30
8	58	3.9	2.92	0.059	6.63	30
9	58	3.9	2.92	0.059	6.63	30
10	38	3.2	2.22	0.046	6.82	22
11	38	3.2	2.22	0.046	6.82	22
12	38	3.2	2.22	0.046	6.82	22
13	38	3.6	2.61	0.053	6.82	22
14	38	3.6	2.61	0.053	6.82	22
15	38	3.6	2.61	0.053	6.82	22
16	38	4.0	3.00	0.060	6.82	22
17	38	4.0	3.00	0.060	6.82	22
18	38	4.0	3.00	0.060	6.82	22
19	36	2.8	1.87	0.039	6.82	20
20	36	2.8	1.87	0.039	6.82	20
21	36	2.8	1.87	0.039	6.82	20
22	38	3.2	2.21	0.046	6.80	22
23	38	3.2	2.21	0.046	6.80	22
24	38	3.2	2.21	0.046	6.80	22
25	38	3.6	2.60	0.053	6.80	22
26	38	3.6	2.60	0.053	6.80	22
27	38	3.6	2.60	0.053	6.80	22

Table B-2: Baseline DBP formation for 27 Scenarios evaluated.

Distribution System Residence Time (hr)	Scenario #1		Scenario #2		Scenario #3		Scenario #4	
	TTHM (µg/L)	*HAA5 (µg/L)*	*TTHM (µg/L)*	*HAA5 (µg/L)*	*TTHM (µg/L)*	*HAA5 (µg/L)*	*TTHM (µg/L)*	*HAA5 (µg/L)*
0	13.5	24.3	17.0	22.2	18.7	20.4	15.3	27.6
12	29.9	35.5	37.4	32.4	41.3	29.8	33.7	40.3
24	36.2	39.1	45.1	35.8	49.8	32.9	40.7	44.5
36	40.5	41.5	50.4	38.0	55.6	34.9	45.6	47.2
48	43.8	43.3	54.5	39.7	60.2	36.5	49.3	49.3
60	46.6	44.8	58.0	41.1	63.9	37.7	52.4	50.9
72	49.0	46.0	60.9	42.2	67.2	38.8	55.1	52.3
84	51.2	47.1	63.5	43.2	70.1	39.7	57.5	53.6
96	53.1	48.1	65.9	44.1	72.6	40.6	59.7	54.7
108	54.8	48.9	68.0	44.9	75.0	41.3	61.7	55.7
120	56.5	49.7	70.0	45.7	77.2	42.0	63.5	56.6
132	58.0	50.5	71.8	46.3	79.2	42.6	65.2	57.4
144	59.4	51.1	73.5	47.0	81.1	43.2	66.7	58.2
156	60.7	51.8	75.2	47.6	82.8	43.8	68.2	58.9
168	61.9	52.4	76.7	48.1	84.5	44.3	69.6	59.5
180	63.1	52.9	78.1	48.6	86.1	44.8	70.9	60.2
192	64.2	53.4	79.5	49.1	87.6	45.2	72.2	60.8
204	65.3	53.9	80.8	49.6	89.0	45.6	73.4	61.3
216	66.3	54.4	82.0	50.0	90.4	46.1	74.6	61.9
228	67.3	54.9	83.3	50.4	91.7	46.5	75.7	62.4
240	68.3	55.3	84.4	50.9	93.0	46.8	76.7	62.9

(Continued)

Distribution System Residence Time (hr)	Scenario #5		Scenario #6		Scenario #7		Scenario #8	
	TTHM (µg/L)	*HAA5 (µg/L)*	*TTHM (µg/L)*	*HAA5 (µg/L)*	*TTHM (µg/L)*	*HAA5 (µg/L)*	*TTHM (µg/L)*	*HAA5 (µg/L)*
0	19.2	25.3	21.2	23.4	14.8	27.8	18.6	25.6
12	42.1	37.1	46.5	34.2	32.5	40.7	40.5	37.5
24	50.7	41.0	56.0	37.8	39.2	45.0	48.8	41.5
36	56.7	43.5	62.5	40.2	43.8	47.7	54.5	44.1
48	61.3	45.4	67.6	42.0	47.4	49.8	58.9	46.0
60	65.1	47.0	71.8	43.4	50.4	51.5	62.6	47.6
72	68.4	48.3	75.4	44.7	53.0	53.0	65.7	49.0
84	71.4	49.5	78.7	45.8	55.2	54.2	68.5	50.2
96	74.0	50.5	81.5	46.7	57.3	55.3	71.0	51.2
108	76.4	51.4	84.2	47.6	59.2	56.3	73.3	52.1
120	78.6	52.3	86.6	48.4	60.9	57.2	75.5	53.0
132	80.6	53.0	88.9	49.1	62.5	58.1	77.4	53.8
144	82.6	53.8	91.0	49.8	64.0	58.8	79.3	54.5
156	84.4	54.4	92.9	50.4	65.5	59.6	81.0	55.2
168	86.1	55.1	94.8	51.0	66.8	60.3	82.6	55.9
180	87.7	55.7	96.6	51.6	68.1	60.9	84.2	56.5
192	89.2	56.2	98.3	52.1	69.3	61.5	85.6	57.0
204	90.7	56.8	99.9	52.6	70.4	62.1	87.0	57.6
216	92.1	57.3	101.4	53.1	71.5	62.6	88.4	58.1
228	93.4	57.7	102.9	53.5	72.6	63.1	89.7	58.6
240	94.7	58.2	104.3	54.0	73.6	63.7	90.9	59.1

(Continued)

Distribution System Residence Time (hr)	Scenario #9		Scenario #10		Scenario #11		Scenario #12	
	TTHM (µg/L)	*HAA5 (µg/L)*	*TTHM (µg/L)*	*HAA5 (µg/L)*	*TTHM (µg/L)*	*HAA5 (µg/L)*	*TTHM (µg/L)*	*HAA5 (µg/L)*
0	20.5	23.7	14.4	24.7	18.1	22.1	20.0	20.0
12	44.7	34.7	31.5	36.2	39.4	32.4	43.5	29.1
24	53.8	38.4	38.0	40.0	47.4	35.8	52.3	32.2
36	60.1	40.8	42.5	42.4	52.9	38.1	58.4	34.3
48	65.0	42.7	46.0	44.3	57.2	39.8	63.1	35.8
60	69.0	44.1	48.9	45.8	60.7	41.1	67.0	37.1
72	72.5	45.4	51.4	47.1	63.8	42.3	70.4	38.1
84	75.6	46.5	53.6	48.2	66.5	43.3	73.4	39.1
96	78.3	47.5	55.6	49.2	68.9	44.3	76.0	39.9
108	80.9	48.4	57.4	50.1	71.1	45.1	78.5	40.6
120	83.2	49.2	59.1	50.9	73.2	45.8	80.7	41.3
132	85.3	49.9	60.6	51.6	75.1	46.5	82.8	42.0
144	87.3	50.6	62.1	52.3	76.8	47.2	84.8	42.5
156	89.2	51.2	63.5	53.0	78.5	47.7	86.6	43.1
168	91.0	51.9	64.8	53.6	80.1	48.3	88.3	43.6
180	92.7	52.4	66.0	54.1	81.6	48.8	89.9	44.1
192	94.3	53.0	67.2	54.7	83.0	49.3	91.5	44.6
204	95.9	53.5	68.3	55.2	84.3	49.8	93.0	45.0
216	97.3	54.0	69.3	55.7	85.6	50.3	94.4	45.4
228	98.8	54.4	70.4	56.2	86.9	50.7	95.8	45.8
240	100.1	54.9	71.4	56.6	88.1	51.1	97.1	46.2

(Continued)

Distribution System Residence Time (hr)	Scenario #13		Scenario #14		Scenario #15		Scenario #16	
	TTHM (µg/L)	*HAA5 (µg/L)*	*TTHM (µg/L)*	*HAA5 (µg/L)*	*TTHM (µg/L)*	*HAA5 (µg/L)*	*TTHM (µg/L)*	*HAA5 (µg/L)*
0	16.8	29.0	21.0	26.2	23.2	23.8	19.1	33.4
12	36.4	42.6	45.4	38.5	50.1	34.9	41.2	49.1
24	43.8	47.0	54.6	42.6	60.2	38.7	49.6	54.3
36	48.9	49.9	60.8	45.3	67.1	41.1	55.4	57.6
48	52.9	52.1	65.7	47.3	72.5	43.0	59.9	60.2
60	56.3	53.9	69.8	48.9	77.0	44.5	63.6	62.2
72	59.1	55.4	73.3	50.3	80.9	45.8	66.9	64.0
84	61.7	56.7	76.4	51.6	84.3	46.9	69.7	65.5
96	64.0	57.9	79.2	52.7	87.3	47.9	72.3	66.8
108	66.1	59.0	81.7	53.6	90.1	48.8	74.7	68.1
120	68.0	59.9	84.1	54.5	92.7	49.7	76.9	69.2
132	69.8	60.8	86.2	55.3	95.1	50.4	78.9	70.2
144	71.5	61.6	88.3	56.1	97.3	51.1	80.8	71.1
156	73.0	62.4	90.2	56.8	99.4	51.8	82.5	72.0
168	74.5	63.1	92.0	57.5	101.4	52.4	84.2	72.8
180	75.9	63.8	93.7	58.1	103.2	53.0	85.8	73.6
192	77.3	64.4	95.3	58.7	105.0	53.5	87.3	74.4
204	78.5	65.0	96.9	59.3	106.7	54.1	88.7	75.1
216	79.8	65.6	98.3	59.8	108.3	54.6	90.1	75.7
228	81.0	66.1	99.8	60.3	109.9	55.1	91.5	76.4
240	82.1	66.7	101.1	60.8	111.4	55.5	92.7	77.0

(Continued)

Distribution System Residence Time (hr)	Scenario #17		Scenario #18		Scenario #19		Scenario #20	
	TTHM (µg/L)	*HAA5 (µg/L)*	*TTHM (µg/L)*	*HAA5 (µg/L)*	*TTHM (µg/L)*	*HAA5 (µg/L)*	*TTHM (µg/L)*	*HAA5 (µg/L)*
0	23.9	30.3	26.4	27.7	14.3	23.5	17.9	20.5
12	51.3	44.7	56.7	40.9	30.7	34.5	38.4	30.1
24	61.7	49.5	68.1	45.3	37.0	38.1	46.2	33.4
36	68.7	52.6	75.8	48.2	41.3	40.4	51.4	35.5
48	74.2	55.0	81.9	50.4	44.6	42.2	55.5	37.1
60	78.8	56.9	86.9	52.2	47.4	43.7	59.0	38.4
72	82.8	58.6	91.3	53.7	49.8	44.9	61.9	39.5
84	86.3	60.0	95.1	55.0	52.0	46.0	64.5	40.5
96	89.4	61.3	98.5	56.2	53.9	46.9	66.8	41.3
108	92.3	62.4	101.7	57.3	55.6	47.8	69.0	42.1
120	94.9	63.4	104.5	58.2	57.3	48.6	70.9	42.8
132	97.3	64.4	107.2	59.1	58.8	49.3	72.7	43.5
144	99.6	65.3	109.7	60.0	60.2	50.0	74.4	44.1
156	101.8	66.1	112.1	60.7	61.5	50.6	76.0	44.7
168	103.8	66.9	114.3	61.5	62.7	51.2	77.6	45.2
180	105.7	67.6	116.4	62.2	63.9	51.7	79.0	45.7
192	107.5	68.3	118.4	62.8	65.0	52.2	80.3	46.2
204	109.3	69.0	120.3	63.4	66.1	52.7	81.6	46.6
216	111.0	69.6	122.1	64.0	67.1	53.2	82.9	47.0
228	112.6	70.2	123.9	64.6	68.1	53.6	84.1	47.5
240	114.1	70.8	125.6	65.1	69.1	54.1	85.2	47.8

(Continued)

Distribution System Residence Time (hr)	Scenario #21		Scenario #22		Scenario #23		Scenario #24	
	TTHM (µg/L)	*HAA5 (µg/L)*	*TTHM (µg/L)*	*HAA5 (µg/L)*	*TTHM (µg/L)*	*HAA5 (µg/L)*	*TTHM (µg/L)*	*HAA5 (µg/L)*
0	19.8	18.3	16.8	28.1	21.0	24.8	23.2	22.2
12	42.5	26.6	36.7	41.1	45.8	36.3	50.6	32.4
24	51.0	29.5	44.2	45.3	55.1	40.2	60.8	35.8
36	56.8	31.3	49.4	48.1	61.4	42.7	67.8	38.1
48	61.4	32.8	53.5	50.2	66.4	44.6	73.3	39.8
60	65.1	33.9	56.8	51.9	70.5	46.2	77.8	41.2
72	68.4	34.9	59.8	53.4	74.1	47.5	81.7	42.4
84	71.2	35.8	62.3	54.6	77.2	48.7	85.2	43.5
96	73.8	36.6	64.6	55.8	80.0	49.7	88.3	44.4
108	76.2	37.3	66.8	56.8	82.6	50.6	91.1	45.2
120	78.3	37.9	68.7	57.7	84.9	51.5	93.7	46.0
132	80.3	38.5	70.5	58.5	87.1	52.2	96.1	46.7
144	82.2	39.0	72.2	59.3	89.2	53.0	98.4	47.4
156	84.0	39.5	73.8	60.1	91.1	53.6	100.5	48.0
168	85.6	40.0	75.3	60.8	92.9	54.3	102.5	48.6
180	87.2	40.5	76.7	61.4	94.7	54.9	104.4	49.1
192	88.7	40.9	78.1	62.0	96.3	55.4	106.2	49.6
204	90.1	41.3	79.4	62.6	97.9	56.0	107.9	50.1
216	91.5	41.7	80.6	63.1	99.4	56.5	109.5	50.6
228	92.8	42.1	81.8	63.7	100.8	57.0	111.1	51.0
240	94.0	42.4	83.0	64.2	102.2	57.4	112.6	51.5

(Continued)

Distribution System Residence Time (hr)	Scenario #25		Scenario #26		Scenario #27		
	TTHM (µg/L)	*HAA5 (µg/L)*	*TTHM (µg/L)*	*HAA5 (µg/L)*	*TTHM (µg/L)*	*HAA5 (µg/L)*	
0	19.5	33.0	24.4	29.4	26.9	26.5	
12	42.3	48.3	52.7	43.2	58.2	38.9	
24	51.0	53.4	63.4	47.8	70.0	43.0	
36	56.9	56.7	70.6	50.9	78.0	45.8	
48	61.6	59.2	76.3	53.2	84.2	47.9	
60	65.4	61.2	81.0	55.0	89.4	49.6	
72	68.8	62.9	85.1	56.6	93.9	51.1	
84	71.7	64.4	88.7	58.0	97.8	52.3	
96	74.4	65.7	91.9	59.2	101.3	53.4	
108	76.8	66.9	94.8	60.3	104.6	54.5	
120	79.0	68.0	97.5	61.3	107.5	55.4	
132	81.1	69.0	100.1	62.3	110.3	56.3	
144	83.1	69.9	102.4	63.1	112.8	57.1	
156	84.9	70.8	104.6	63.9	115.3	57.8	
168	86.6	71.6	106.7	64.7	117.5	58.5	
180	88.3	72.4	108.7	65.4	119.7	59.2	
192	89.8	73.1	110.5	66.1	121.8	59.8	
204	91.3	73.8	112.3	66.7	123.7	60.4	
216	92.7	74.4	114.1	67.3	125.6	60.9	
228	94.1	75.0	115.7	67.9	127.4	61.5	
240	95.4	75.6	117.3	68.5	129.1	62.0	

(Continued)

Table B-3: Population-weighted RHI values for KY2.

Scenario #	Baseline	Booster Chlorination	Optimized Coagulation	WTP Effluent GAC	DS GAC	Spray Aeration	Bubble Aeration
1	3.29×10^{-5}	2.96×10^{-5}	3.29×10^{-5}	3.29×10^{-5}	3.29×10^{-5}	3.29×10^{-5}	3.29×10^{-5}
2*	3.72×10^{-5}	3.40×10^{-5}	3.57×10^{-5}	3.53×10^{-5}	3.72×10^{-5}	3.72×10^{-5}	3.72×10^{-5}
3**	4.07×10^{-5}	3.75×10^{-5}	3.52×10^{-5}	3.50×10^{-5}	4.06×10^{-5}	4.06×10^{-5}	4.06×10^{-5}
4†	3.74×10^{-5}	3.40×10^{-5}	3.55×10^{-5}	3.57×10^{-5}	3.74×10^{-5}	3.74×10^{-5}	3.74×10^{-5}
5**	4.21×10^{-5}	3.87×10^{-5}	3.60×10^{-5}	3.55×10^{-5}	4.18×10^{-5}	4.19×10^{-5}	4.19×10^{-5}
6**	4.58×10^{-5}	4.25×10^{-5}	3.55×10^{-5}	3.51×10^{-5}	4.30×10^{-5}	4.37×10^{-5}	4.38×10^{-5}
7†	3.72×10^{-5}	3.37×10^{-5}	3.57×10^{-5}	3.72×10^{-5}	3.72×10^{-5}	3.72×10^{-5}	3.72×10^{-5}
8**	4.17×10^{-5}	3.83×10^{-5}	3.53×10^{-5}	3.67×10^{-5}	4.16×10^{-5}	4.16×10^{-5}	4.16×10^{-5}
9**	4.53×10^{-5}	4.19×10^{-5}	3.59×10^{-5}	3.61×10^{-5}	4.34×10^{-5}	4.39×10^{-5}	4.40×10^{-5}
10	3.38×10^{-5}	3.04×10^{-5}	3.38×10^{-5}	3.38×10^{-5}	3.38×10^{-5}	3.38×10^{-5}	3.38×10^{-5}
11*	3.83×10^{-5}	3.50×10^{-5}	3.51×10^{-5}	3.48×10^{-5}	3.83×10^{-5}	3.83×10^{-5}	3.83×10^{-5}
12**	4.19×10^{-5}	3.86×10^{-5}	3.27×10^{-5}	3.45×10^{-5}	4.10×10^{-5}	4.12×10^{-5}	4.12×10^{-5}
13*†	3.96×10^{-5}	3.56×10^{-5}	3.62×10^{-5}	3.57×10^{-5}	3.94×10^{-5}	3.96×10^{-5}	3.96×10^{-5}
14**†	4.45×10^{-5}	4.06×10^{-5}	3.46×10^{-5}	3.52×10^{-5}	4.26×10^{-5}	4.33×10^{-5}	4.33×10^{-5}
15**	4.85×10^{-5}	4.46×10^{-5}	3.66×10^{-5}	3.47×10^{-5}	4.27×10^{-5}	4.37×10^{-5}	4.40×10^{-5}
16**††	4.55×10^{-5}	4.08×10^{-5}	3.57×10^{-5}	3.57×10^{-5}	3.88×10^{-5}	4.55×10^{-5}	4.55×10^{-5}
17**††	5.08×10^{-5}	4.63×10^{-5}	3.54×10^{-5}	3.56×10^{-5}	4.44×10^{-5}	4.66×10^{-5}	4.67×10^{-5}
18**†	5.51×10^{-5}	5.06×10^{-5}	3.47×10^{-5}	3.50×10^{-5}	4.18×10^{-5}	4.38×10^{-5}	4.38×10^{-5}
19	3.22×10^{-5}	2.93×10^{-5}	3.22×10^{-5}	3.22×10^{-5}	3.22×10^{-5}	3.22×10^{-5}	3.22×10^{-5}
20*	3.67×10^{-5}	3.41×10^{-5}	3.42×10^{-5}	3.45×10^{-5}	3.67×10^{-5}	3.67×10^{-5}	3.67×10^{-5}
21**	4.00×10^{-5}	3.77×10^{-5}	3.35×10^{-5}	3.40×10^{-5}	3.98×10^{-5}	3.99×10^{-5}	3.99×10^{-5}
22*†	3.86×10^{-5}	3.48×10^{-5}	3.61×10^{-5}	3.60×10^{-5}	3.86×10^{-5}	3.86×10^{-5}	3.86×10^{-5}
23**	4.36×10^{-5}	3.98×10^{-5}	3.42×10^{-5}	3.41×10^{-5}	4.10×10^{-5}	4.18×10^{-5}	4.19×10^{-5}
24**	4.75×10^{-5}	4.38×10^{-5}	3.39×10^{-5}	3.36×10^{-5}	4.16×10^{-5}	4.24×10^{-5}	2.27×10^{-5}
25**††	4.52×10^{-5}	4.07×10^{-5}	3.57×10^{-5}	3.61×10^{-5}	3.99×10^{-5}	4.51×10^{-5}	4.51×10^{-5}
26**†	5.06×10^{-5}	4.62×10^{-5}	3.48×10^{-5}	3.45×10^{-5}	4.16×10^{-5}	4.41×10^{-5}	4.43×10^{-5}
27**†	5.49×10^{-5}	5.06×10^{-5}	3.42×10^{-5}	3.39×10^{-5}	4.10×10^{-5}	4.25×10^{-5}	4.30×10^{-5}

* = TTHM Violation < 10 µg/L
** = TTHM Violation ≥ 10 µg/L
† = HAA5 Violation < 10 µg/L
†† = HAA5 Violation ≥ 10 µg/L

Table B-4: Population-weighted RHI values for KY7.

Scenario #	Baseline	Booster Chlorination	Optimized Coagulation	WTP Effluent GAC	DS GAC	Spray Aeration	Bubble Aeration
1	3.32×10^{-5}	3.05×10^{-5}	3.32×10^{-5}	3.32×10^{-5}	3.32×10^{-5}	3.32×10^{-5}	3.32×10^{-5}
2*	3.76×10^{-5}	3.52×10^{-5}	3.60×10^{-5}	3.56×10^{-5}	3.70×10^{-5}	3.73×10^{-5}	3.73×10^{-5}
3**	4.11×10^{-5}	3.89×10^{-5}	3.55×10^{-5}	3.53×10^{-5}	3.94×10^{-5}	4.00×10^{-5}	4.00×10^{-5}
4†	3.78×10^{-5}	3.50×10^{-5}	3.59×10^{-5}	3.61×10^{-5}	3.73×10^{-5}	3.78×10^{-5}	3.78×10^{-5}
5**	4.25×10^{-5}	4.00×10^{-5}	3.63×10^{-5}	3.59×10^{-5}	4.05×10^{-5}	4.14×10^{-5}	4.14×10^{-5}
6**	4.63×10^{-5}	4.40×10^{-5}	3.58×10^{-5}	3.54×10^{-5}	4.27×10^{-5}	4.39×10^{-5}	4.40×10^{-5}
7†	3.76×10^{-5}	3.47×10^{-5}	3.61×10^{-5}	3.54×10^{-5}	3.69×10^{-5}	3.76×10^{-5}	3.76×10^{-5}
8**	4.21×10^{-5}	3.95×10^{-5}	3.56×10^{-5}	3.70×10^{-5}	4.06×10^{-5}	4.13×10^{-5}	4.13×10^{-5}
9**	4.57×10^{-5}	4.33×10^{-5}	3.59×10^{-5}	3.65×10^{-5}	4.27×10^{-5}	4.38×10^{-5}	4.39×10^{-5}
10	3.41×10^{-5}	3.13×10^{-5}	3.41×10^{-5}	3.41×10^{-5}	3.41×10^{-5}	3.41×10^{-5}	3.41×10^{-5}
11*	3.87×10^{-5}	3.62×10^{-5}	3.54×10^{-5}	3.51×10^{-5}	3.77×10^{-5}	3.81×10^{-5}	3.81×10^{-5}
12**	4.23×10^{-5}	3.99×10^{-5}	3.34×10^{-5}	3.48×10^{-5}	3.99×10^{-5}	4.06×10^{-5}	4.07×10^{-5}
13*†	4.00×10^{-5}	3.67×10^{-5}	3.65×10^{-5}	3.60×10^{-5}	3.88×10^{-5}	3.99×10^{-5}	3.99×10^{-5}
14**†	4.50×10^{-5}	4.20×10^{-5}	3.49×10^{-5}	3.56×10^{-5}	4.19×10^{-5}	4.32×10^{-5}	4.32×10^{-5}
15**	4.89×10^{-5}	4.62×10^{-5}	3.51×10^{-5}	3.51×10^{-5}	4.34×10^{-5}	4.50×10^{-5}	4.52×10^{-5}
16**††	4.60×10^{-5}	4.20×10^{-5}	3.60×10^{-5}	3.60×10^{-5}	4.09×10^{-5}	4.52×10^{-5}	4.52×10^{-5}
17**††	5.13×10^{-5}	4.78×10^{-5}	3.57×10^{-5}	3.60×10^{-5}	4.53×10^{-5}	4.78×10^{-5}	4.79×10^{-5}
18**†	5.56×10^{-5}	5.23×10^{-5}	3.50×10^{-5}	3.53×10^{-5}	4.56×10^{-5}	4.81×10^{-5}	4.84×10^{-5}
19	3.26×10^{-5}	3.02×10^{-5}	3.26×10^{-5}	3.26×10^{-5}	3.26×10^{-5}	3.26×10^{-5}	3.26×10^{-5}
20*	3.71×10^{-5}	3.53×10^{-5}	3.46×10^{-5}	3.48×10^{-5}	3.64×10^{-5}	3.67×10^{-5}	3.67×10^{-5}
21**	4.05×10^{-5}	3.90×10^{-5}	3.42×10^{-5}	3.44×10^{-5}	3.86×10^{-5}	3.92×10^{-5}	3.92×10^{-5}
22*†	3.90×10^{-5}	3.58×10^{-5}	3.64×10^{-5}	3.63×10^{-5}	3.82×10^{-5}	3.88×10^{-5}	3.88×10^{-5}
23**	4.40×10^{-5}	4.12×10^{-5}	3.45×10^{-5}	3.44×10^{-5}	4.08×10^{-5}	4.21×10^{-5}	4.21×10^{-5}
24**	3.79×10^{-5}	4.53×10^{-5}	3.42×10^{-5}	3.40×10^{-5}	4.24×10^{-5}	4.37×10^{-5}	4.39×10^{-5}
25**††	4.57×10^{-5}	4.19×10^{-5}	3.60×10^{-5}	3.64×10^{-5}	4.14×10^{-5}	4.47×10^{-5}	4.47×10^{-5}
26**†	5.11×10^{-5}	4.77×10^{-5}	3.52×10^{-5}	3.49×10^{-5}	4.39×10^{-5}	4.65×10^{-5}	4.66×10^{-5}
27**†	5.55×10^{-5}	5.23×10^{-5}	3.45×10^{-5}	3.42×10^{-5}	4.49×10^{-5}	4.71×10^{-5}	4.74×10^{-5}

* = TTHM Violation < 10 µg/L
** = TTHM Violation ≥ 10 µg/L
† = HAA5 Violation < 10 µg/L
†† = HAA5 Violation ≥ 10 µg/L

Table B-5: Population-weighted RHI values for KY12.

Scenario #	Baseline	Booster Chlorination	Optimized Coagulation	WTP Effluent GAC	DS GAC	Spray Aeration	Bubble Aeration
1	3.60×10^{-5}	3.26×10^{-5}	3.60×10^{-5}	3.60×10^{-5}	3.60×10^{-5}	3.60×10^{-5}	3.60×10^{-5}
2*	4.08×10^{-5}	3.76×10^{-5}	3.91×10^{-5}	3.87×10^{-5}	4.07×10^{-5}	4.08×10^{-5}	4.08×10^{-5}
3**	4.48×10^{-5}	3.73×10^{-5}	3.89×10^{-5}	3.90×10^{-5}	4.08×10^{-5}	4.09×10^{-5}	4.09×10^{-5}
4†	4.09×10^{-5}	3.73×10^{-5}	3.89×10^{-5}	3.90×10^{-5}	4.08×10^{-5}	4.09×10^{-5}	4.09×10^{-5}
5**	4.61×10^{-5}	4.27×10^{-5}	3.95×10^{-5}	3.89×10^{-5}	4.54×10^{-5}	4.57×10^{-5}	4.57×10^{-5}
6**	5.04×10^{-5}	4.71×10^{-5}	3.91×10^{-5}	3.86×10^{-5}	4.65×10^{-5}	4.75×10^{-5}	4.77×10^{-5}
7†	4.07×10^{-5}	3.70×10^{-5}	3.91×10^{-5}	3.84×10^{-5}	4.05×10^{-5}	4.07×10^{-5}	4.07×10^{-5}
8**	4.56×10^{-5}	4.21×10^{-5}	3.87×10^{-5}	4.02×10^{-5}	4.53×10^{-5}	4.54×10^{-5}	4.55×10^{-5}
9**	4.97×10^{-5}	4.63×10^{-5}	3.95×10^{-5}	3.97×10^{-5}	4.76×10^{-5}	4.82×10^{-5}	4.83×10^{-5}
10	3.70×10^{-5}	3.35×10^{-5}	3.70×10^{-5}	3.70×10^{-5}	3.70×10^{-5}	3.70×10^{-5}	3.70×10^{-5}
11*	4.21×10^{-5}	3.87×10^{-5}	3.85×10^{-5}	3.82×10^{-5}	4.18×10^{-5}	4.19×10^{-5}	4.19×10^{-5}
12**	4.61×10^{-5}	4.28×10^{-5}	3.61×10^{-5}	3.80×10^{-5}	4.50×10^{-5}	4.53×10^{-5}	4.54×10^{-5}
13*†	4.33×10^{-5}	3.92×10^{-5}	3.96×10^{-5}	3.90×10^{-5}	4.29×10^{-5}	4.33×10^{-5}	4.33×10^{-5}
14**†	4.88×10^{-5}	4.48×10^{-5}	3.80×10^{-5}	3.86×10^{-5}	4.67×10^{-5}	4.75×10^{-5}	4.75×10^{-5}
15**	5.33×10^{-5}	4.94×10^{-5}	3.84×10^{-5}	3.82×10^{-5}	4.32×10^{-5}	4.51×10^{-5}	4.55×10^{-5}
16**††	4.98×10^{-5}	4.49×10^{-5}	3.90×10^{-5}	3.91×10^{-5}	4.03×10^{-5}	4.95×10^{-5}	4.95×10^{-5}
17**††	5.57×10^{-5}	5.10×10^{-5}	3.89×10^{-5}	3.91×10^{-5}	4.46×10^{-5}	4.83×10^{-5}	4.85×10^{-5}
18**†	6.05×10^{-5}	5.60×10^{-5}	3.83×10^{-5}	3.85×10^{-5}	4.18×10^{-5}	4.49×10^{-5}	4.57×10^{-5}
19	3.53×10^{-5}	3.23×10^{-5}	3.53×10^{-5}	3.53×10^{-5}	3.53×10^{-5}	3.53×10^{-5}	3.53×10^{-5}
20*	4.03×10^{-5}	3.77×10^{-5}	3.76×10^{-5}	3.79×10^{-5}	4.02×10^{-5}	4.02×10^{-5}	4.02×10^{-5}
21**	4.42×10^{-5}	4.19×10^{-5}	3.75×10^{-5}	3.76×10^{-5}	4.36×10^{-5}	4.37×10^{-5}	4.37×10^{-5}
22*†	4.22×10^{-5}	3.83×10^{-5}	3.96×10^{-5}	3.94×10^{-5}	4.21×10^{-5}	4.22×10^{-5}	4.22×10^{-5}
23**	4.78×10^{-5}	4.40×10^{-5}	3.76×10^{-5}	3.74×10^{-5}	4.44×10^{-5}	4.55×10^{-5}	4.56×10^{-5}
24**	5.23×10^{-5}	4.85×10^{-5}	3.75×10^{-5}	3.71×10^{-5}	4.21×10^{-5}	4.35×10^{-5}	4.39×10^{-5}
25**††	4.95×10^{-5}	4.48×10^{-5}	3.96×10^{-5}	3.96×10^{-5}	4.16×10^{-5}	4.91×10^{-5}	4.91×10^{-5}
26**†	5.55×10^{-5}	5.01×10^{-5}	3.83×10^{-5}	3.79×10^{-5}	4.22×10^{-5}	4.60×10^{-5}	4.63×10^{-5}
27**†	6.05×10^{-5}	5.60×10^{-5}	3.78×10^{-5}	3.73×10^{-5}	4.08×10^{-5}	4.32×10^{-5}	4.40×10^{-5}

* = TTHM Violation < 10 µg/L
** = TTHM Violation ≥ 10 µg/L
† = HAA5 Violation < 10 µg/L
†† = HAA5 Violation ≥ 10 µg/L